Supporting Information

From Hydroborations Catalysed by Sn(II) cations to Photoluminescent Boronic Esters

*Ondřej Moždiak,[a] Tomáš Bíza, [a] Lukáš Střižík, [a] Zdeňka Růžičková, [a] Milan Erben, [a] Libor Dostál, [a] Emanuel Hupf,[b] and Roman Jambor[a]**

[a] Department of General and Inorganic Chemistry, Faculty of Chemistry and Technology, University of Pardubice, 532 10 Pardubice, Czech Republic

Email: roman.jambor@upce.cz

[b] Department of Inorganic Chemistry, Faculty of Chemistry, University of Bremen, Germany

CONTENT

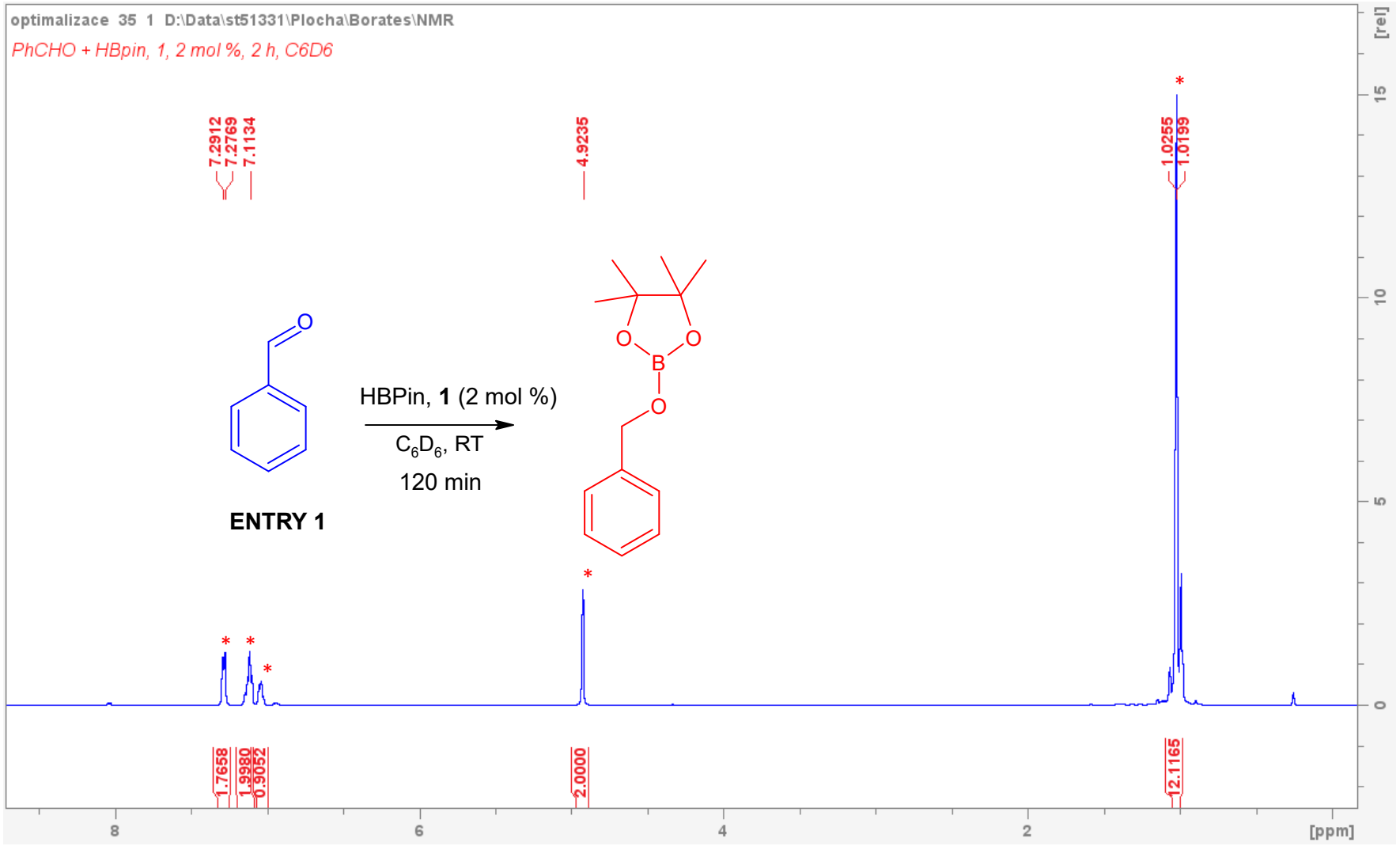

Figure S1. Entry 1: Reaction mixture. Benzaldehyde + HBPin, catalyst **1** (2 mol %), 2 h, RT, C_6D_6.

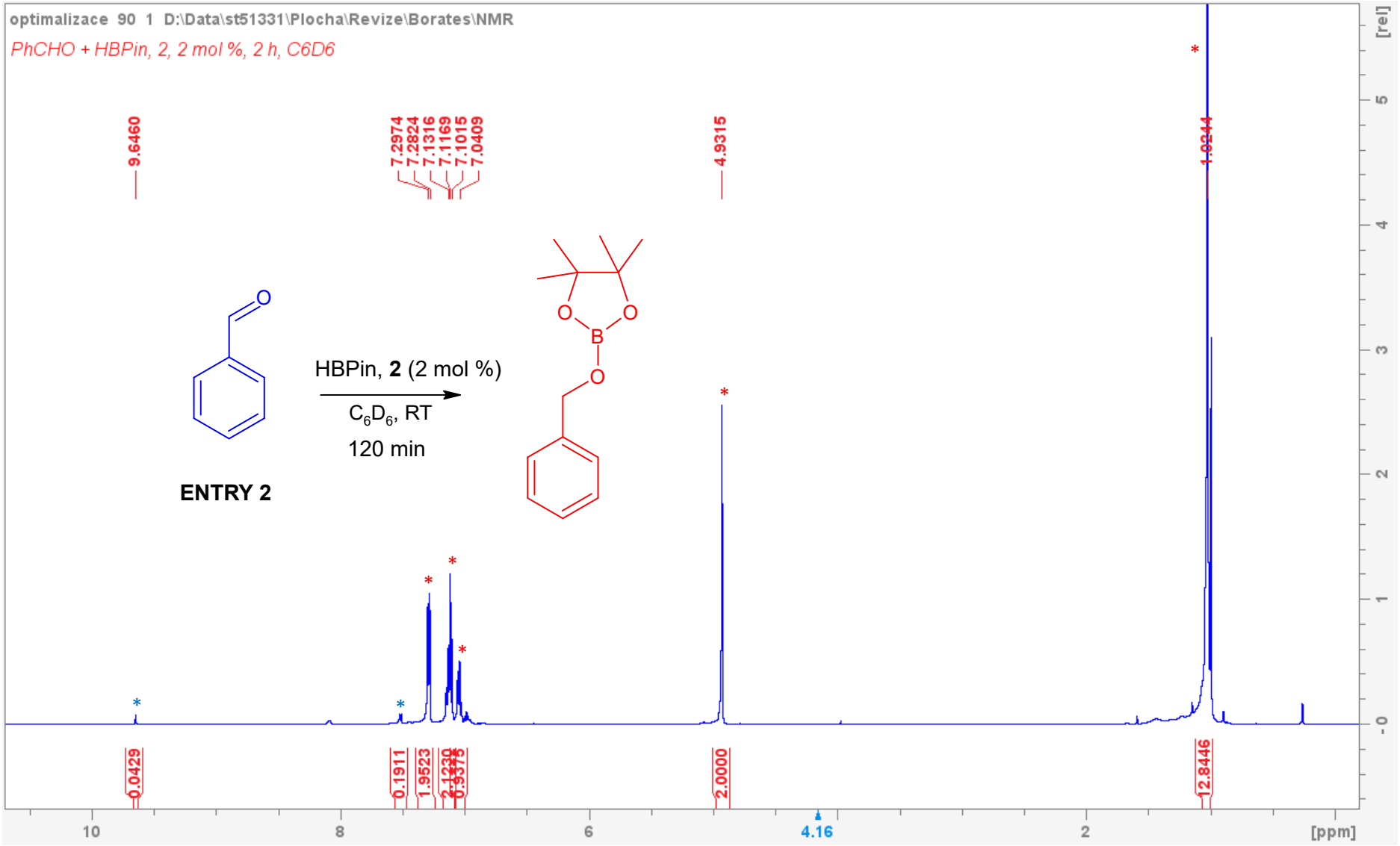

Figure S2. Entry 2: Reaction mixture. Benzaldehyde + HBPin, catalyst **2** (2 mol %), 2 h, RT, C_6D_6.

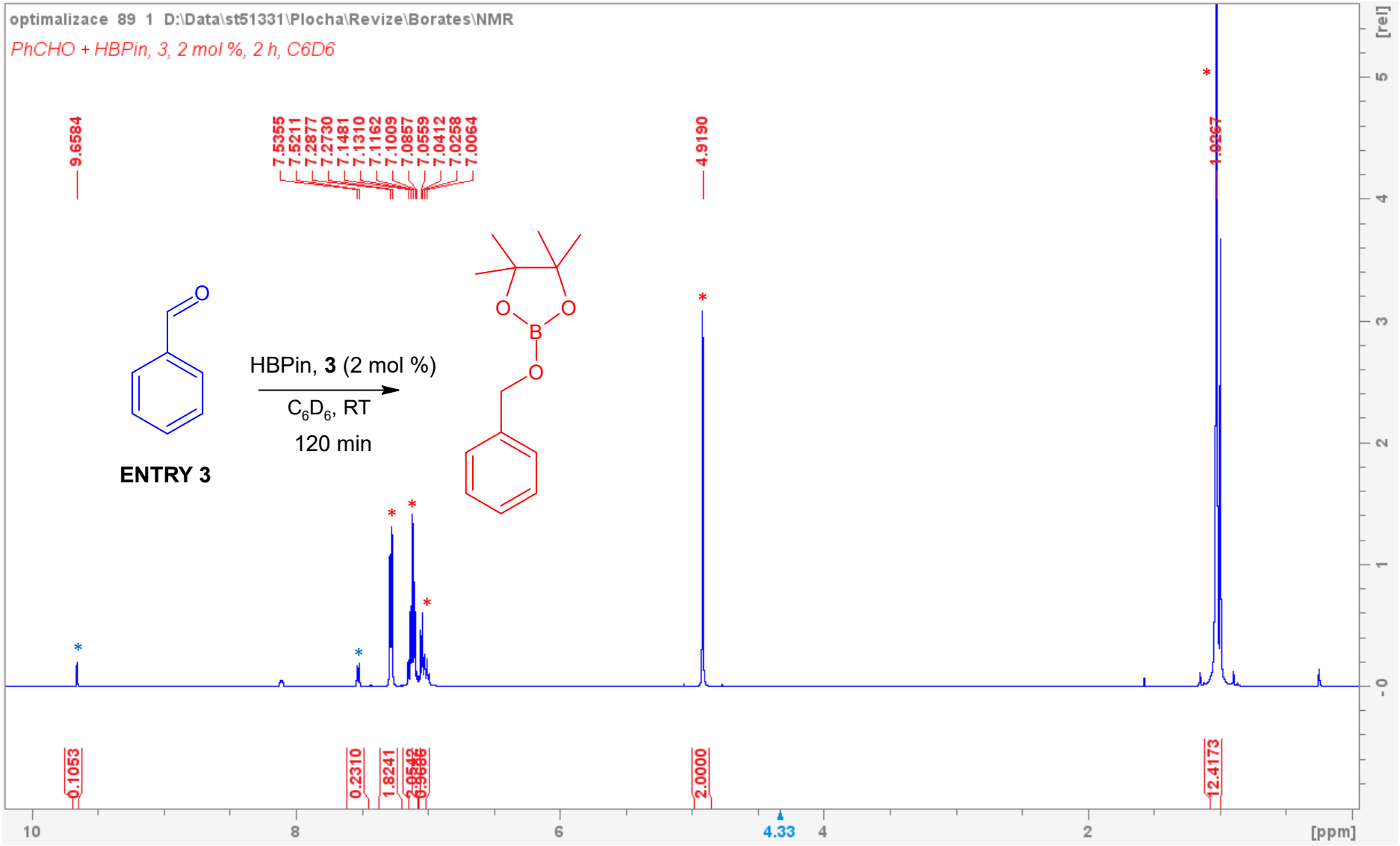

Figure S3. Entry 3: Reaction mixture. Benzaldehyde + HBPin, catalyst **3** (2 mol %), 2 h, RT, C_6D_6.

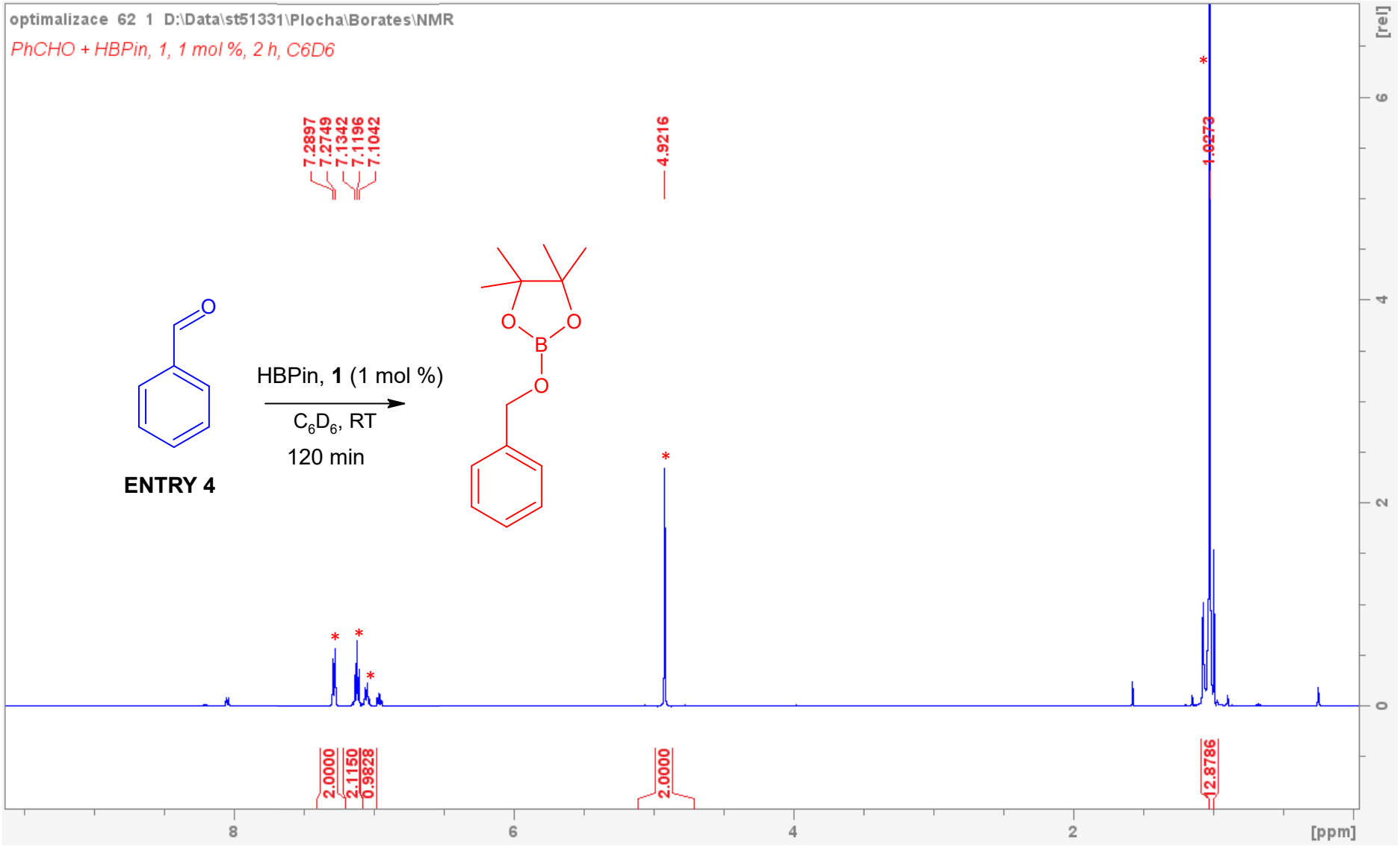

Figure S4. Entry 4: Reaction mixture. Benzaldehyde + HBPin, catalyst **1** (1 mol %), 2 h, RT, C_6D_6.

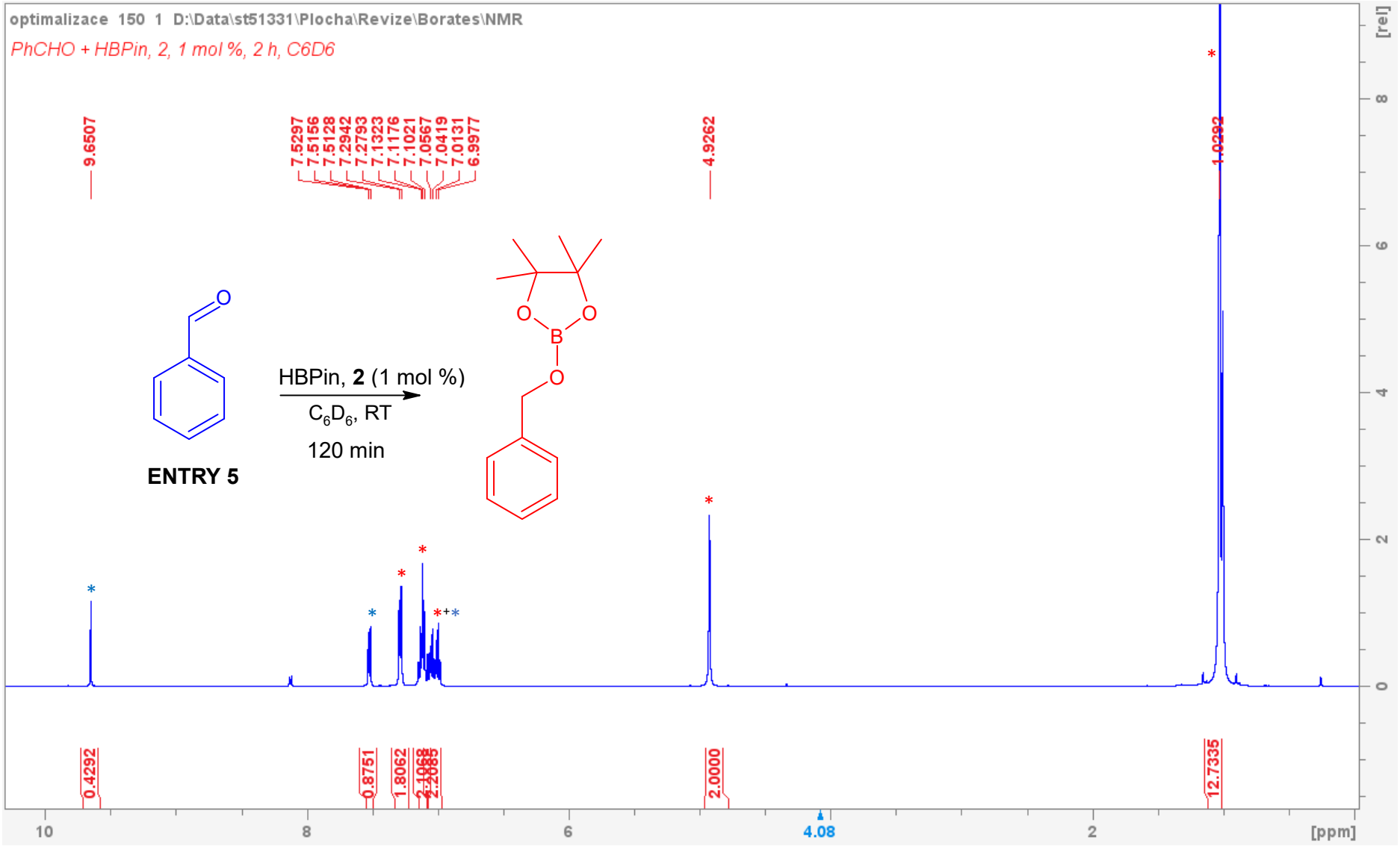

Figure S5. Entry 5: Reaction mixture. Benzaldehyde + HBPin, catalyst **2** (1 mol %), 2 h, RT, C_6D_6.

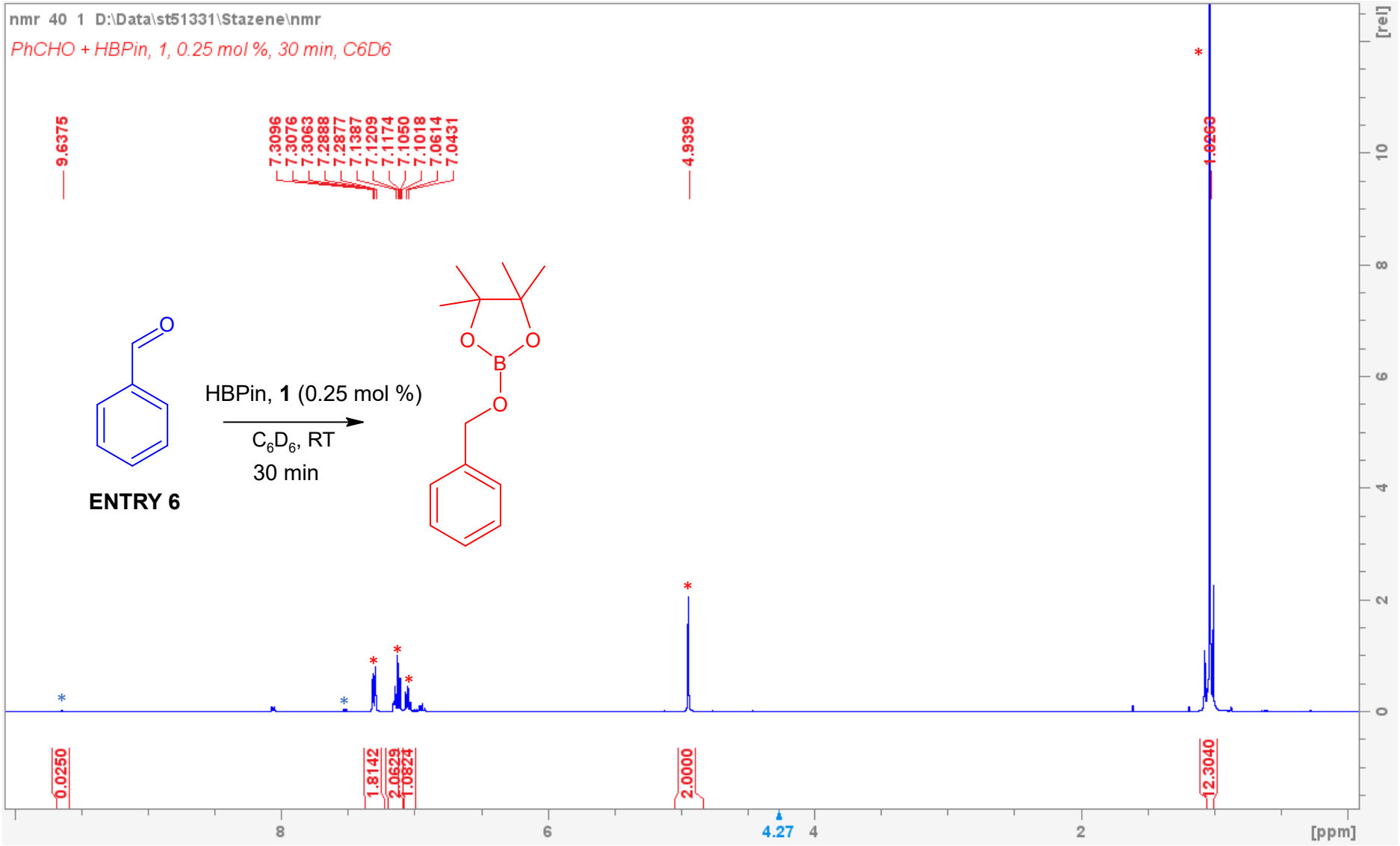

Figure S6. Entry 6: Reaction mixture. Benzaldehyde + HBPin, catalyst **1** (0.25 mol %), 30 min, RT, C_6D_6. Conversion >95 %.

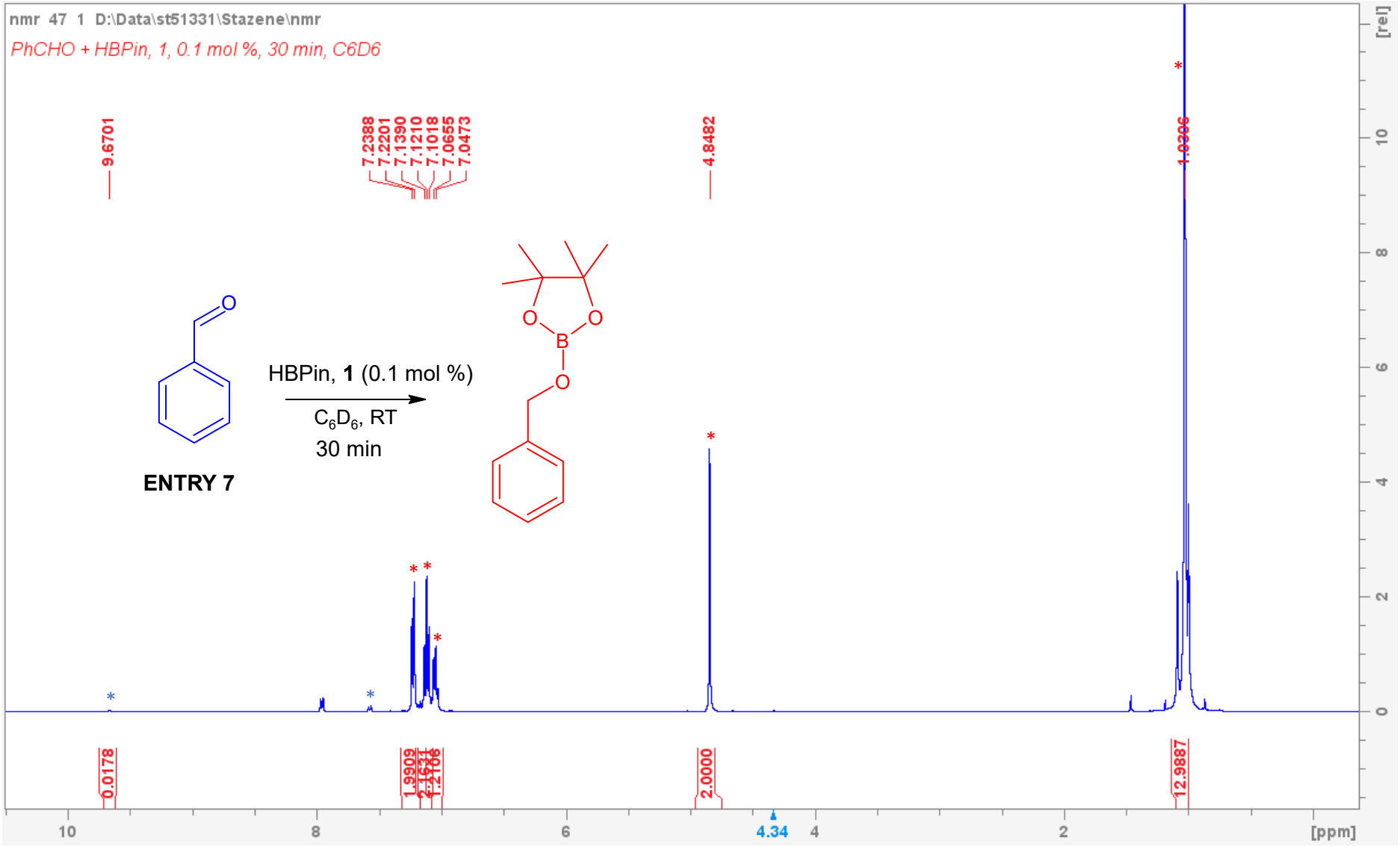

Figure S7. Entry 7: Reaction mixture. Benzaldehyde + HBPin, catalyst **1** (0.1 mol %), 30 min, RT, C_6D_6. Conversion >95 %.

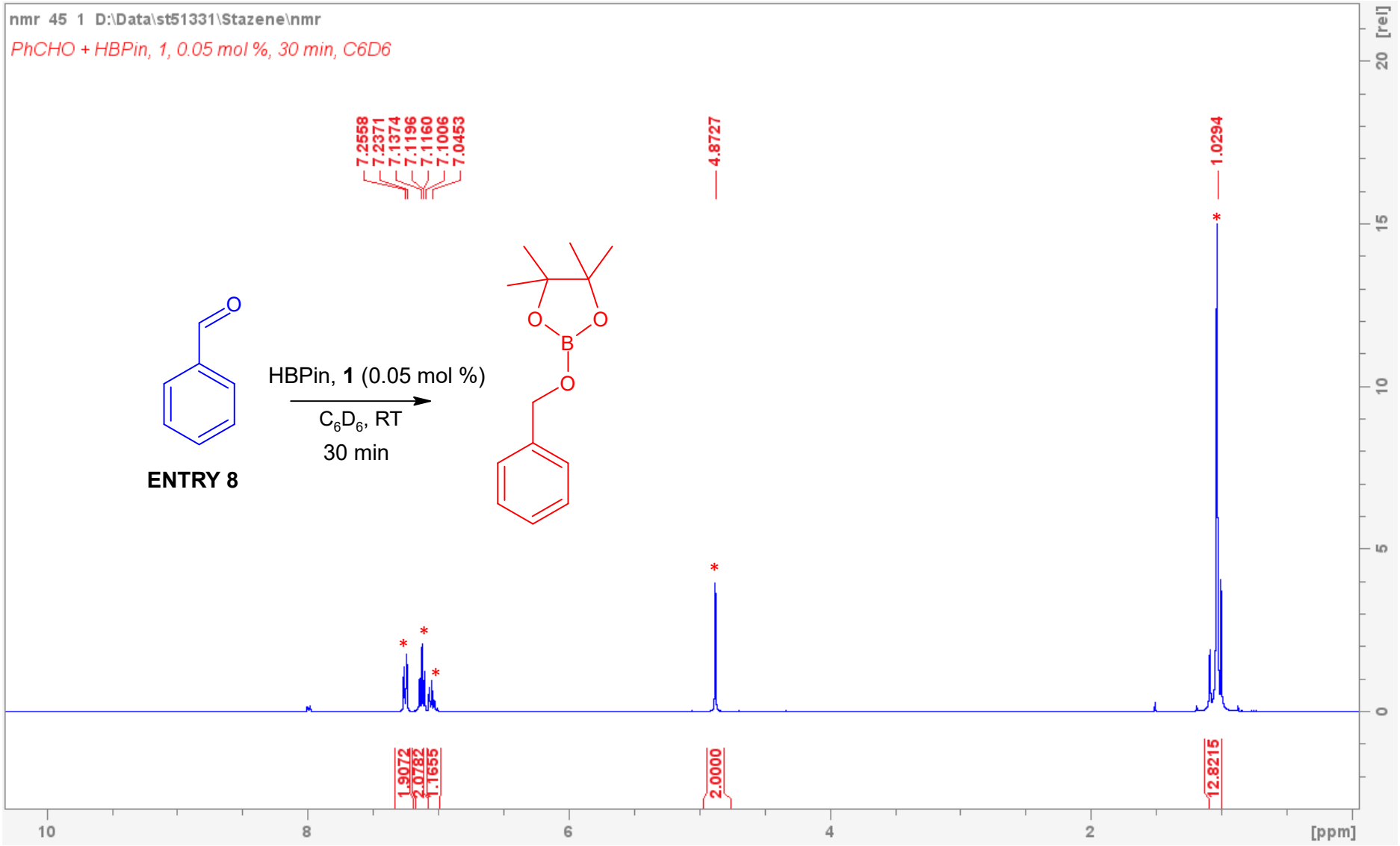

Figure S8. Entry 8: Reaction mixture. Benzaldehyde + HBPin, catalyst **1** (0.05 mol %), 30 min, RT, C_6D_6. Conversion >95 %.

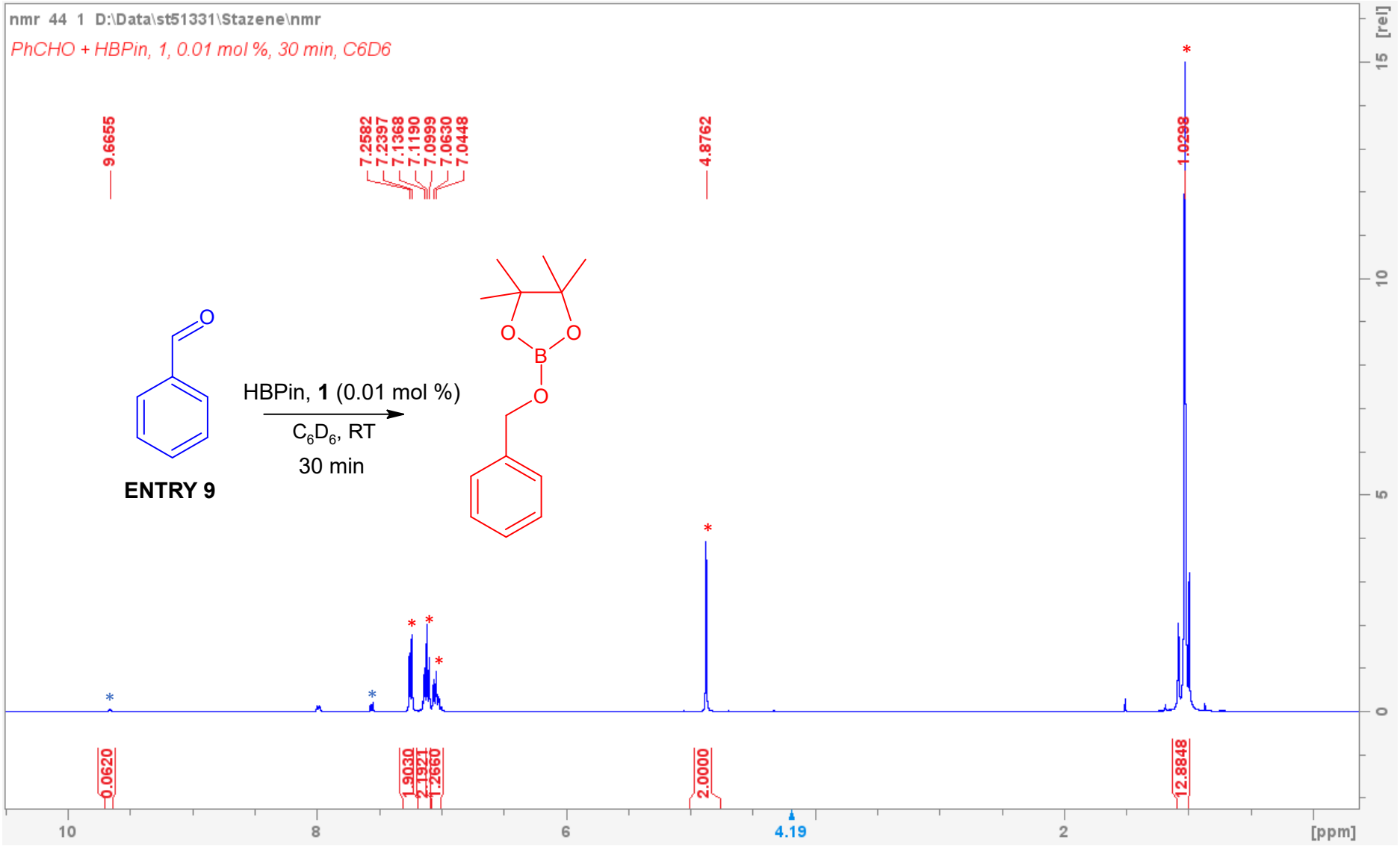

Figure S9. Entry 9: Reaction mixture. Benzaldehyde + HBPin, catalyst **1** (0.01 mol %), 30 min, RT, C_6D_6. Conversion 94 %.

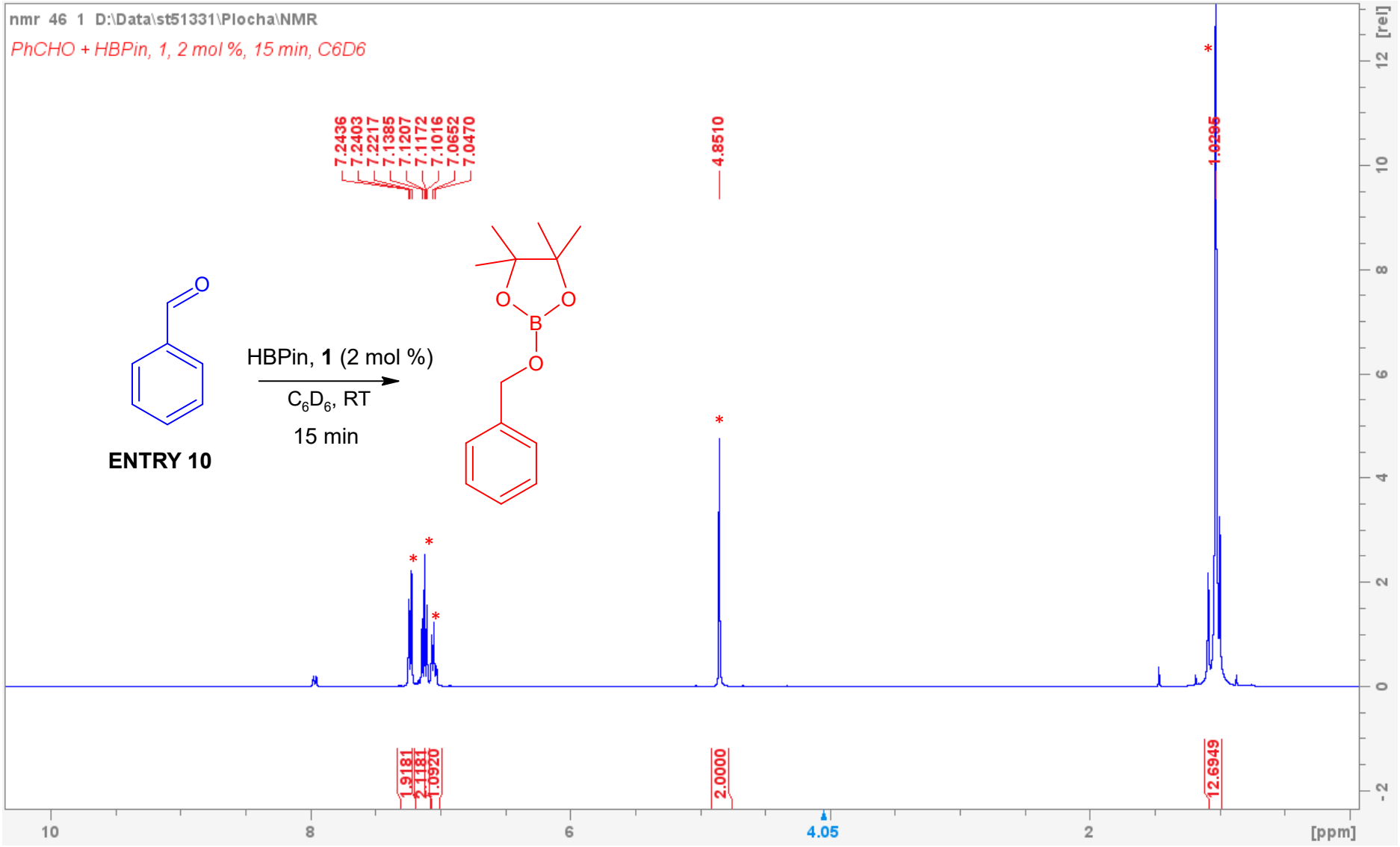

Figure S10. Entry 10: Reaction mixture. Benzaldehyde + HBPin, catalyst **1** (2 mol %), 15 min, RT, C_6D_6. Conversion 99 %.

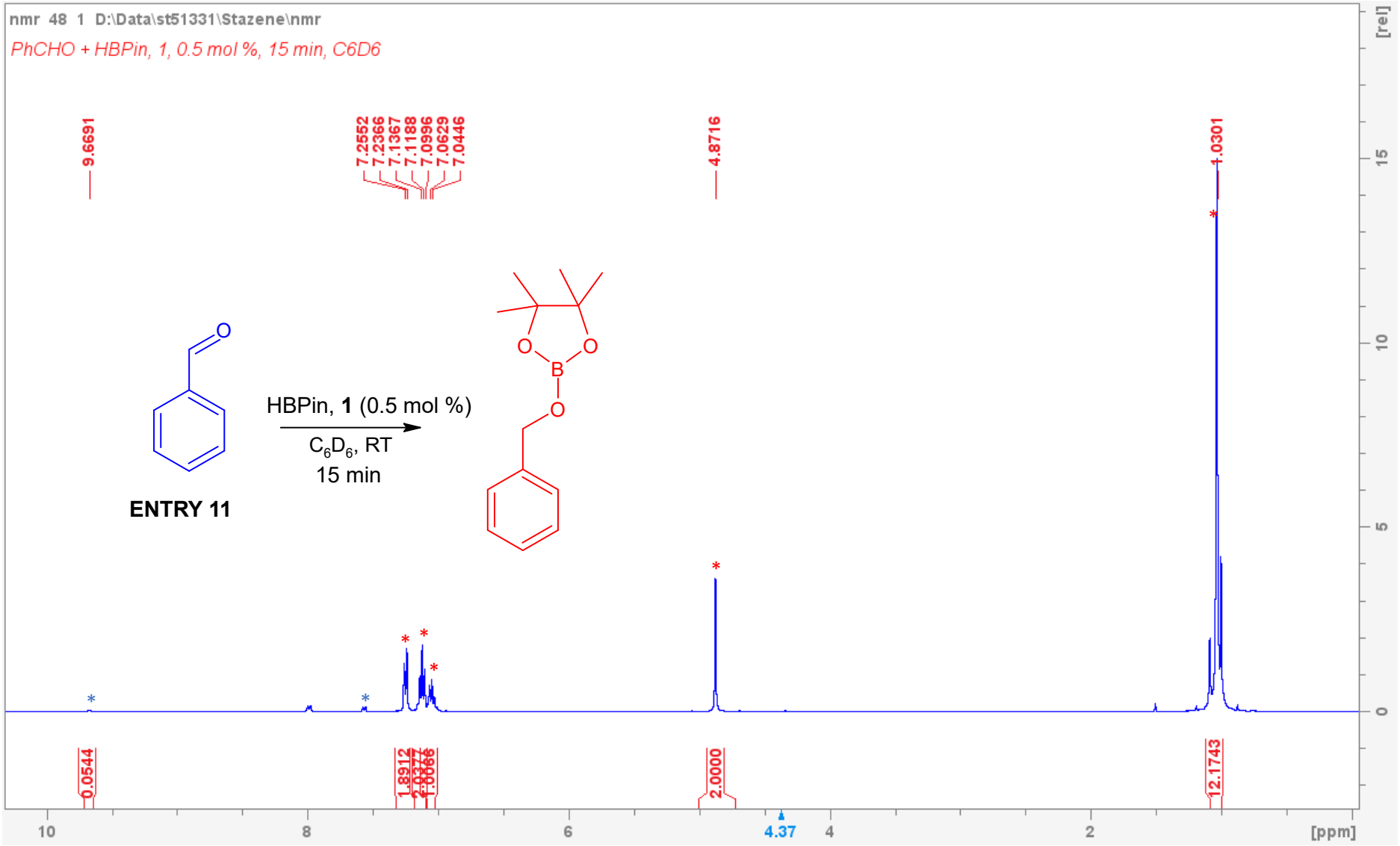

Figure S11. Entry 11: Reaction mixture. Benzaldehyde + HBPin, catalyst **1** (0.5 mol %), 15 min, RT, C_6D_6. Conversion >95 %.

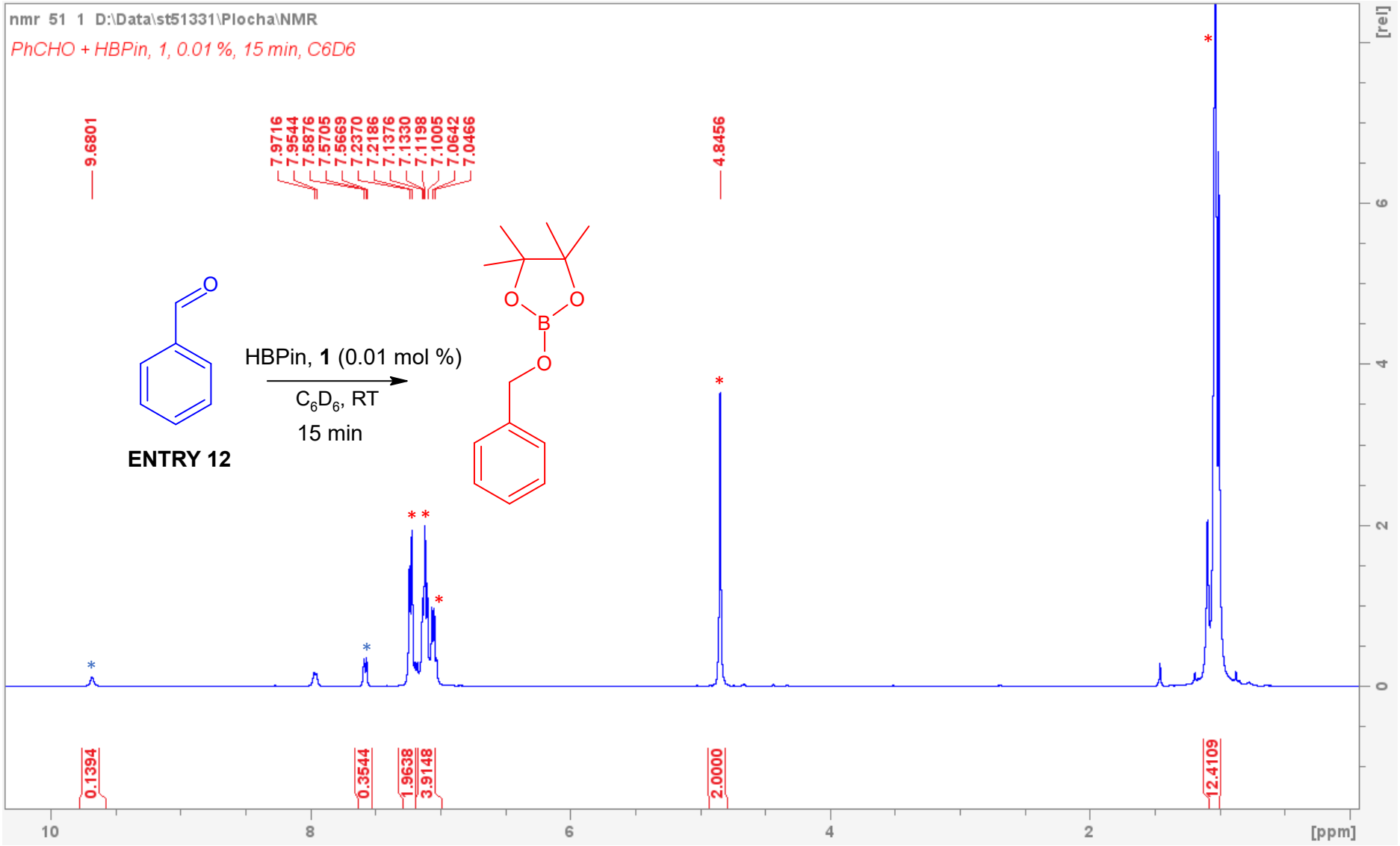

Figure S12. Entry 12: Reaction mixture. Benzaldehyde + HBPin, catalyst **1** (0.01 mol %), 15 min, RT, C_6D_6. Conversion 88 %.

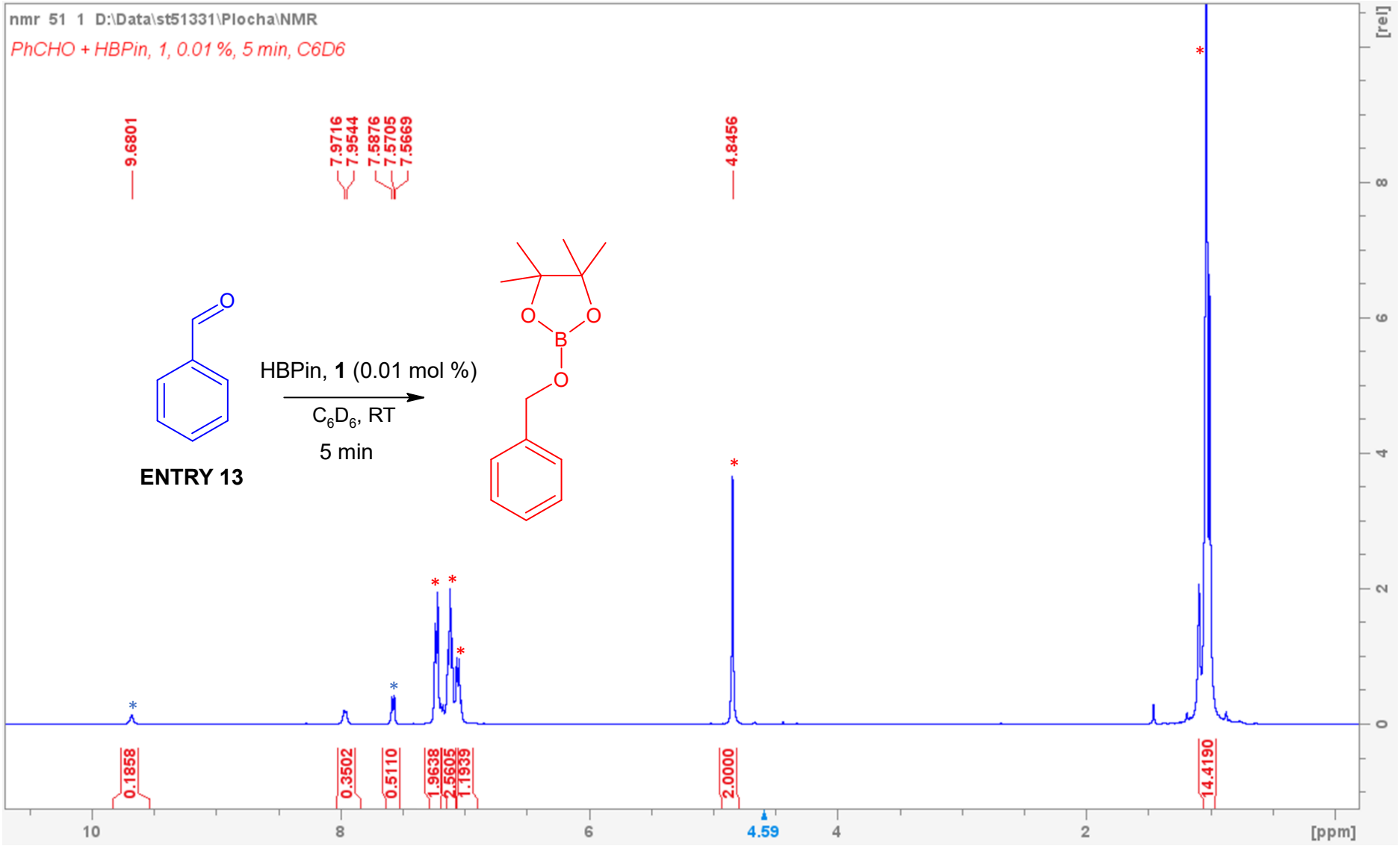

Figure S13. Entry 13: Reaction mixture. Benzaldehyde + HBPin, catalyst **1** (0.01 mol %), 5 min, RT, C_6D_6. Conversion 84 %.

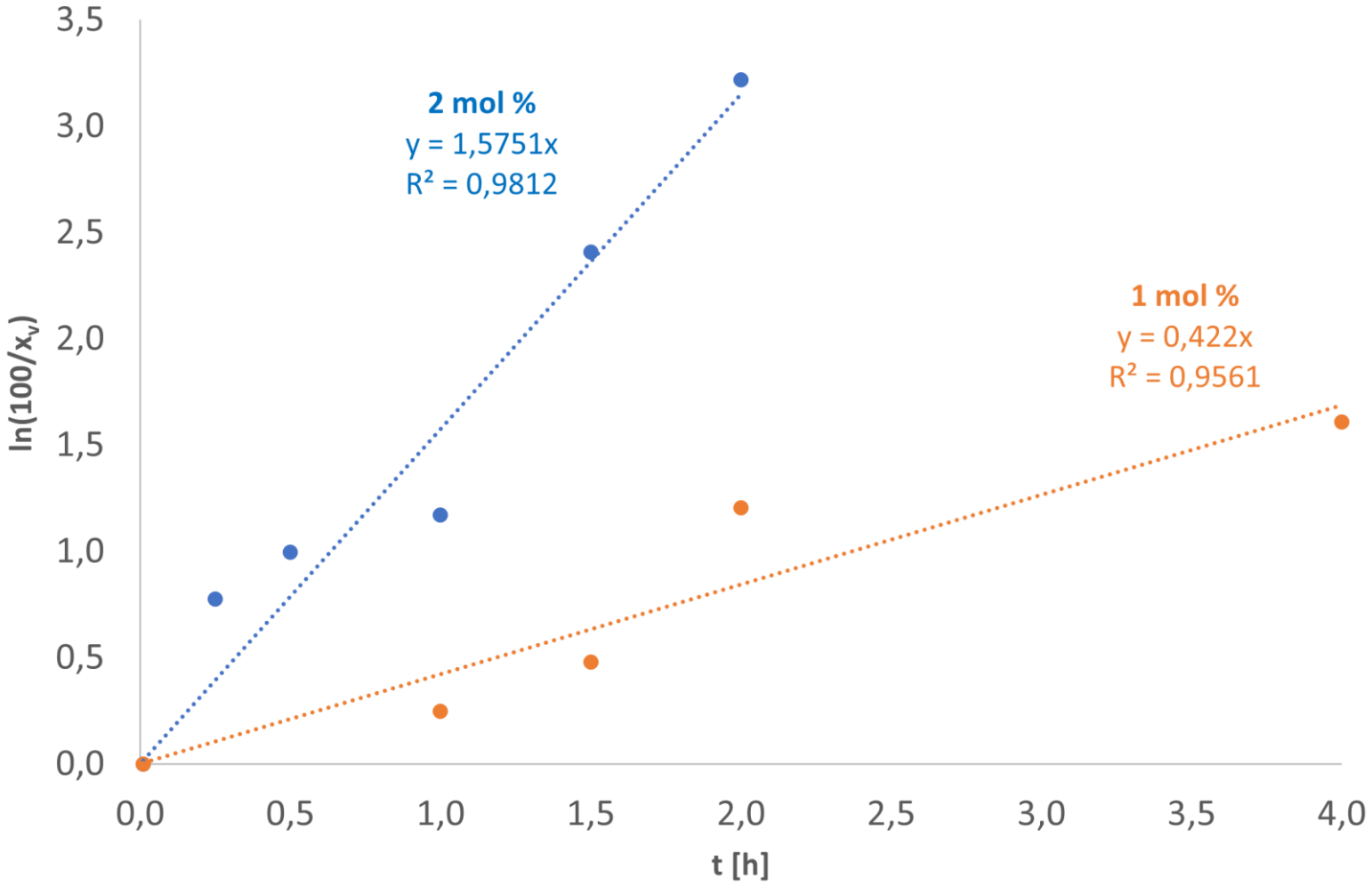

Figure S14. Conversion of benzaldehyde during hydroboration catalysed by **2** (2 mol %, 2 h; 1 mol %, 4 h**)**. ^{1}H NMR study (C_6D_6).

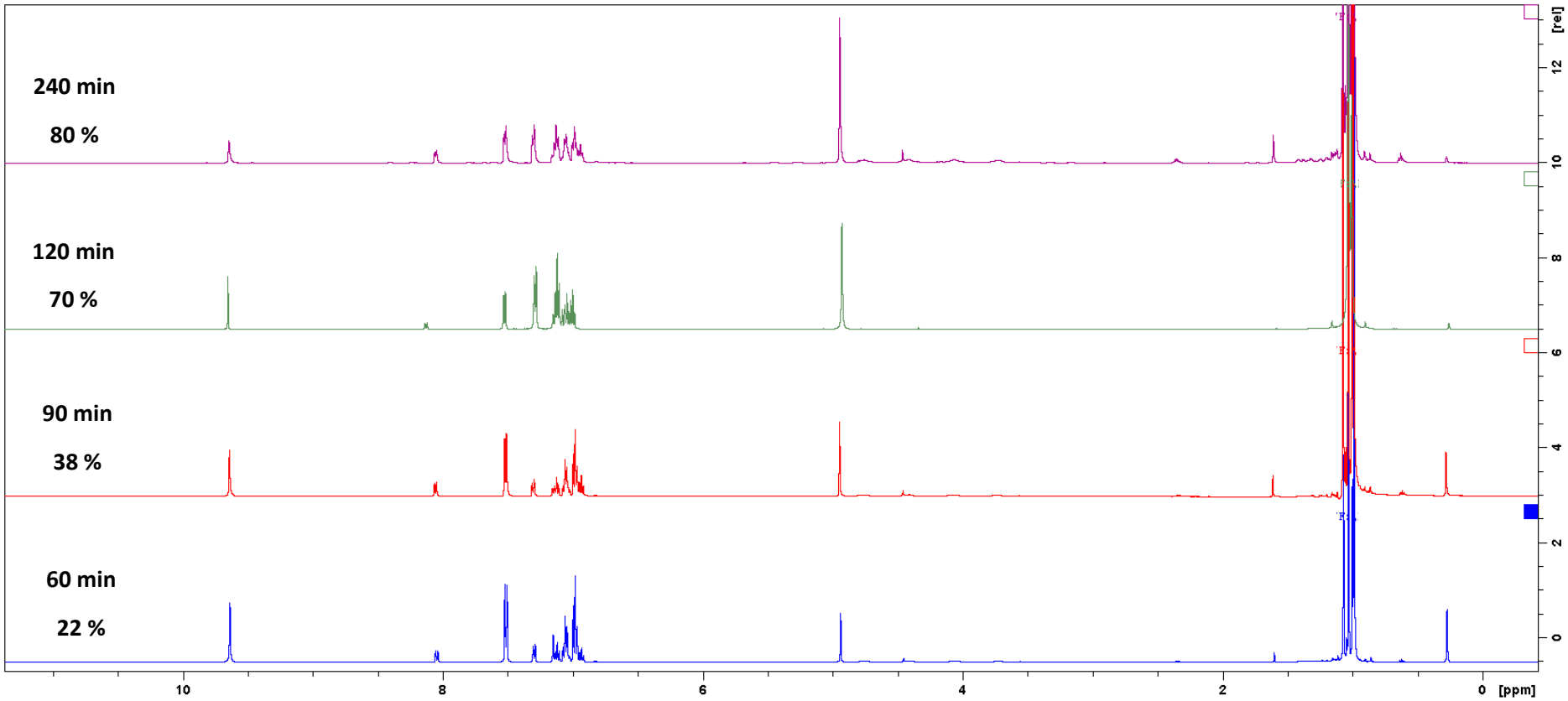

Figure S15. NMR kinetic study of benzaldehyde hydroboration catalysed by **2** (1 mol %), 60–240 min, C_6D_6. Each spectrum represents independent reaction.

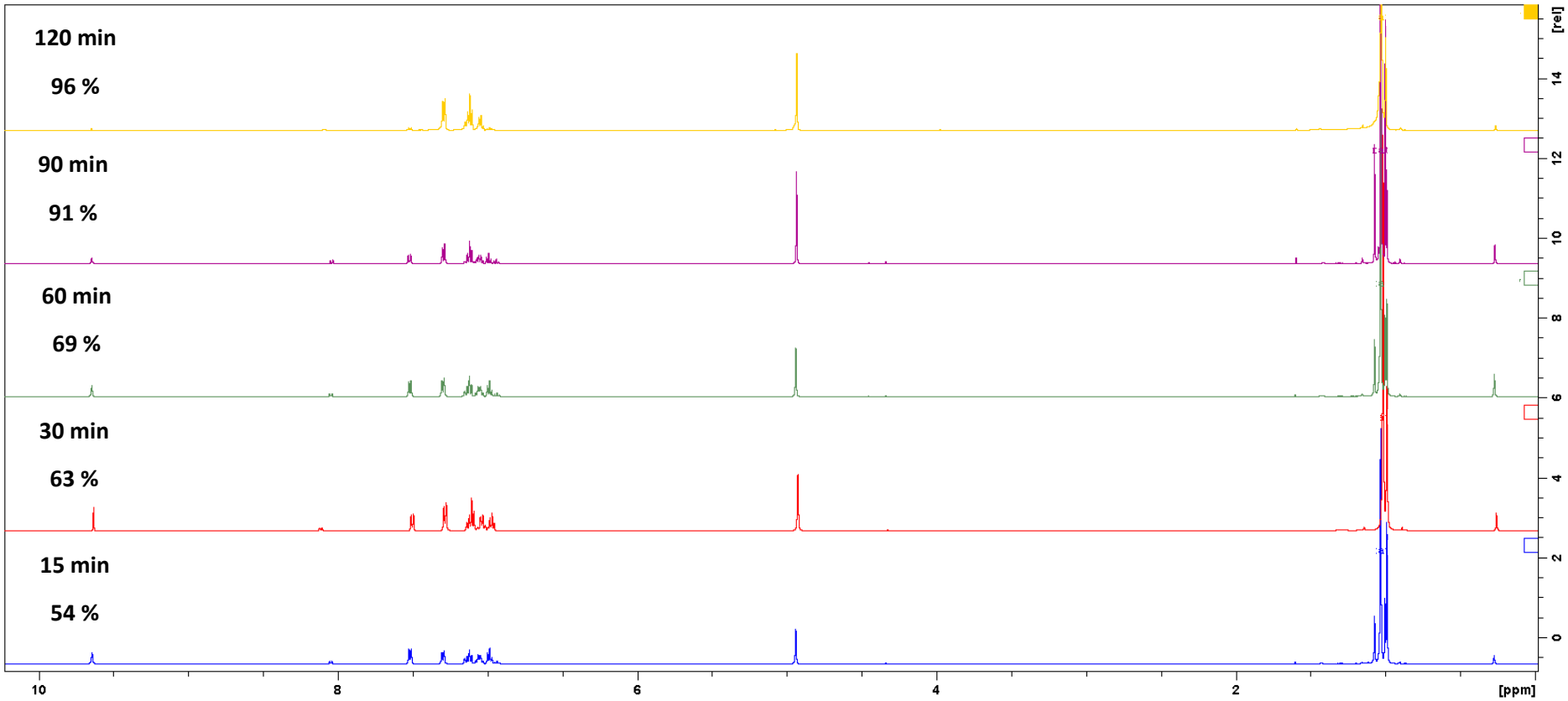

Figure S16. NMR kinetic study of benzaldehyde hydroboration catalysed by **2** (2 mol %), 15–120 min, C_6D_6. Each spectrum represents independent reaction.

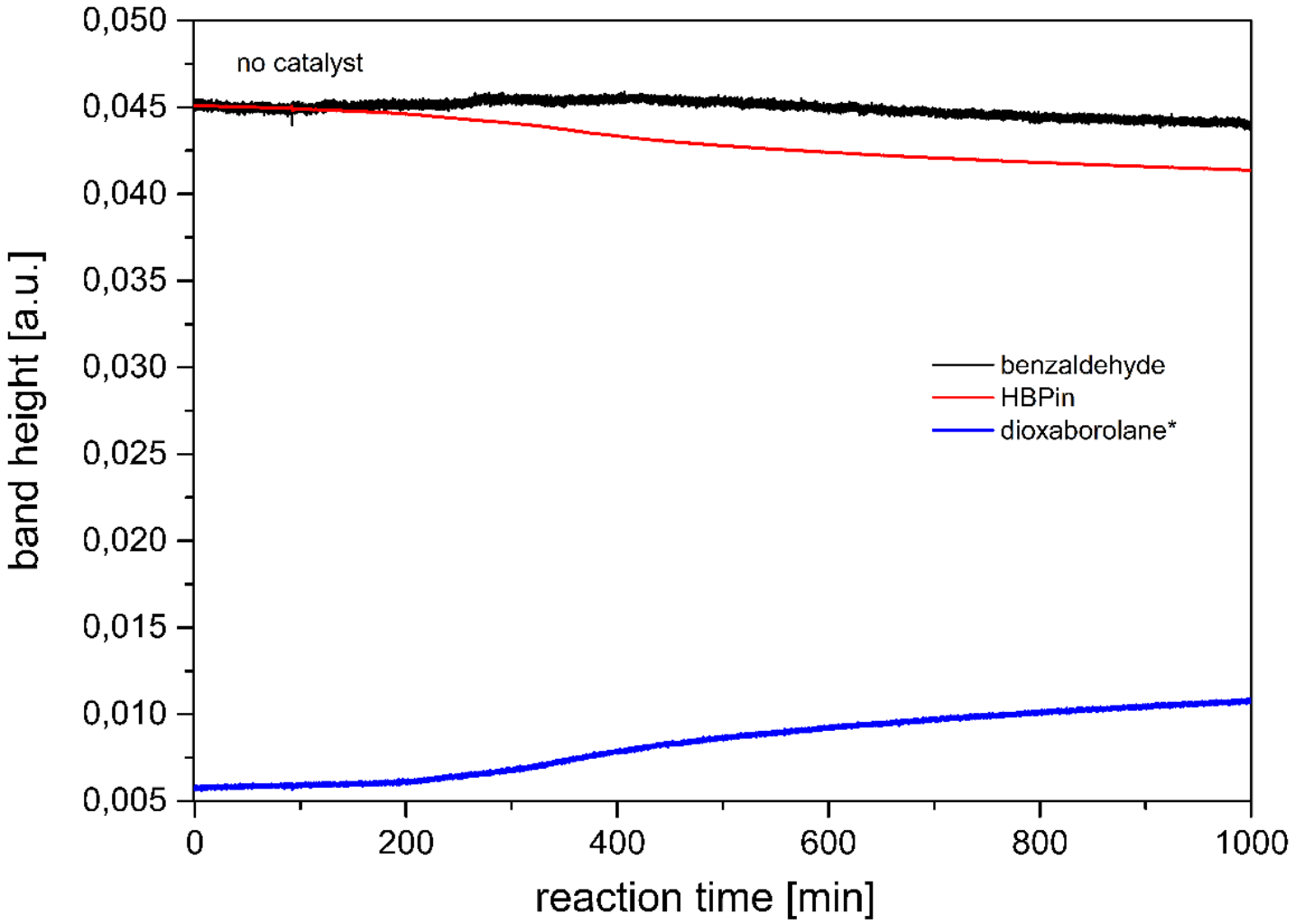

Figure S17. Time-dependent changes in IR spectra in the mixture of benzaldehyde (0.5 mmol) and HBPin (0.5 mmol) in benzene (5 mL). * Observed decrease in the concentration of HBPin is due to slow hydrolysis yielding pinacolboronic acid containing dioxaborolane ring in the molecule.

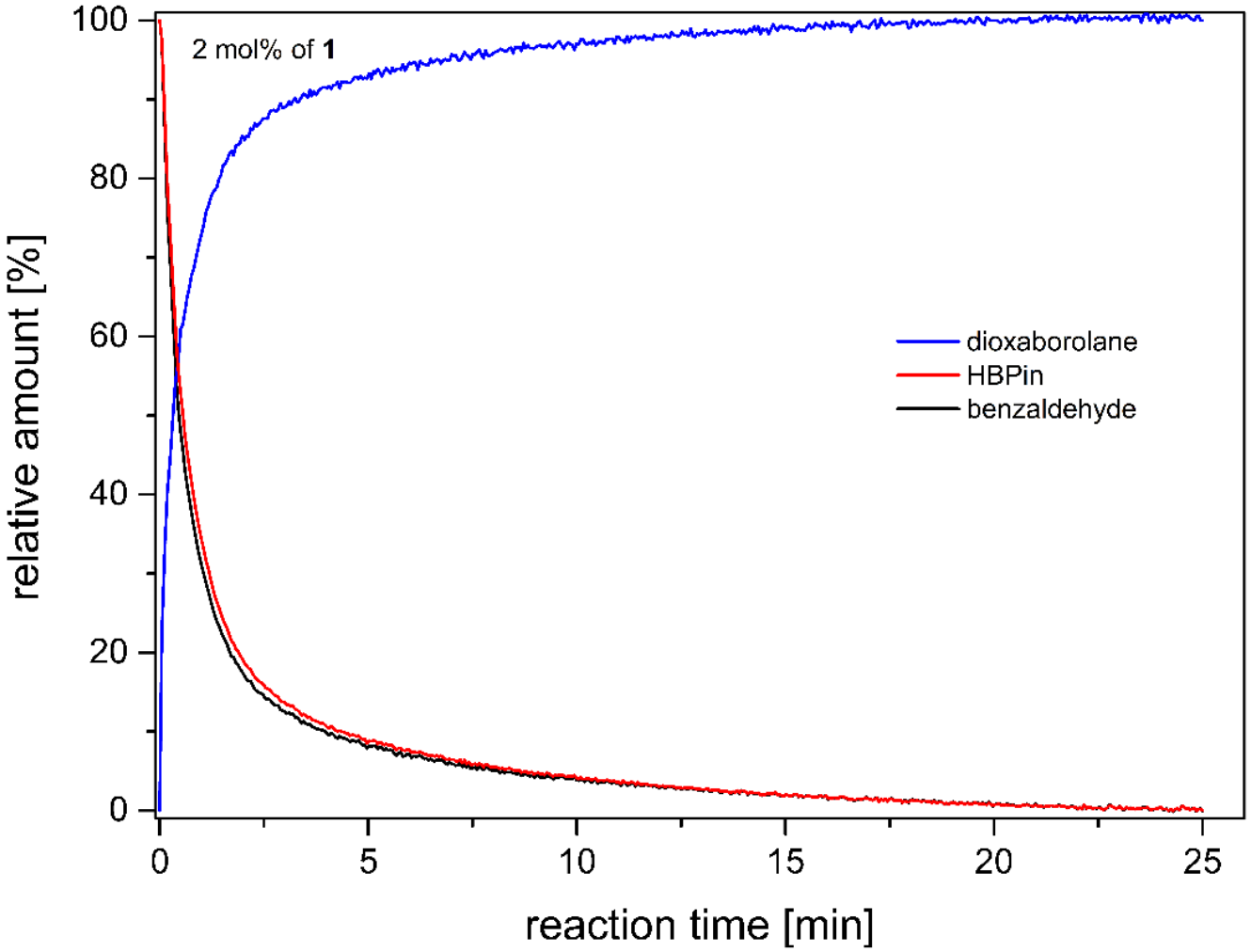

Figure S18. Changes in relative amount of monitored species in the mixture of benzaldehyde (0.5 mmol) and HBPin (0.5 mmol) in benzene (5 mL) catalysed with 2 mol % of **1**.

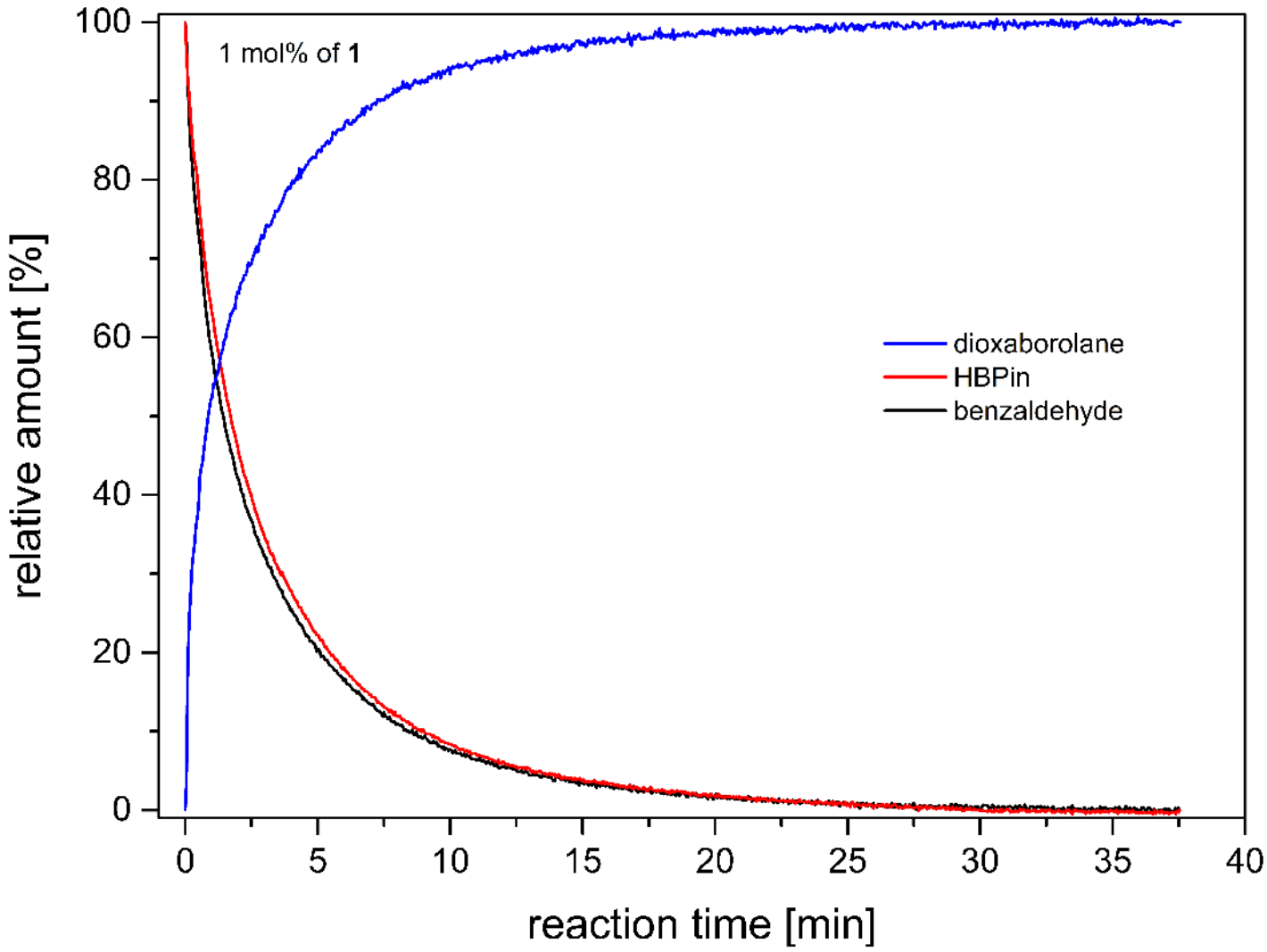

Figure S19. Changes in relative amount of monitored species in the mixture of benzaldehyde (0.5 mmol) and HBPin (0.5 mmol) in benzene (5 mL) catalysed with 1 mol % of **1.**

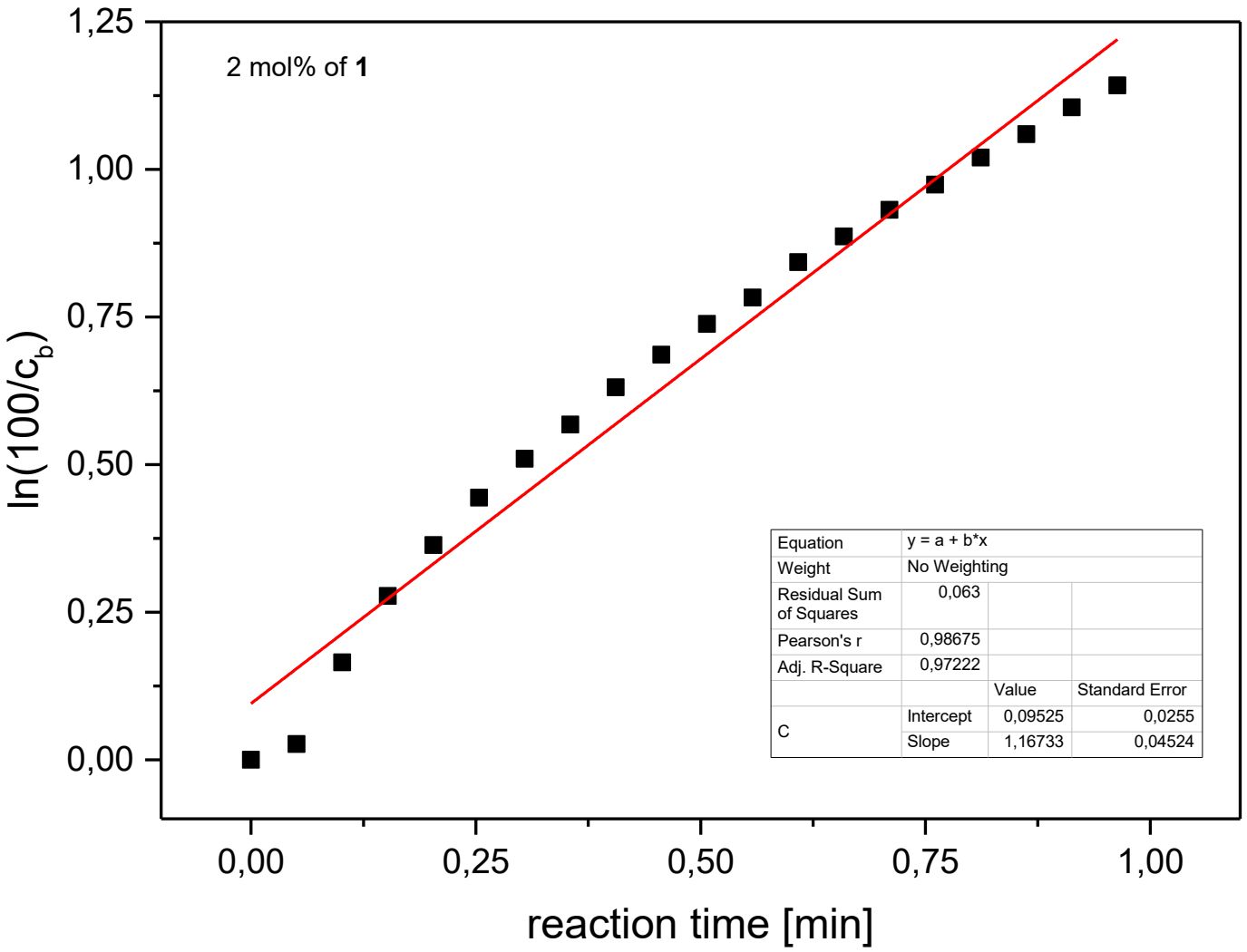

Figure S20. Determination of rate constant for benzaldehyde hydroboration catalysed with 2 mol % of **1.**

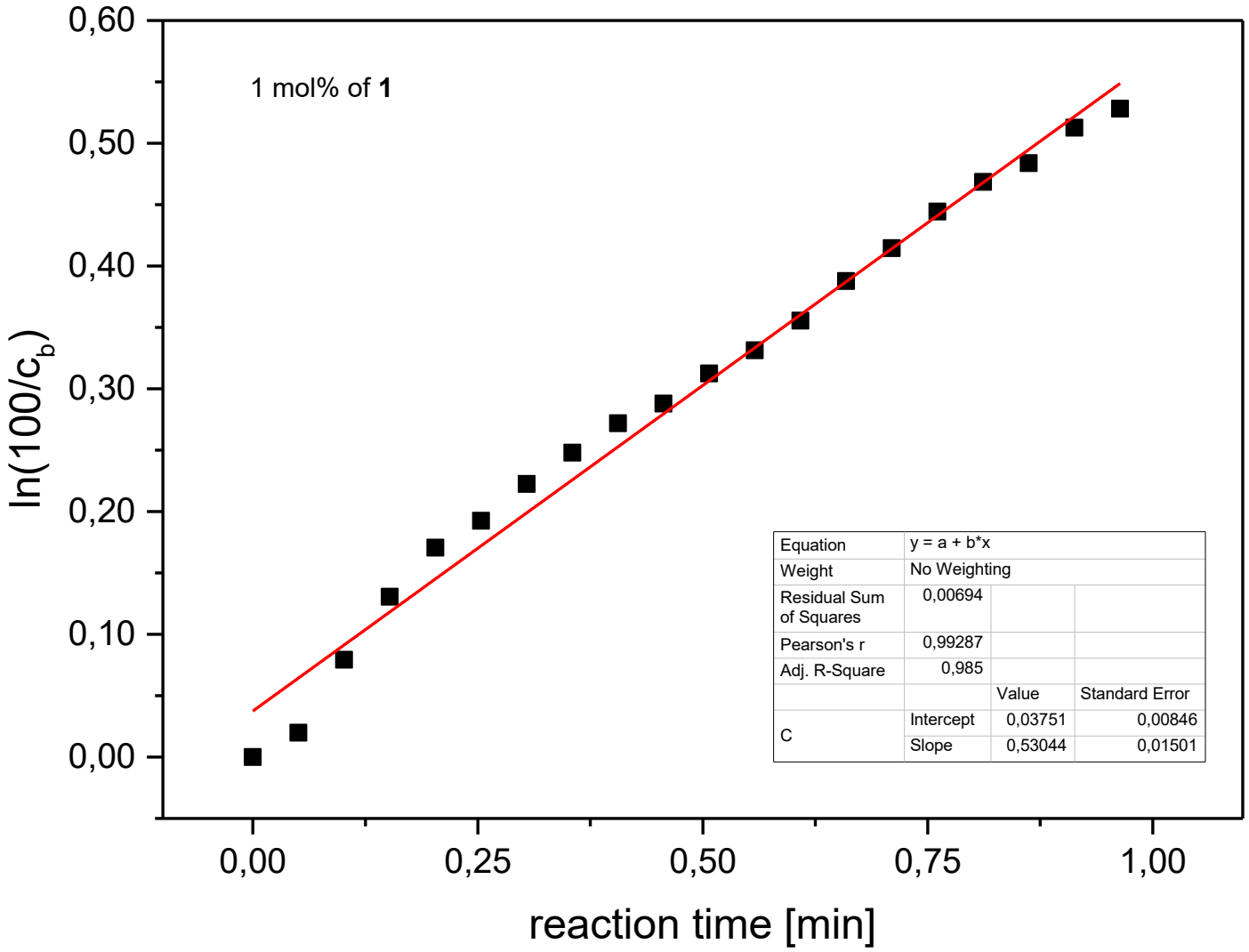

Figure S21.Determination of rate constant for benzaldehyde hydroboration catalysed with 1 mol % of **1.**

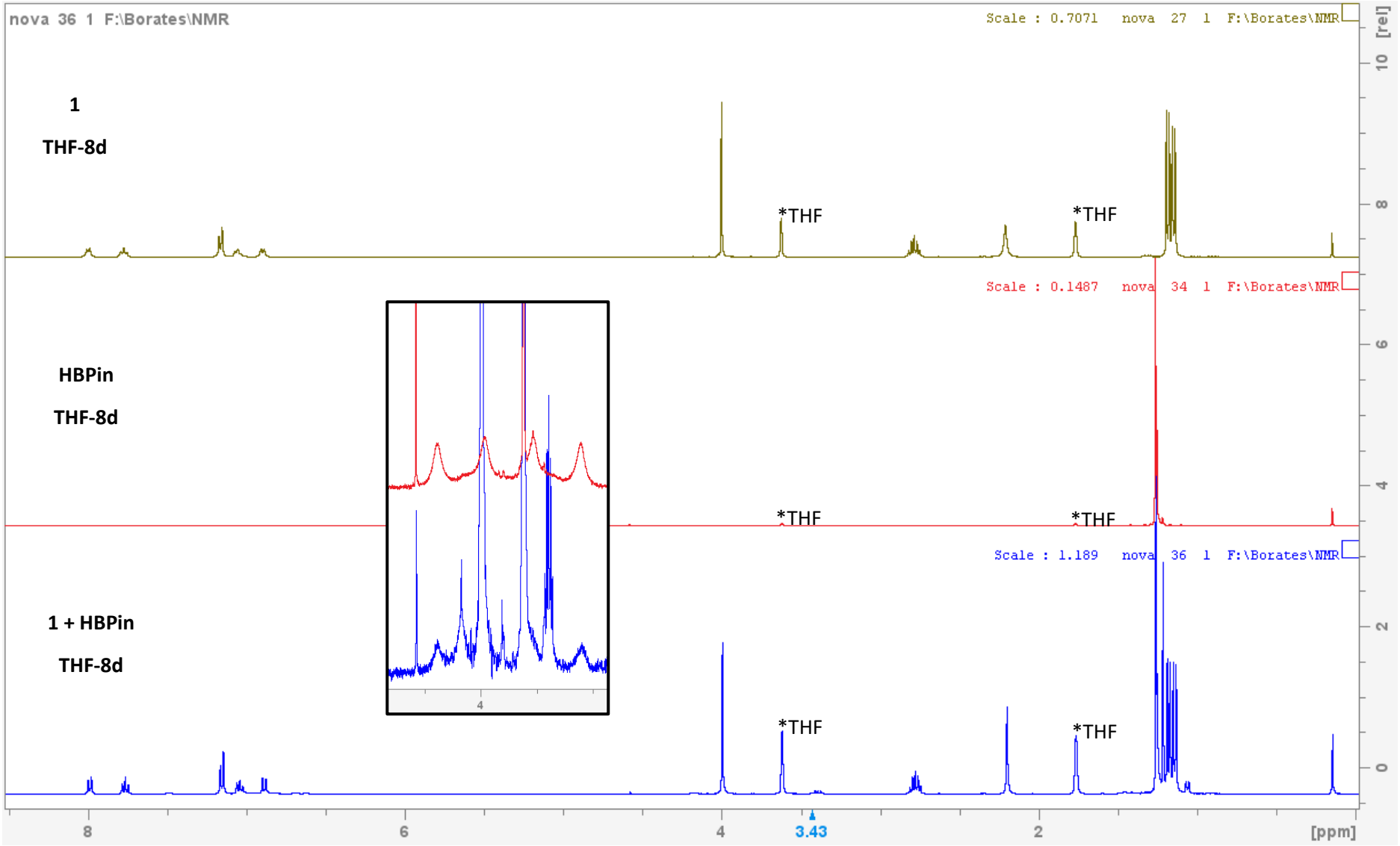

Figure S22. ^{1}H NMR (THF-8d, 500.13 MHz, 300 K) of **1**; HBPin and mixture of **1** + excess of HBPin. Detail of B*H* multiplet.

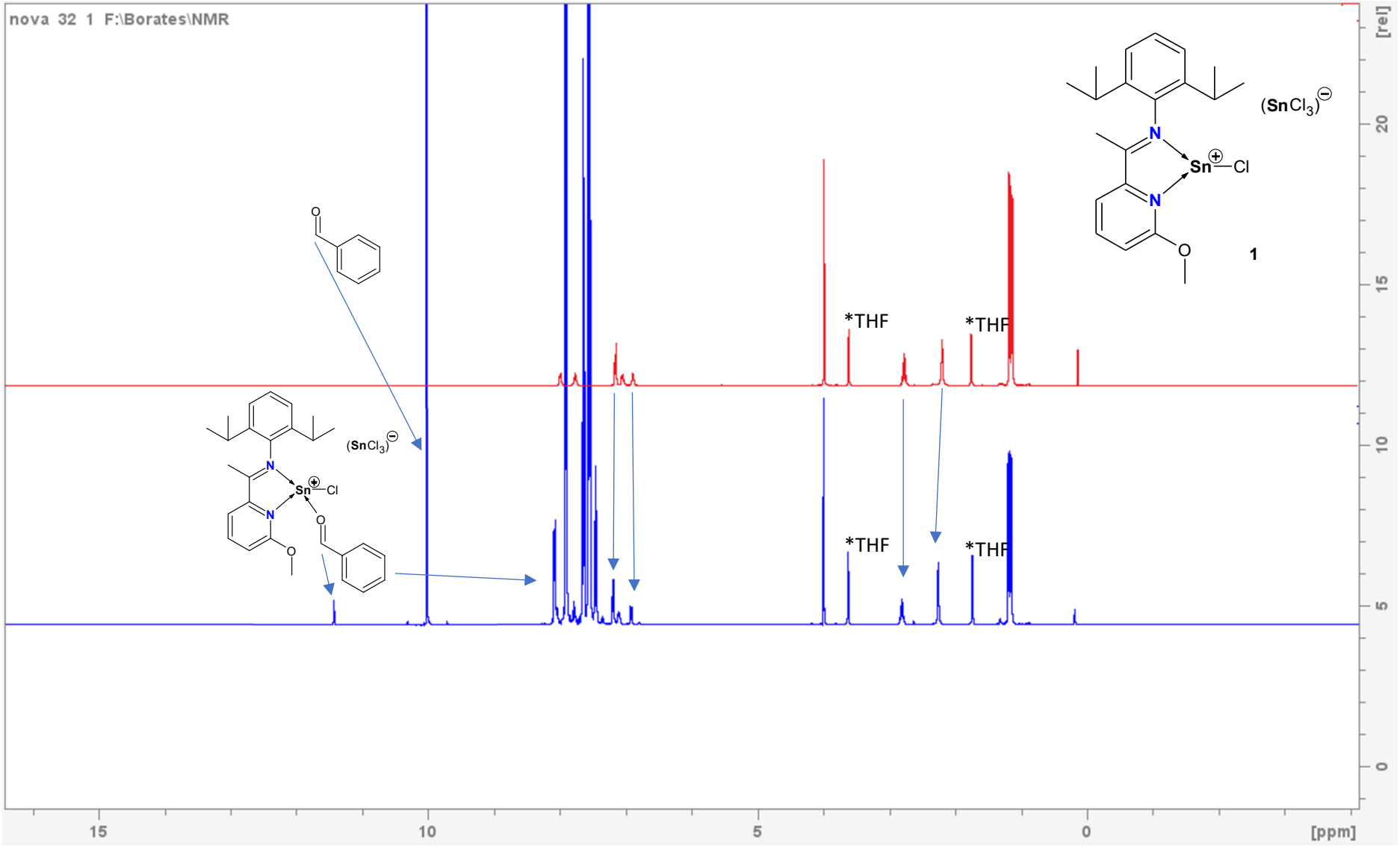

Figure S23. ^{1}H NMR (THF-8d, 500.13 MHz, 300 K) of **1** (red) and **1** + excess of PhCHO (blue).

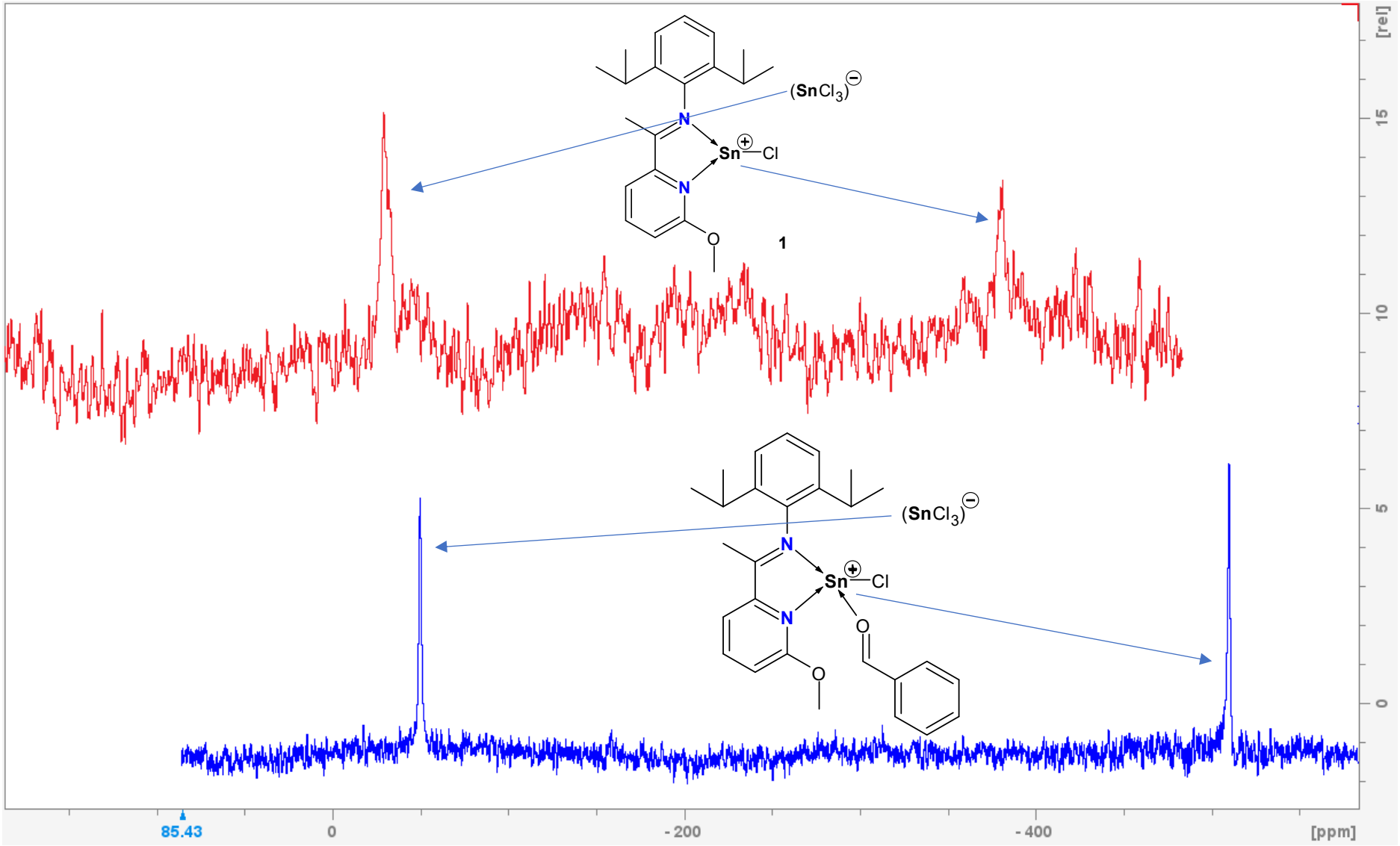

Figure S24. $^{119}Sn\{^{1}H\}$ NMR spectra of free **1** (THF-8d, 500.13 MHz, 300 K) and **1** in the presence of benzaldehyde.

Substrate scope of carbonyl hydroboration catalysed by 1

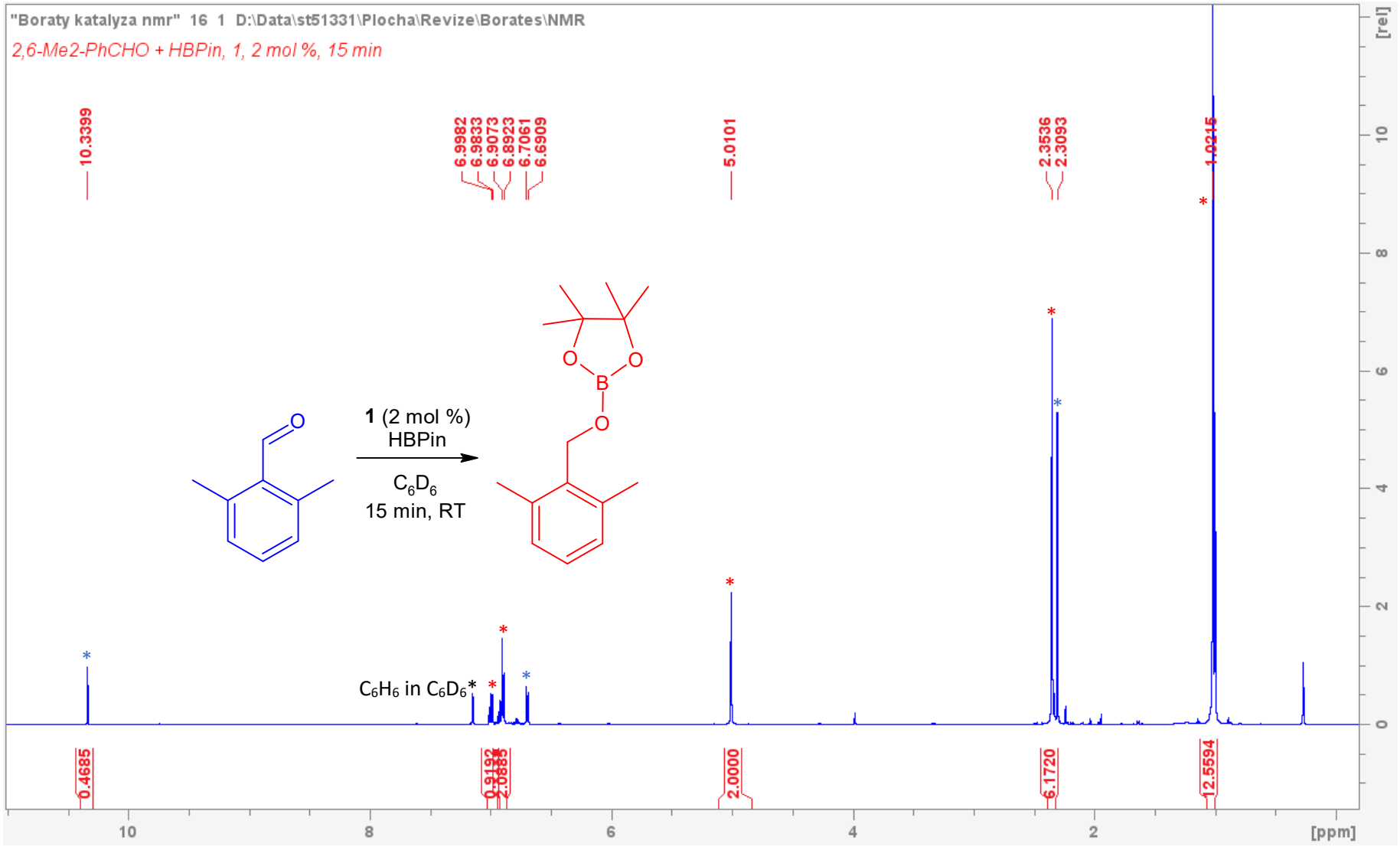

Figure S25. (***b***) Reaction mixture. 2,6-Me_2-PhCHO + HBPin, **1**, 2 mol %, 15 min, RT, C_6D_6. Conversion 68 %.

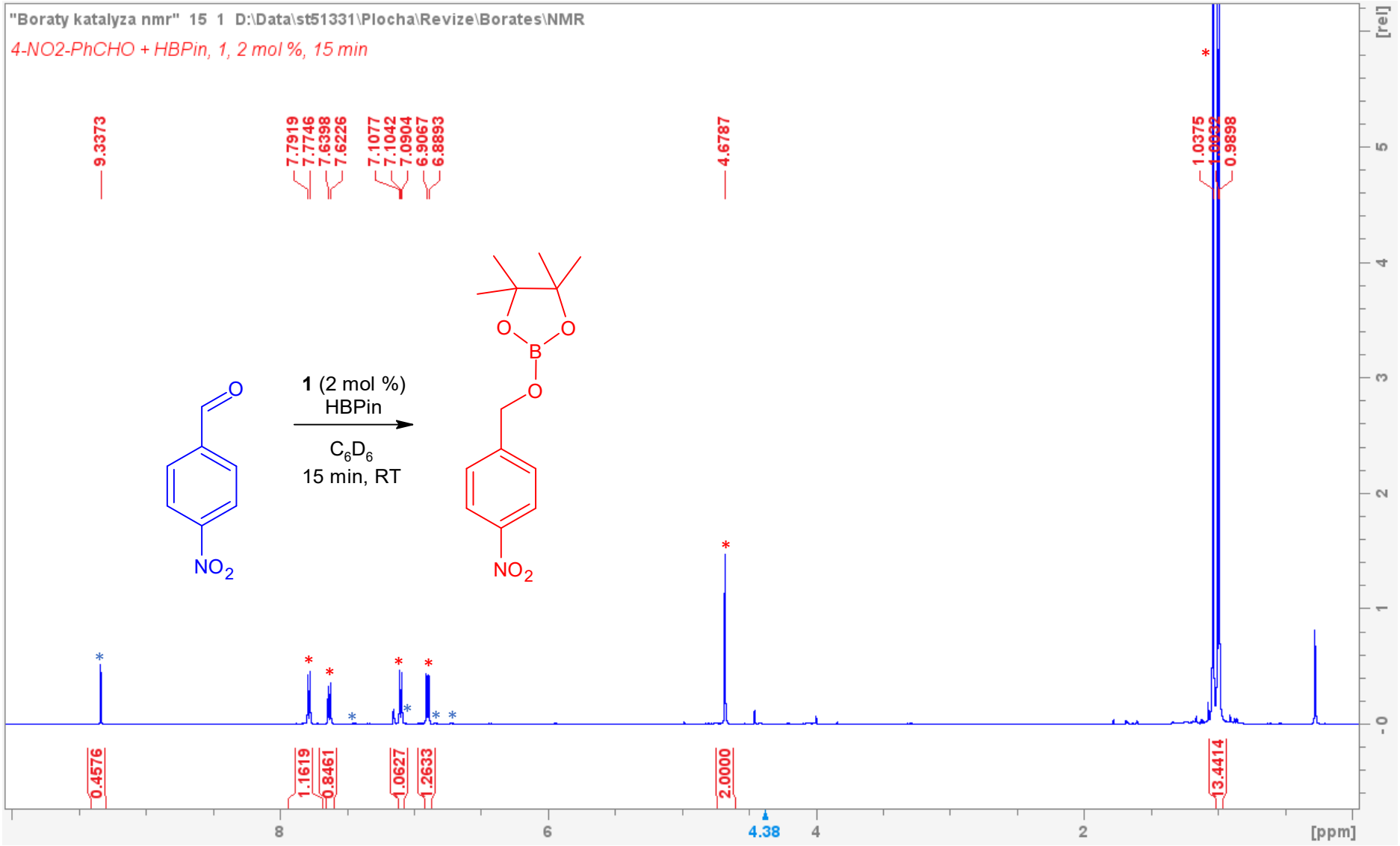

Figure S26. (*c*) Reaction mixture. 4-NO_2-PhCHO + HBPin, **1**, 2 mol %, 15 min, RT, C_6D_6. Conversion 69 %.

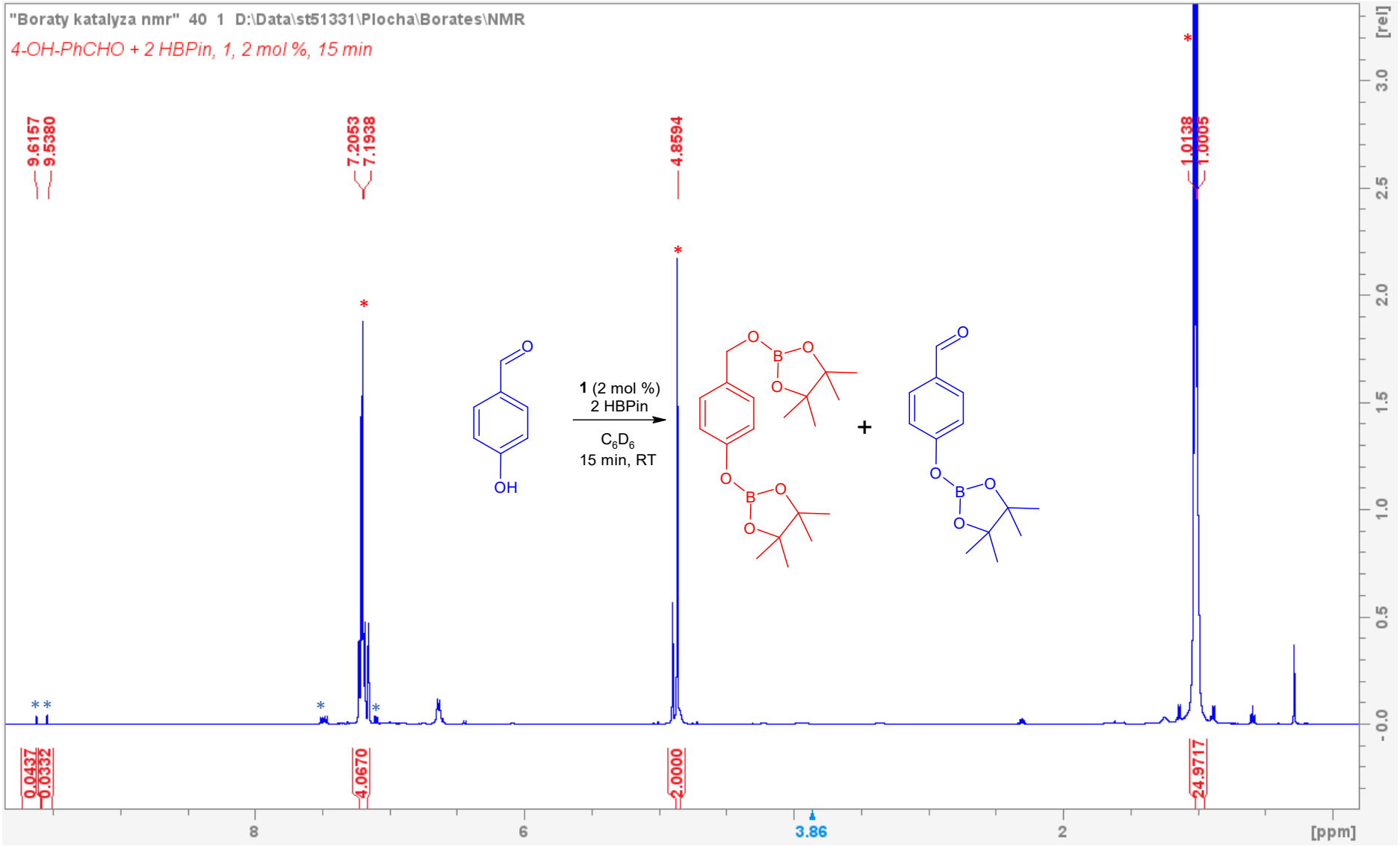

Figure S27. (***d***) Reaction mixture. 4-HO-PhCHO + 2 HBPin, **1**, 2 mol %, 15 min, RT, C_6D_6. Conversion 99 %.

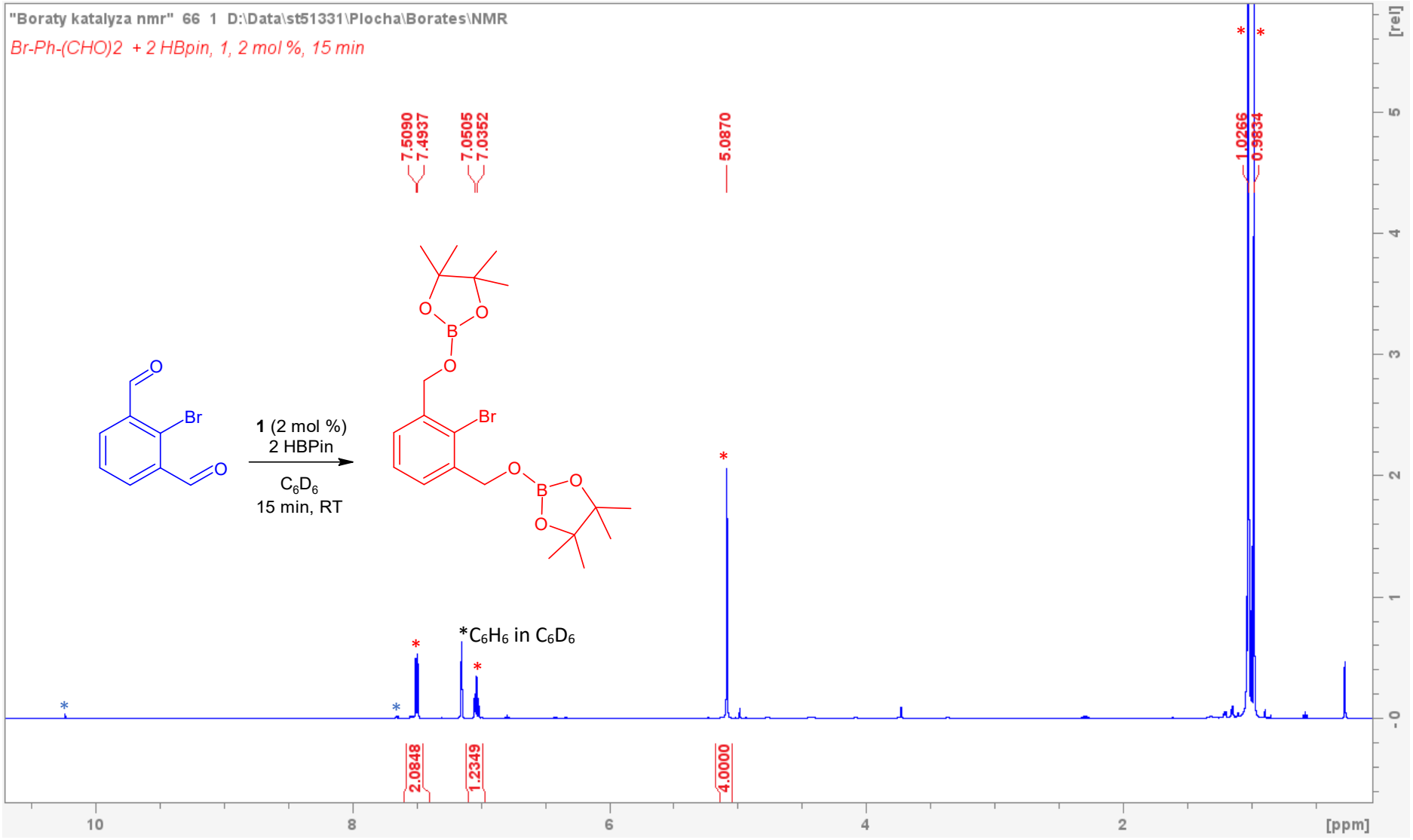

Figure S28. (*e*) Reaction mixture. 6-Br-Ph-1,5-$(CHO)_2$ + 2 HBPin, **1**, 2 mol %, 15 min, RT, C_6D_6. Conversion 99 %.

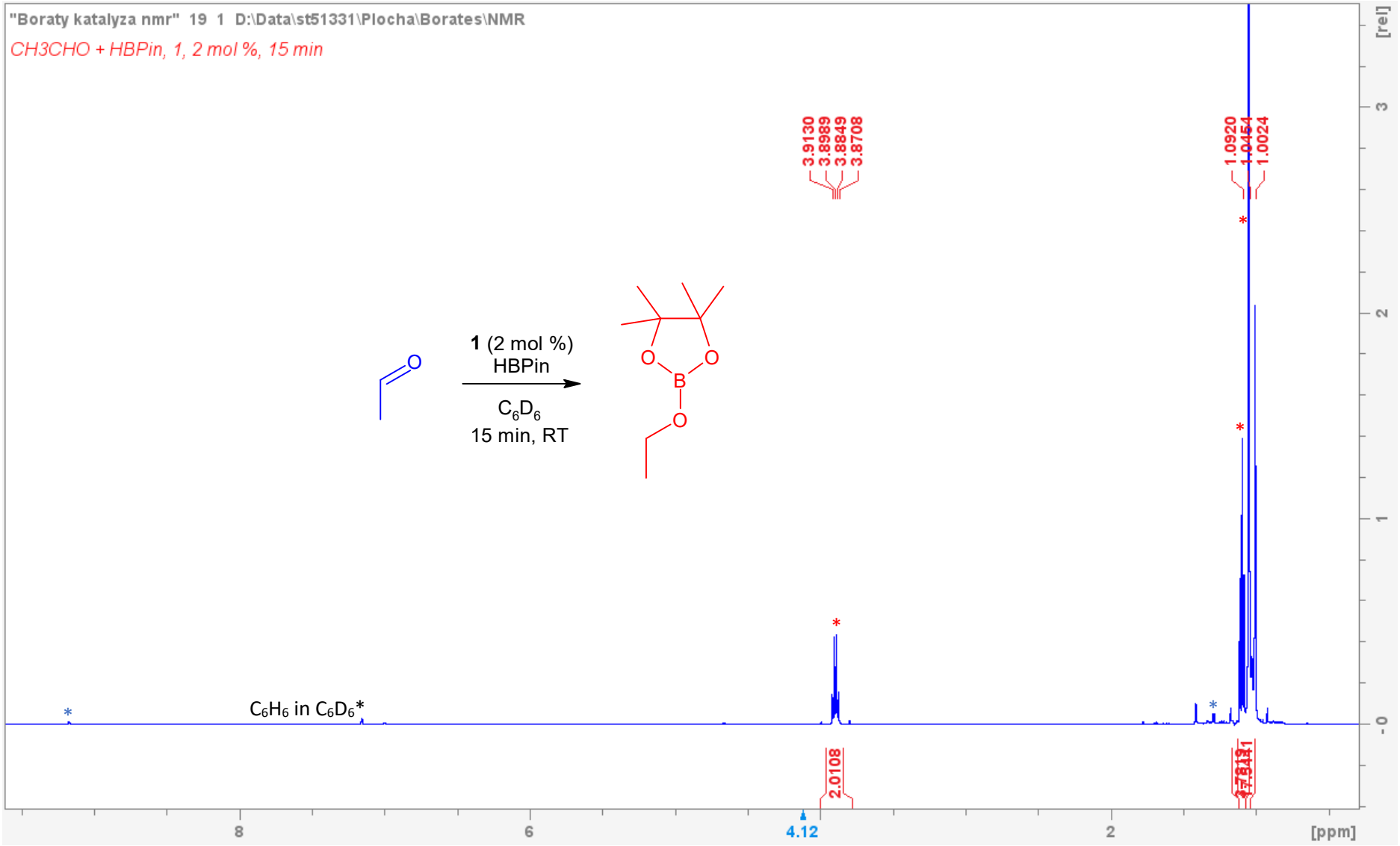

Figure S29. (*f*) Reaction mixture. MeCHO + HBPin, **1**, 2 mol %, 15 min, RT, C_6D_6. Conversion 99 %.

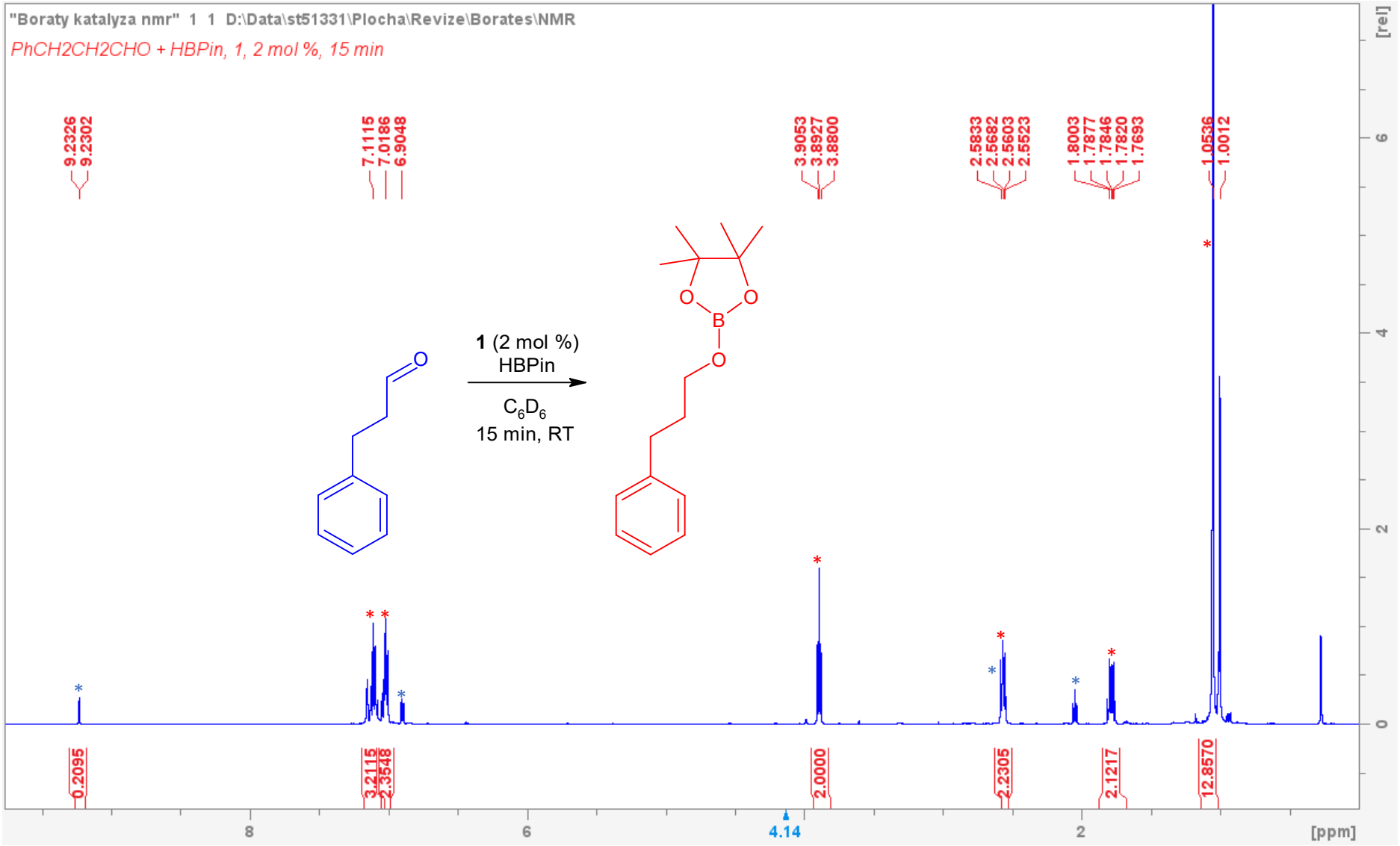

Figure S30. (***g***) Reaction mixture. $PhCH_2CH_2CHO$ + HBPin, **1**, 2 mol %, 15 min, RT, C_6D_6. Conversion 83 %.

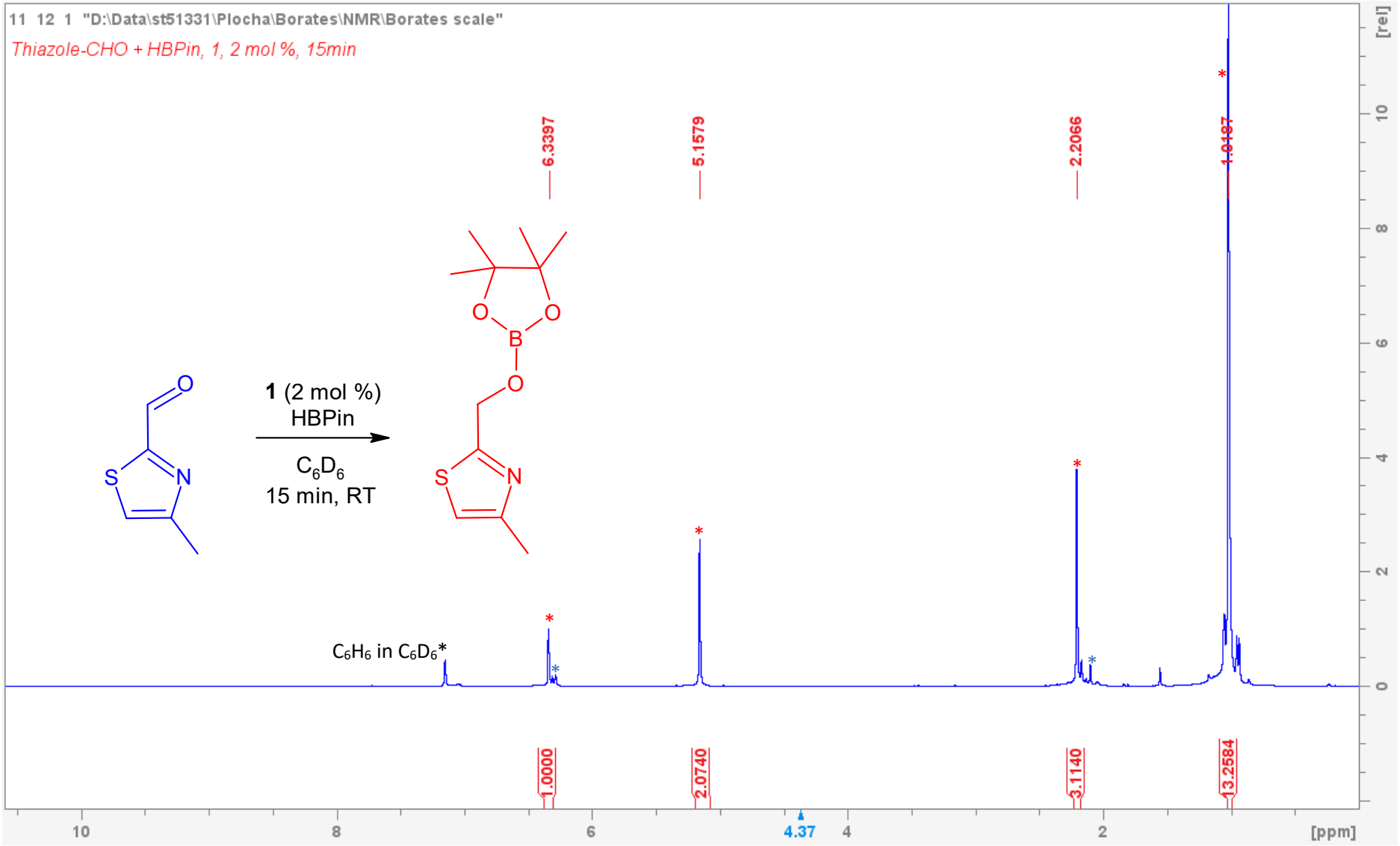

Figure S31. (***h***) Reaction mixture. 5-(C_4H_4SN)-CHO + HBPin, **1**, 2 mol %, 15 min, RT, C_6D_6. Conversion >99 %.

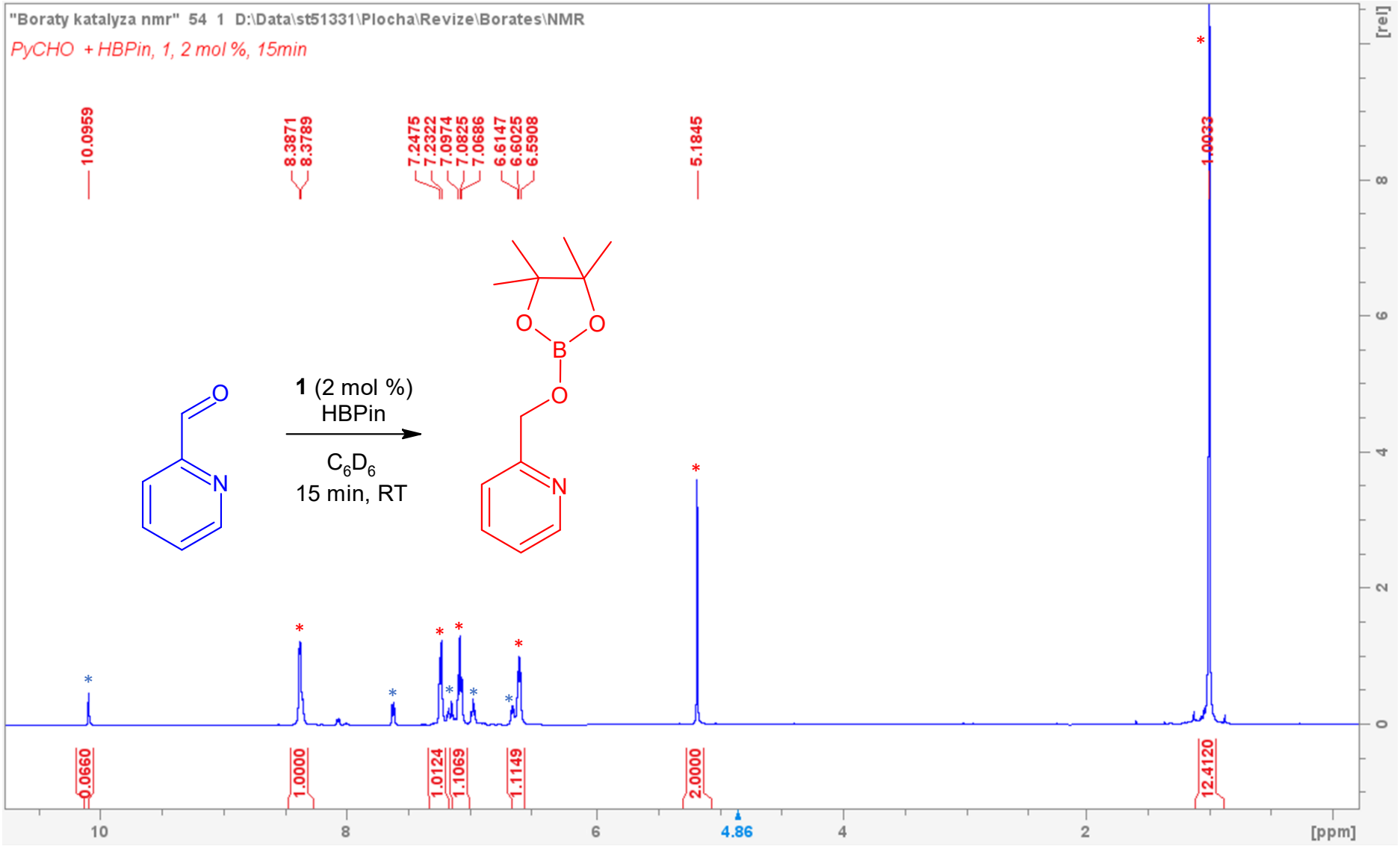

Figure S32. (*i*) Reaction mixture. 6-(C_5H_4N)-CHO + HBPin, **1**, 2 mol %, 15 min, RT, C_6D_6. Conversion >95 %.

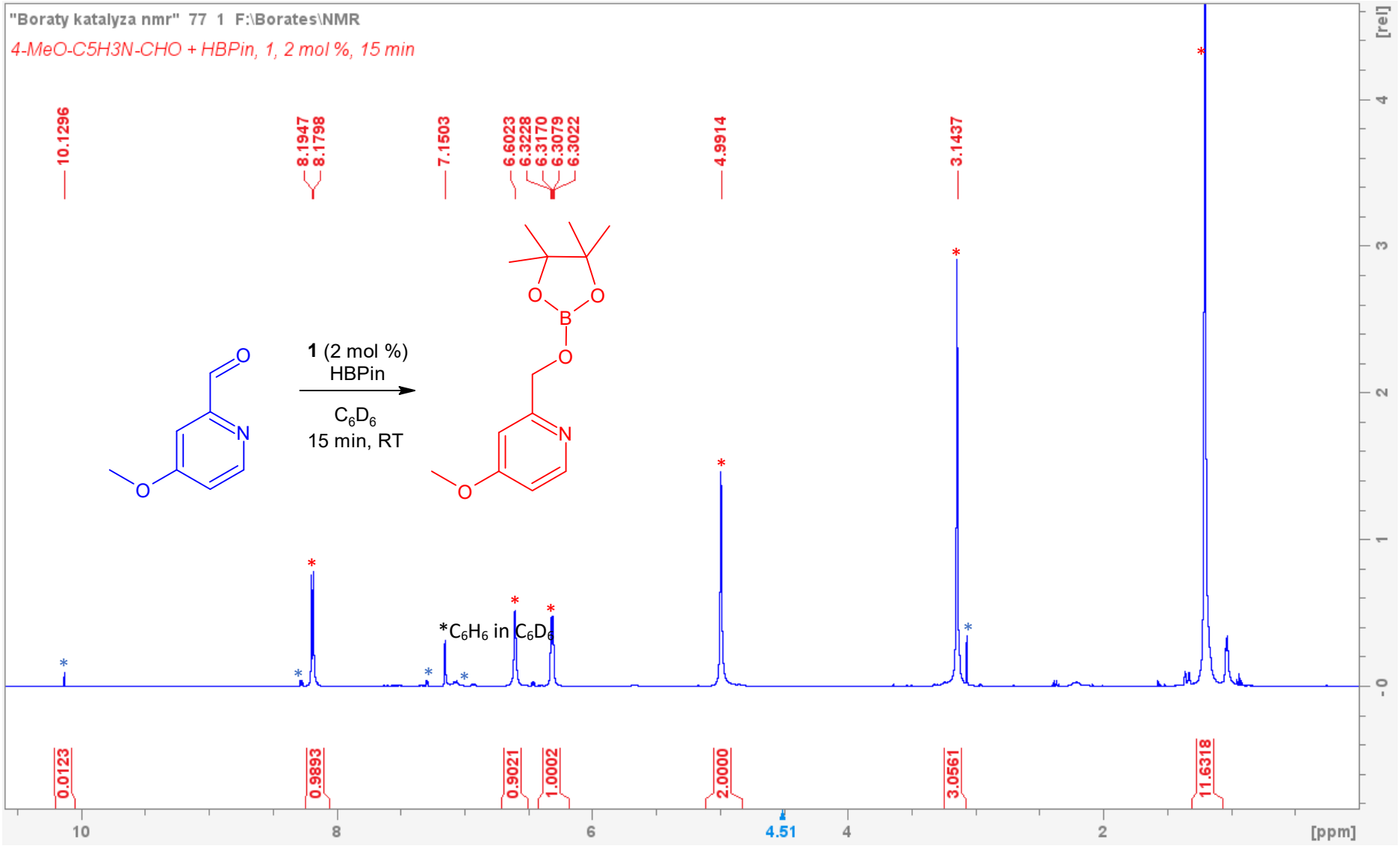

Figure S33. (*j*) Reaction mixture. 4-OMe-(C_5H_4N)-CHO + HBPin, **1**, 2 mol %, 15 min, RT, C_6D_6. Conversion 99 %.

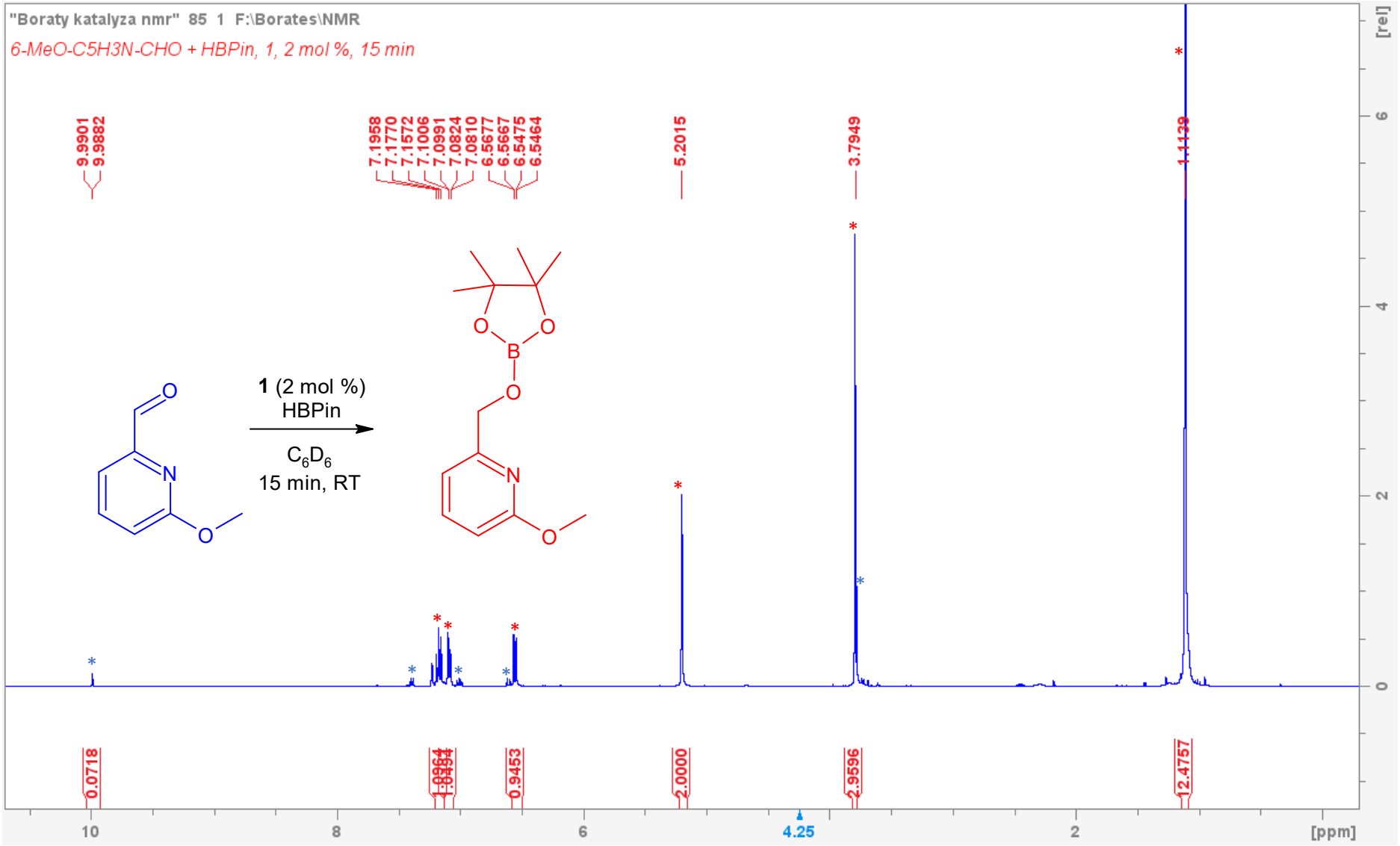

Figure S34. (***k***) Reaction mixture. 6-OMe-(C_5H_4N)-CHO + HBPin, **1**, 2 mol %, 15 min, RT, C_6D_6. Conversion >95 %.

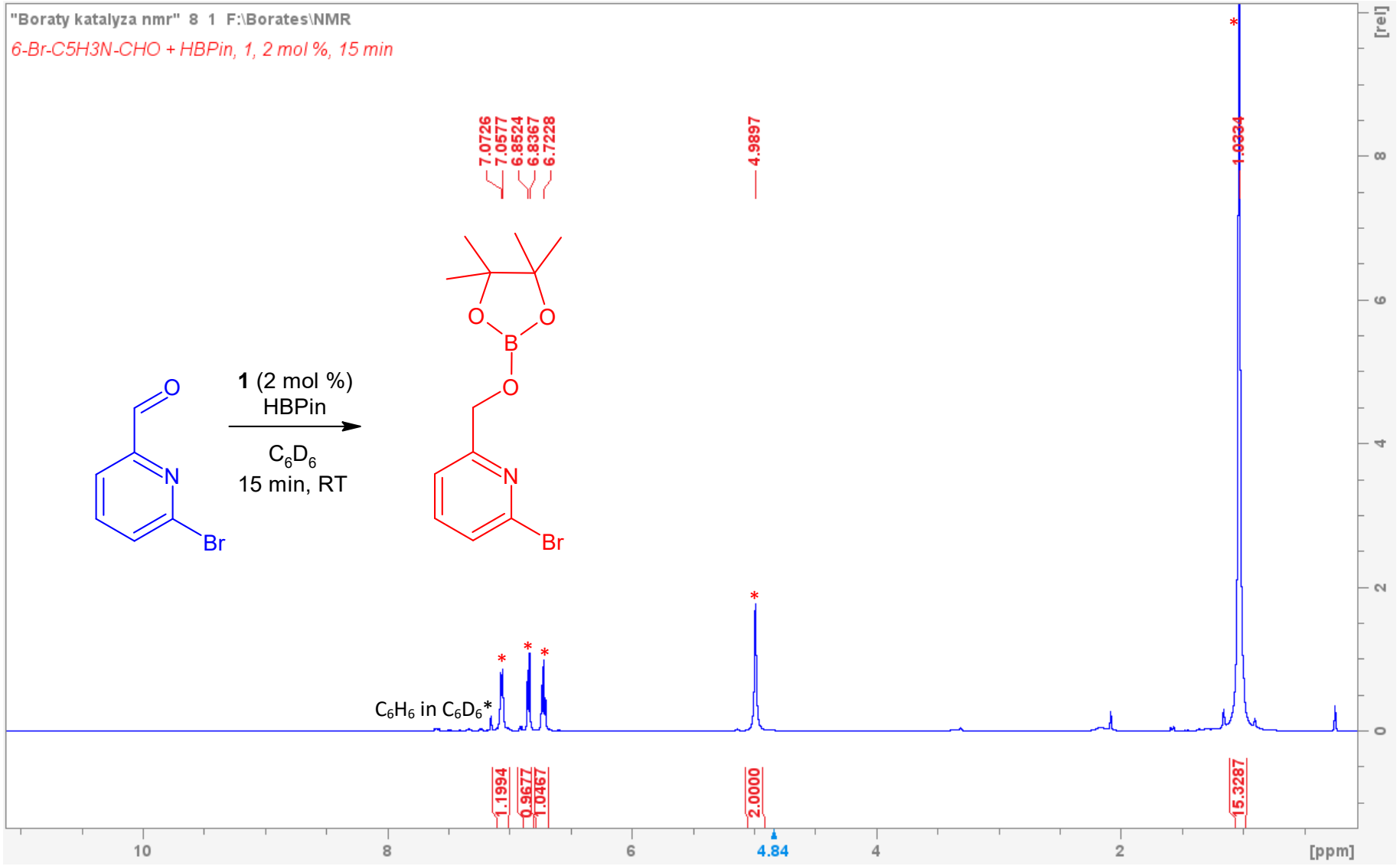

Figure S35. (*l*) Reaction mixture. 6-Br-(C_5H_4N)-CHO + HBPin, **1**, 2 mol %, 15 min, RT, C_6D_6. Conversion 99 %.

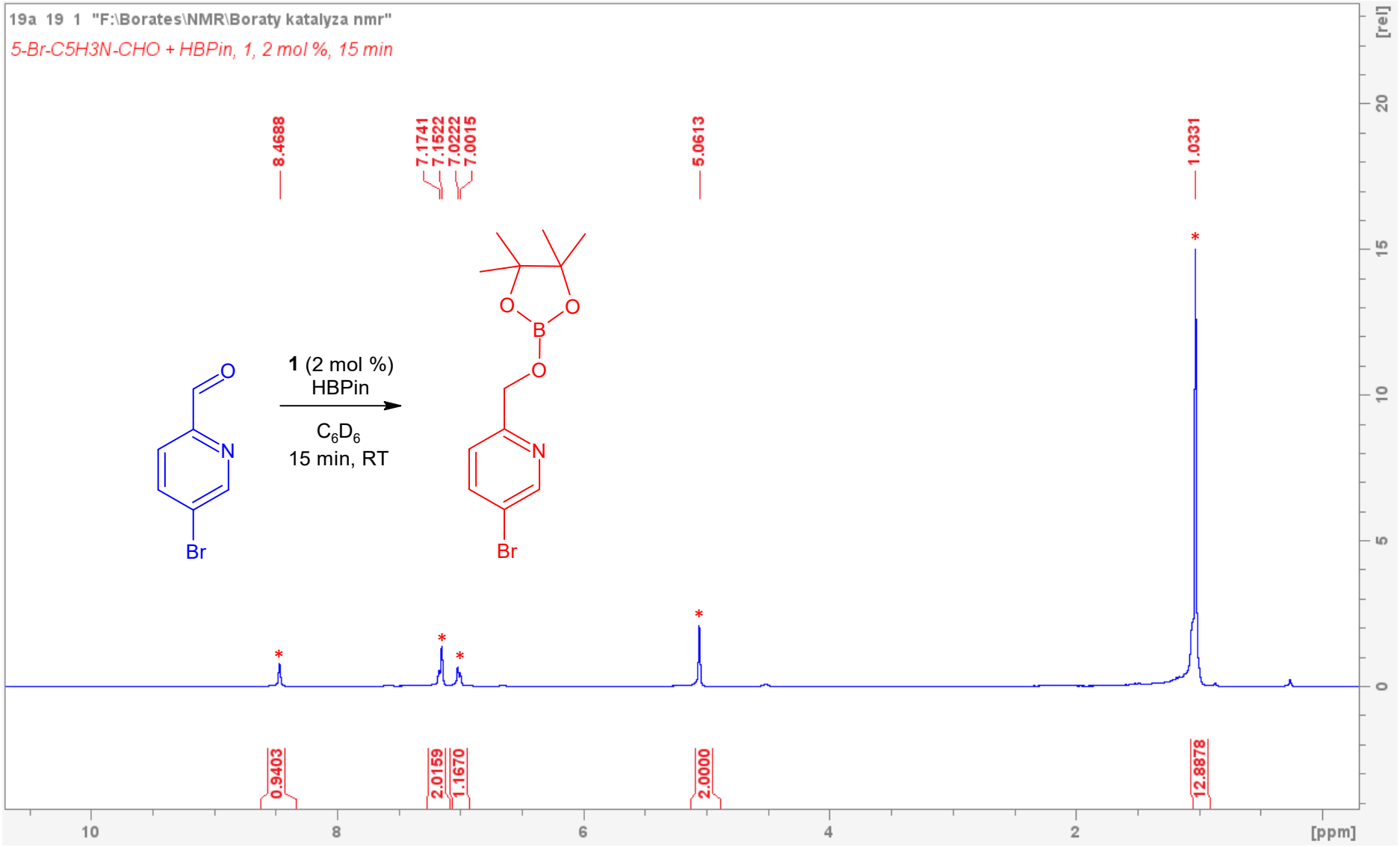

Figure S36. (***m***) Reaction mixture. 5-Br-(C_5H_4N)-CHO + HBPin, **1**, 2 mol %, 15 min, RT, C_6D_6. Conversion 99 %.

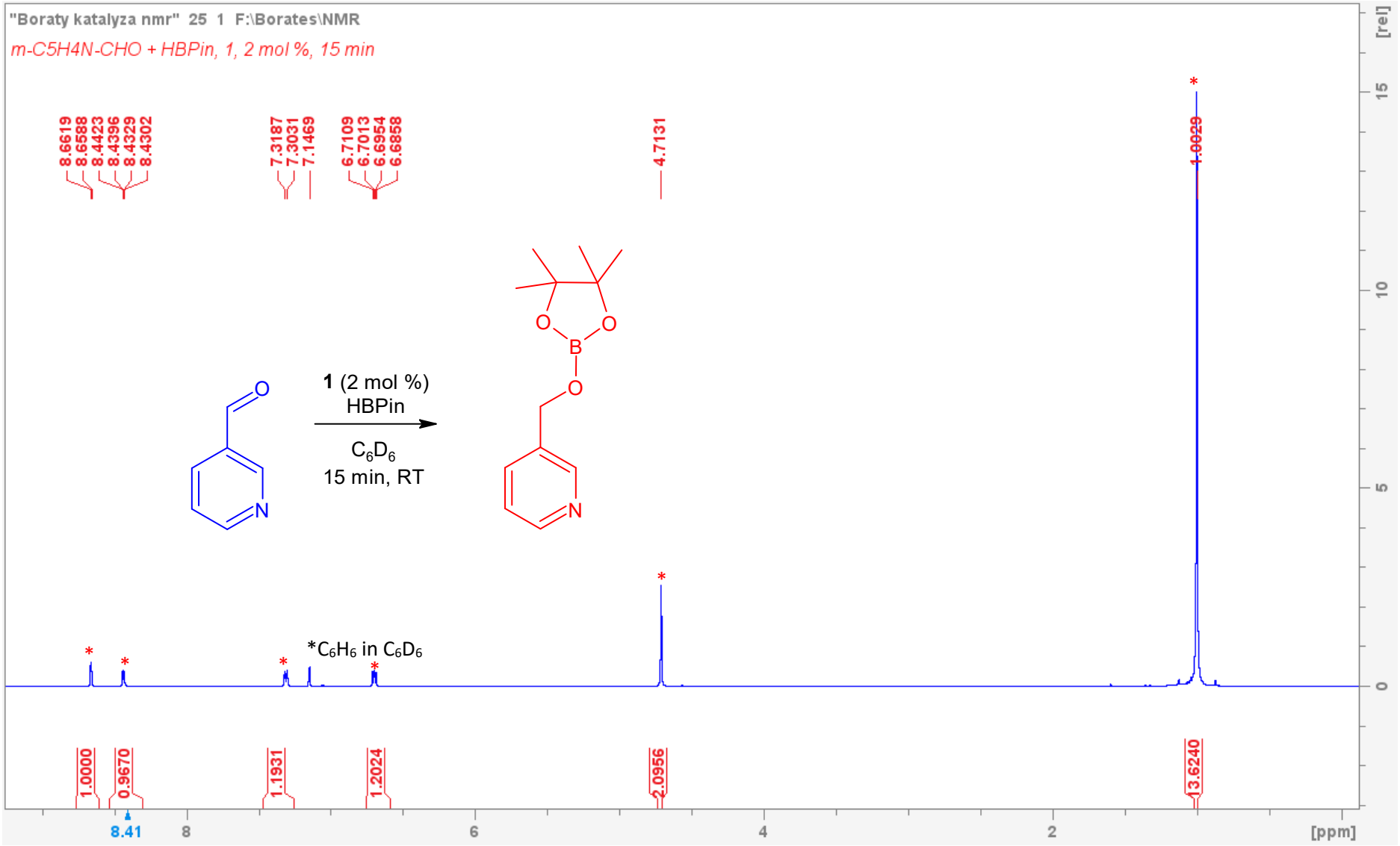

Figure S37. (*n*) Reaction mixture. 5-(C_5H_4N)-CHO + HBPin, **1**, 2 mol %, 15 min, RT, C_6D_6. Conversion >99 %.

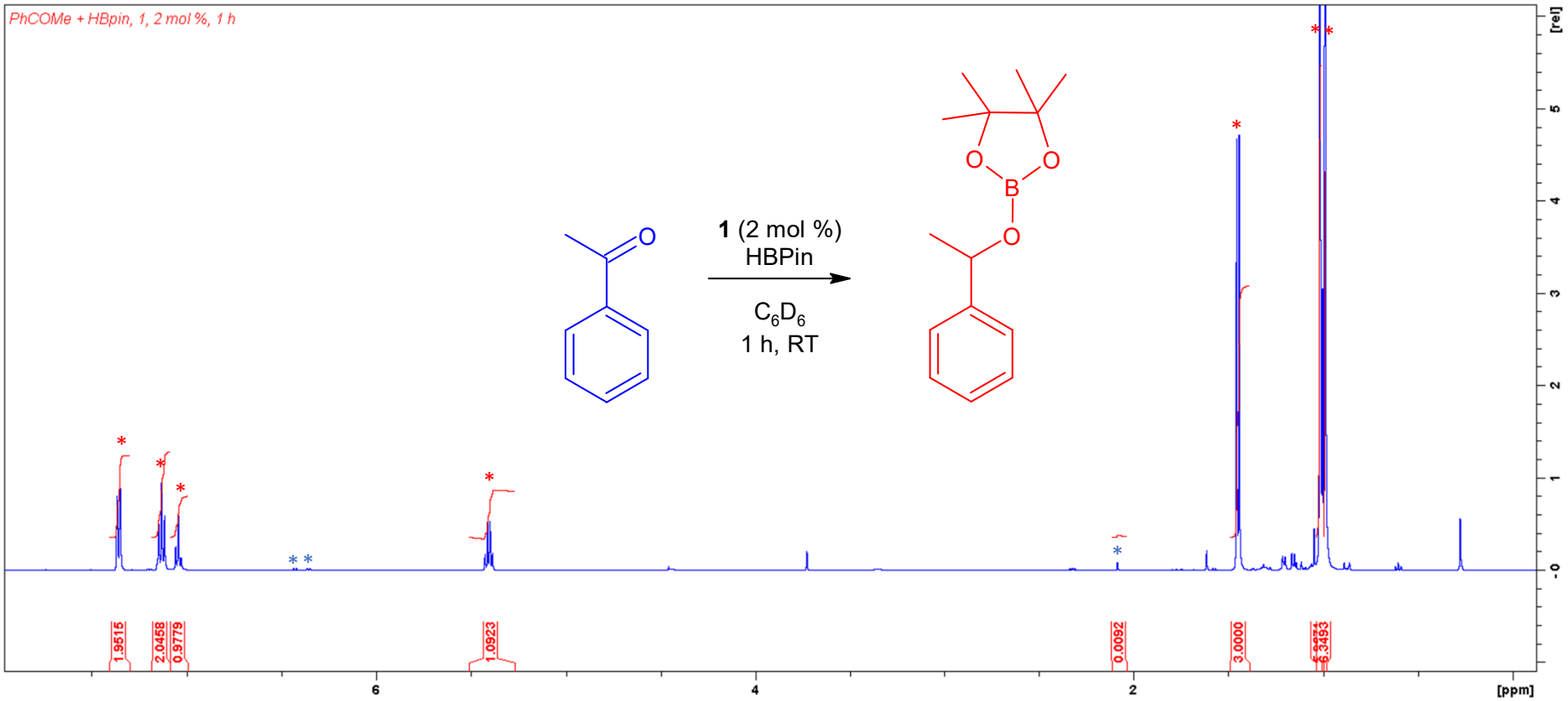

Figure S38. (*o*) Reaction mixture. PhCOMe + HBPin, **1**, 2 mol %, 60 min, RT, C_6D_6. Conversion >99 %.

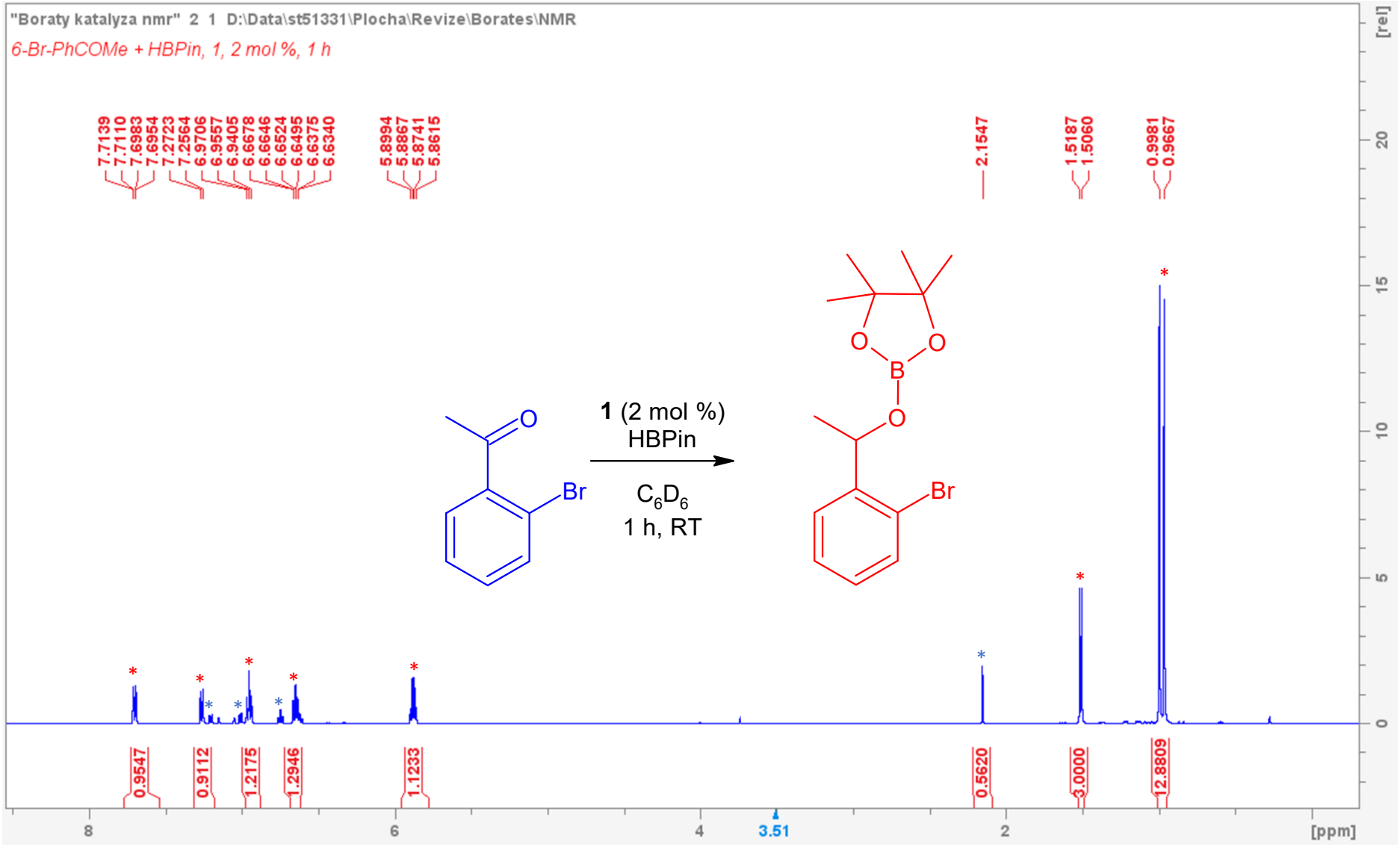

Figure S39. (***p***) Reaction mixture. 2-Br-PhCOMe + HBPin, **1**, 2 mol %, 60 min, RT, C_6D_6. Conversion 84 %.

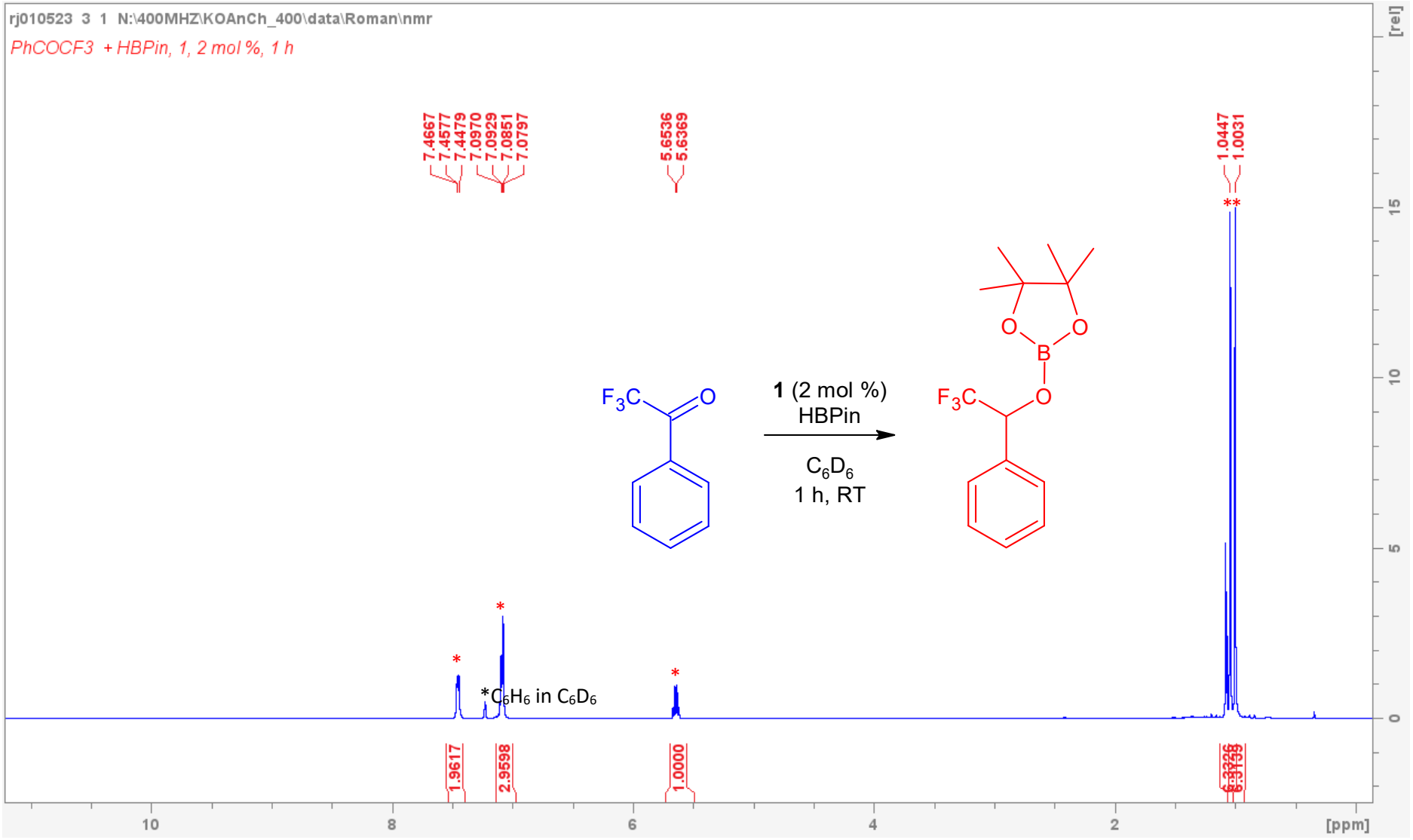

Figure S40. (*q*) Reaction mixture. $PhCOCF_3$ + HBPin, **1**, 2 mol %, 60 min, RT, C_6D_6. Conversion >99 %.

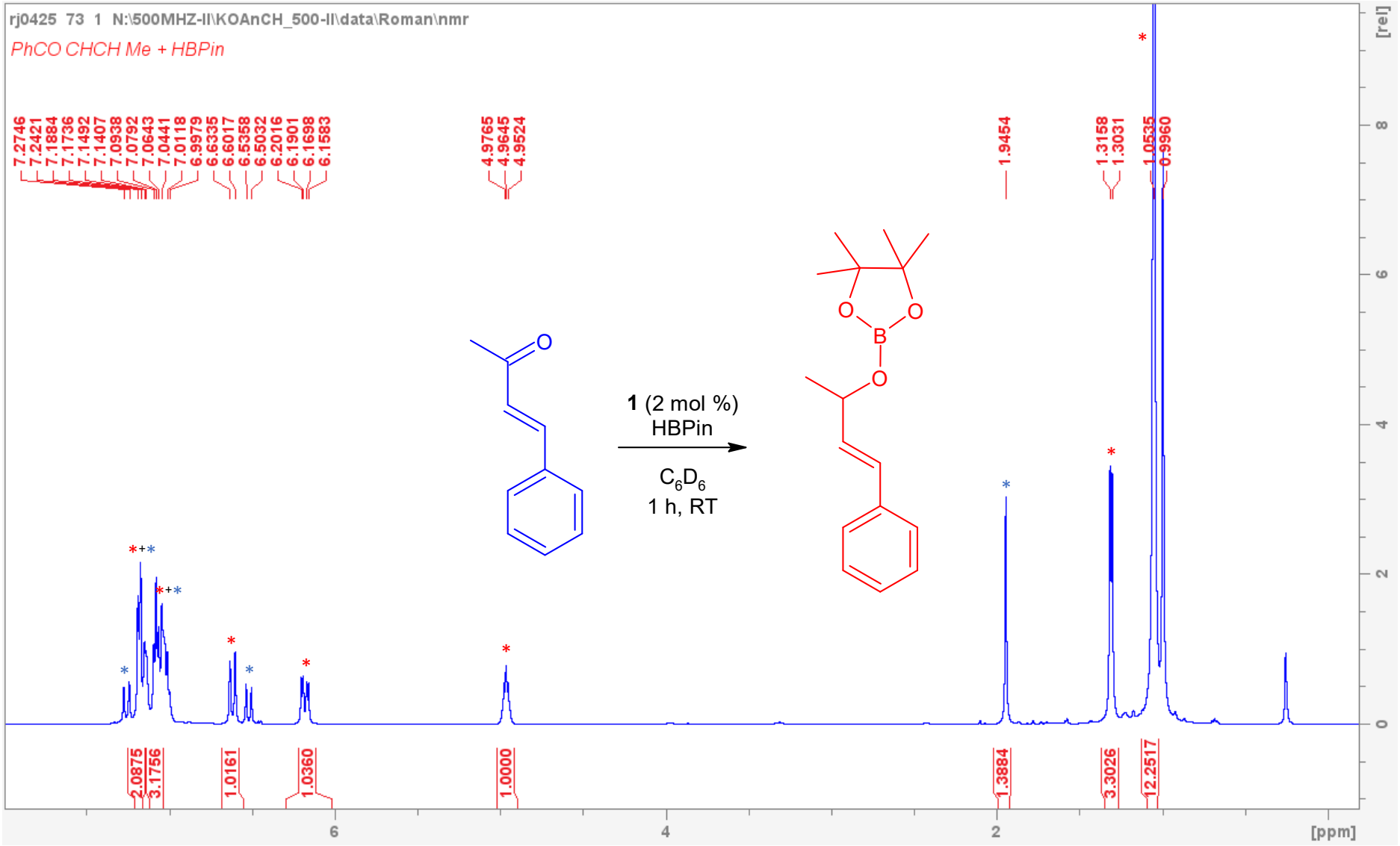

Figure S41. (*r*) Reaction mixture. PhCOCH=CHMe + HBPin, **1**, 2 mol %, 60 min, RT, C_6D_6. Conversion 67 %.

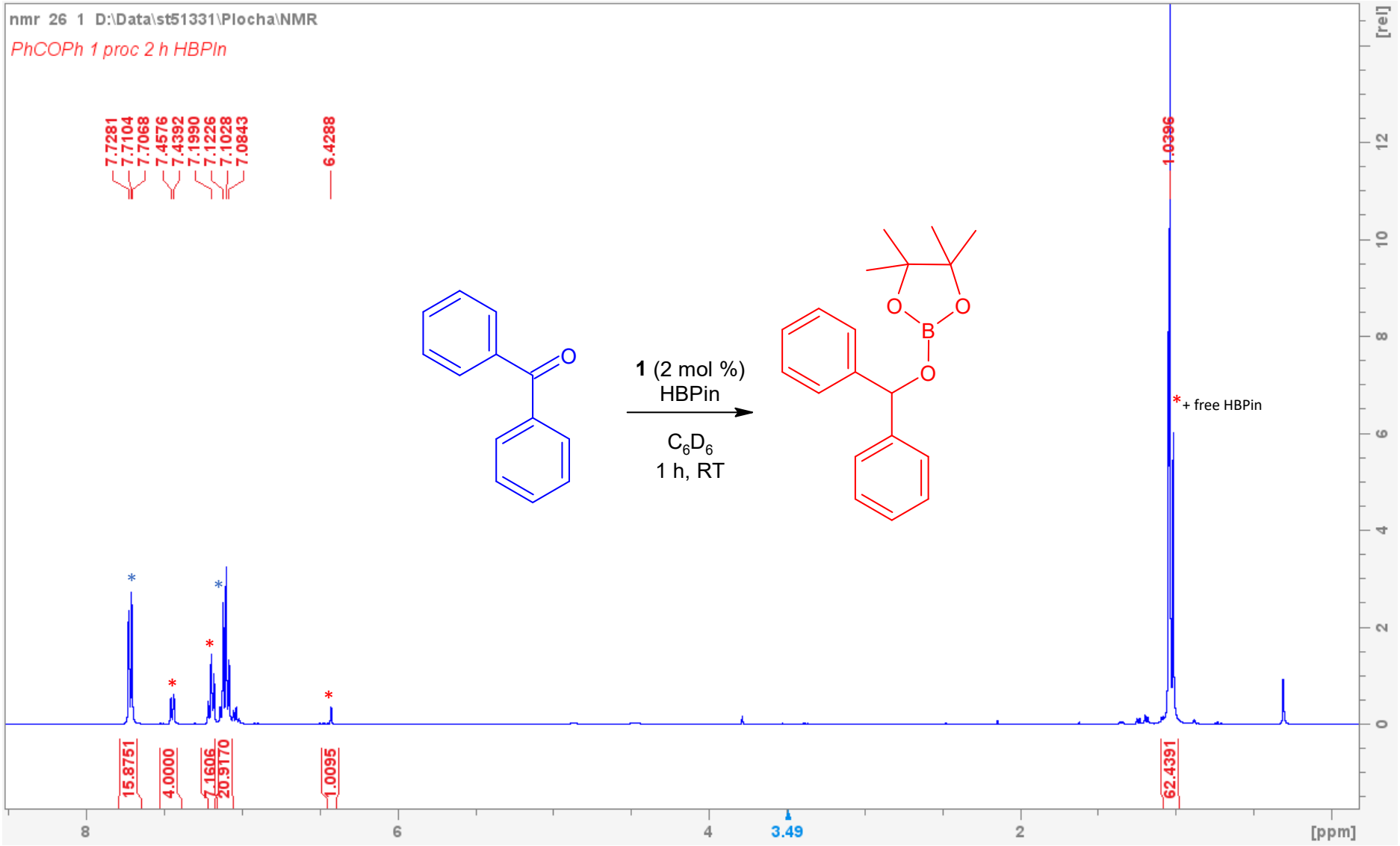

Figure S42. (**s**) Reaction mixture. PhCOPh + HBPin, **1**, 2 mol %, 60 min, RT, C_6D_6. Conversion 20 %.

NMR characterization of N-substituted boron esters 4–10

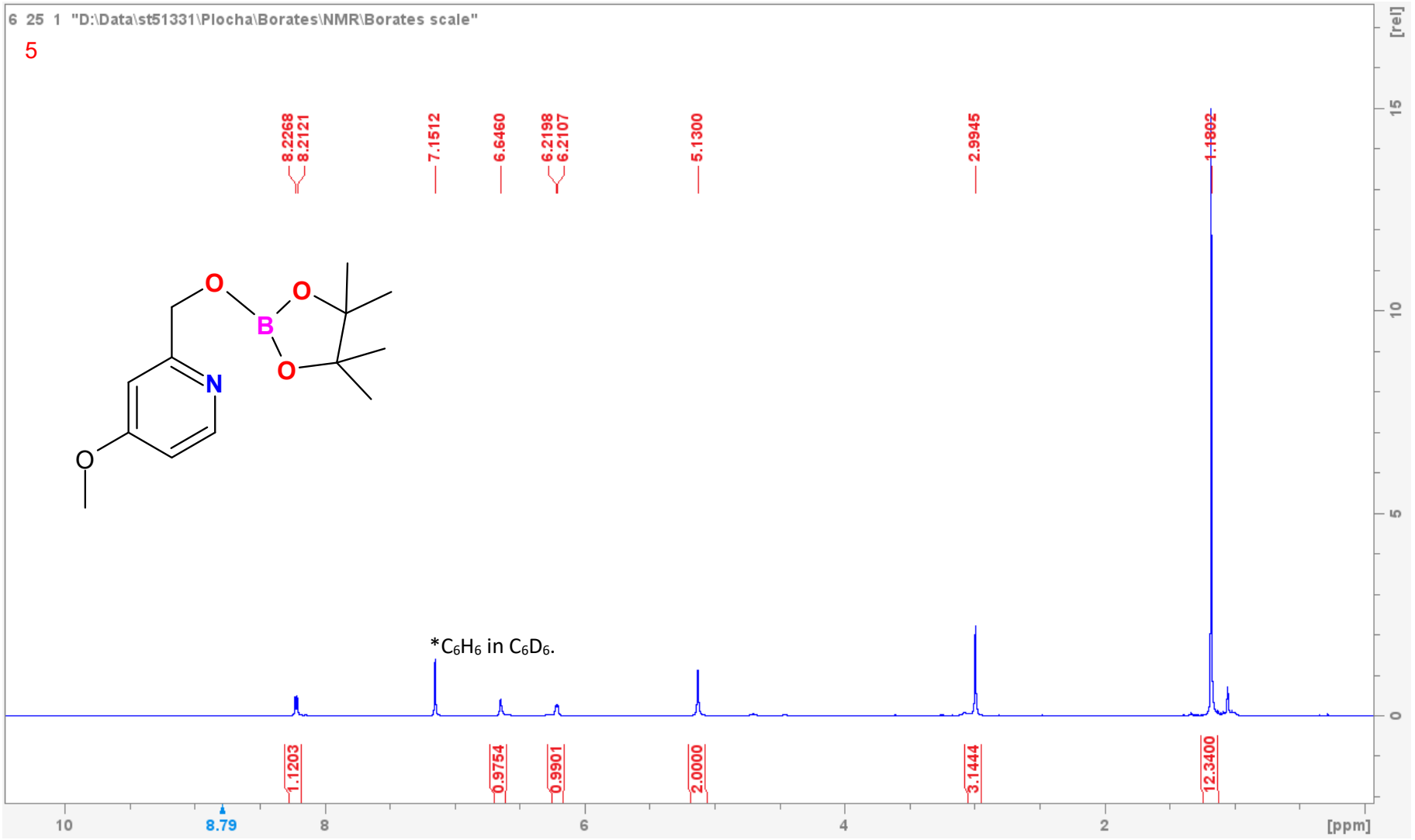

Figure S43. ^{1}H NMR (C_6D_6, 400.13 MHz, 300 K) of **5.**

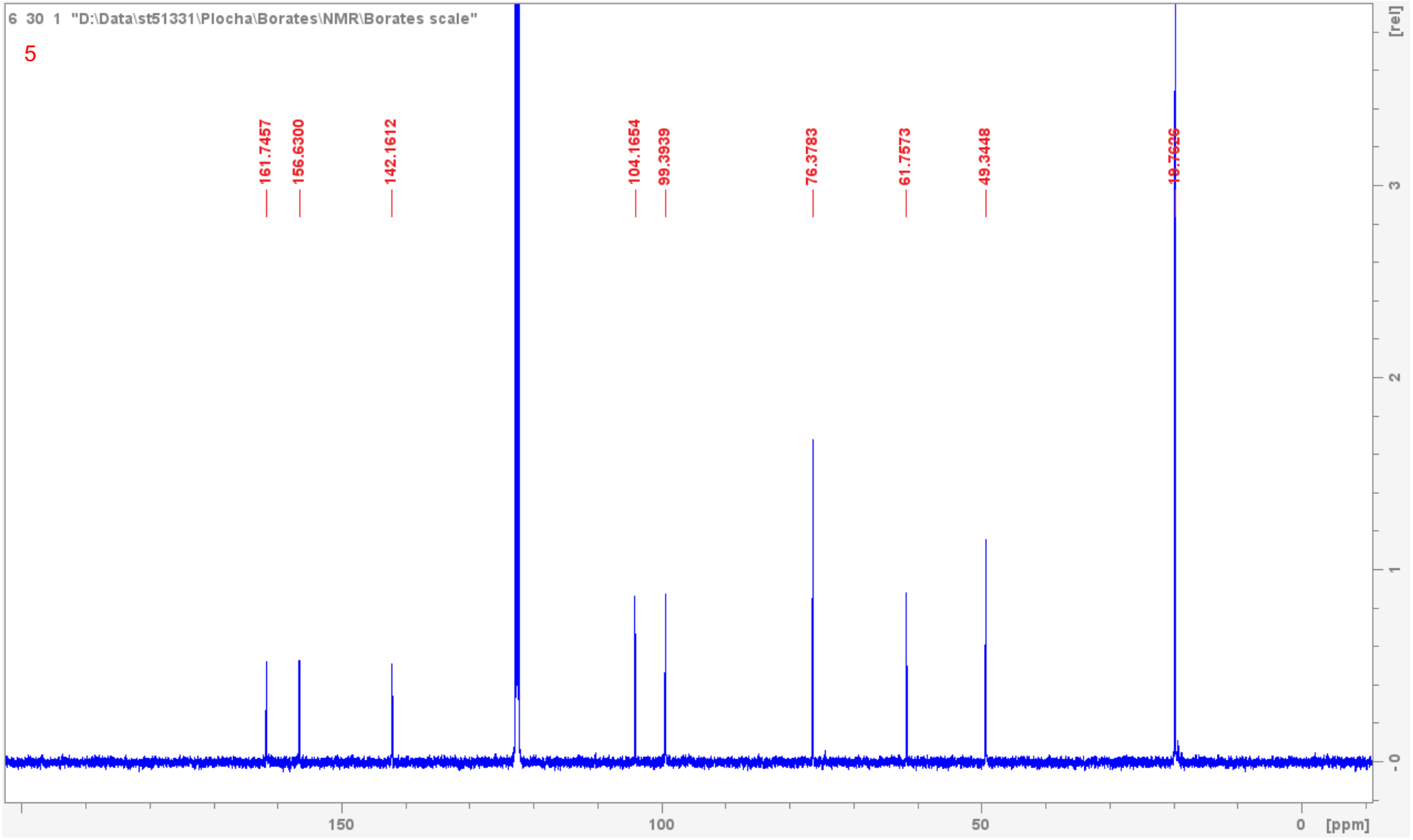

Figure S44. $^{13}C\{^{1}H\}$ NMR (C_6D_6, 100.76 MHz, 300 K) of **5**.

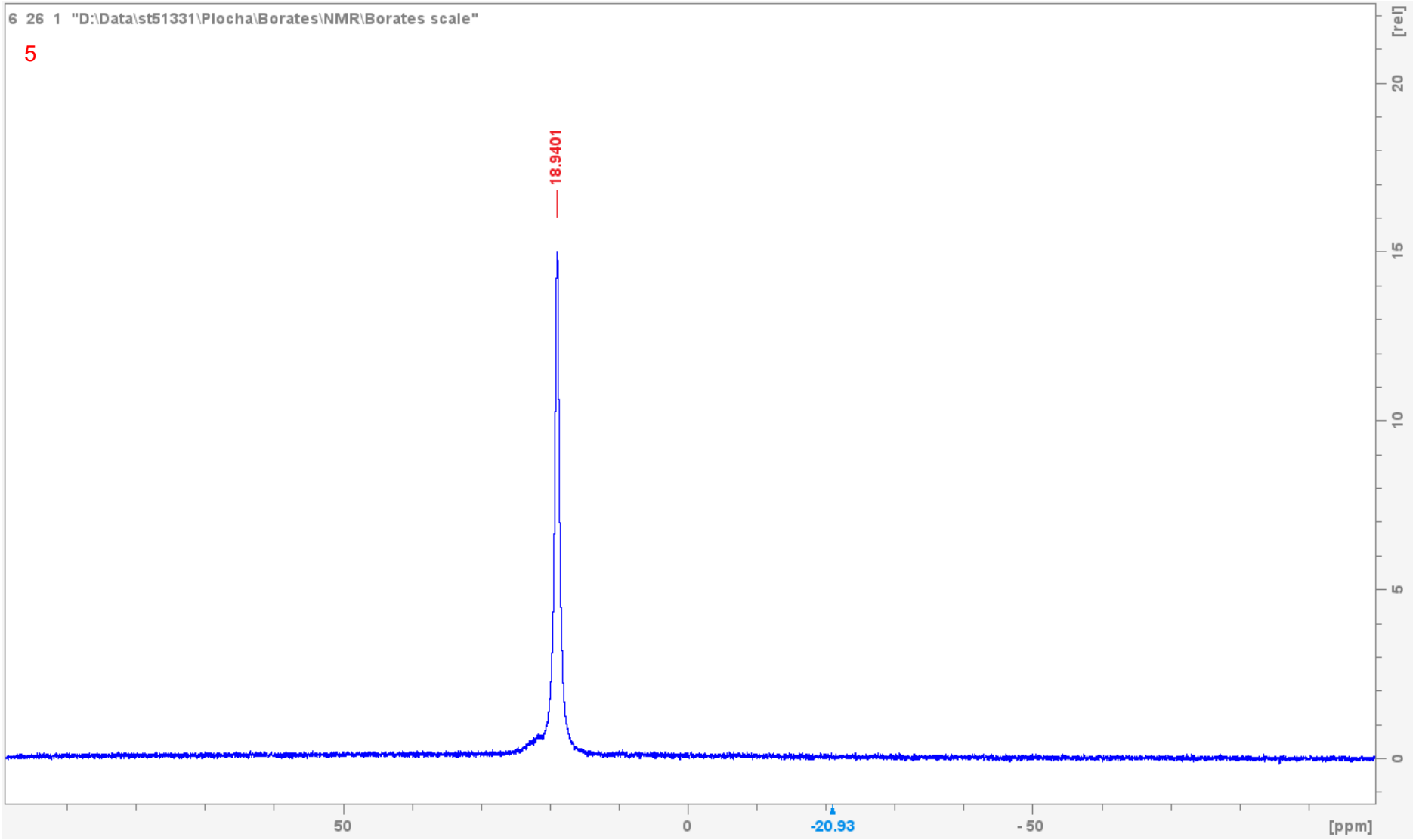

Figure S45. $^{11}B\{^{1}H\}$ NMR (C_6D_6, 128.378 MHz, 300 K) of **5**.

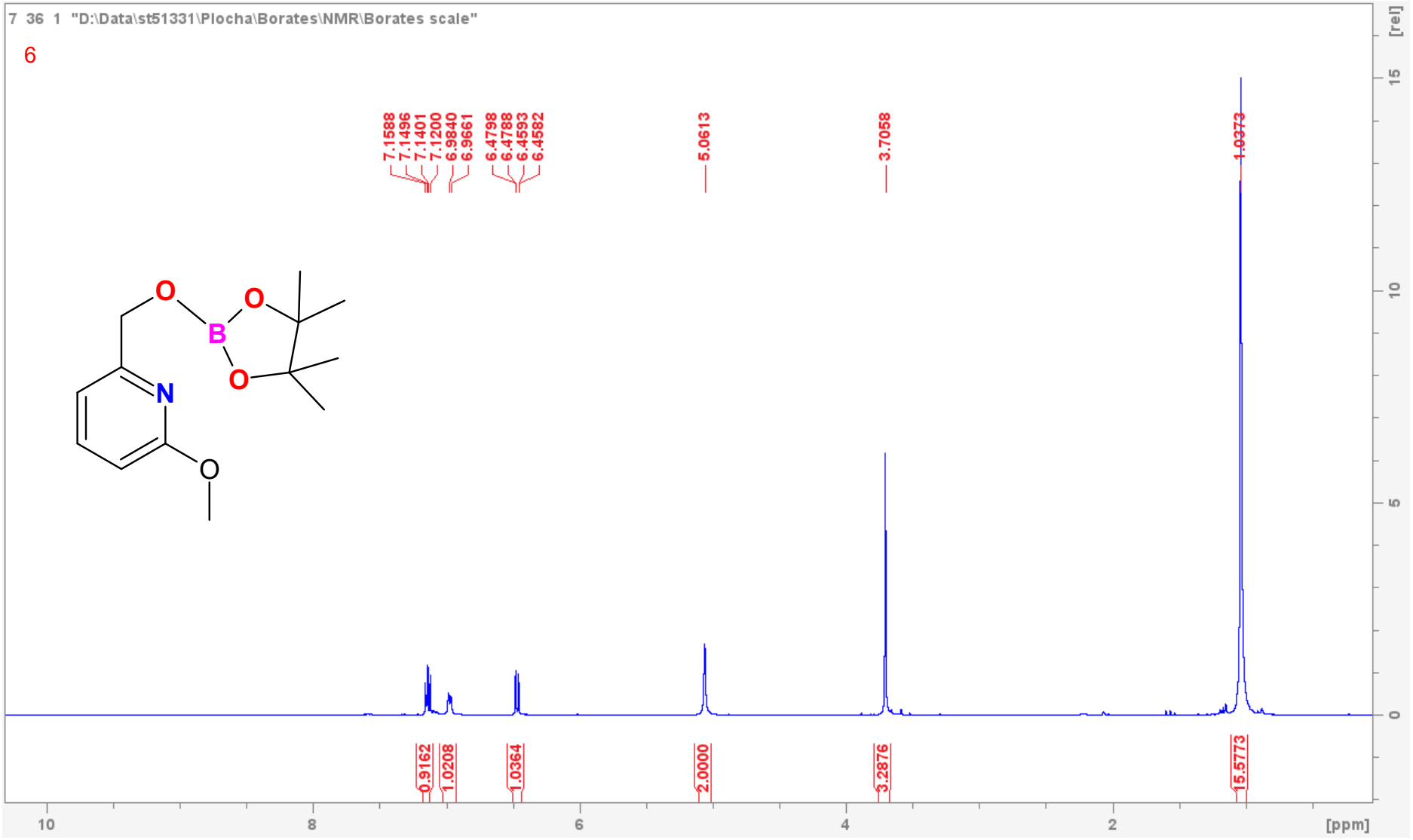

Figure S46. ^{1}H NMR (C_6D_6, 400.13 MHz, 300 K) of **6.**

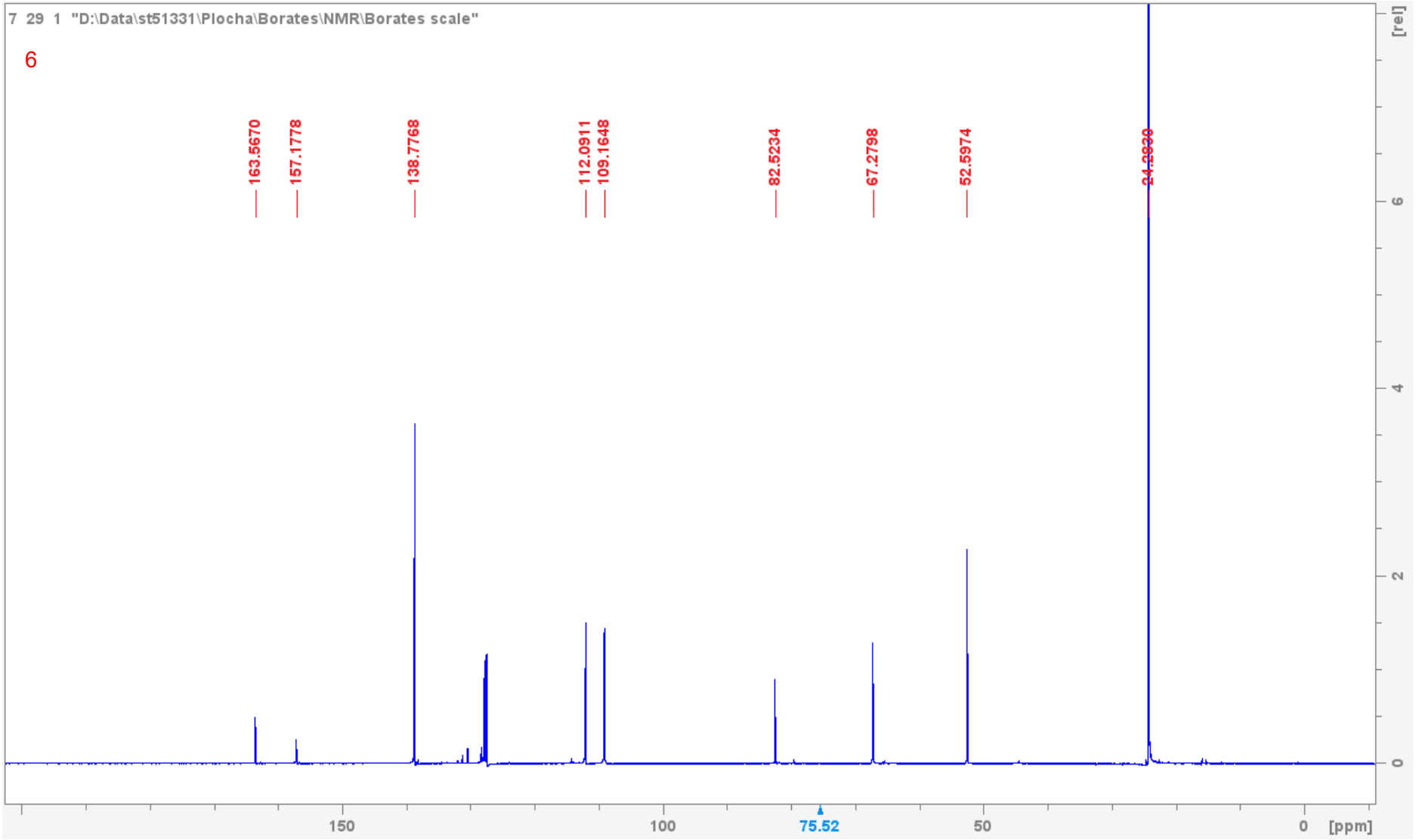

Figure S47. $^{13}C\{^{1}H\}$ NMR (C_6D_6, 125.76 MHz, 300 K) of **6**.

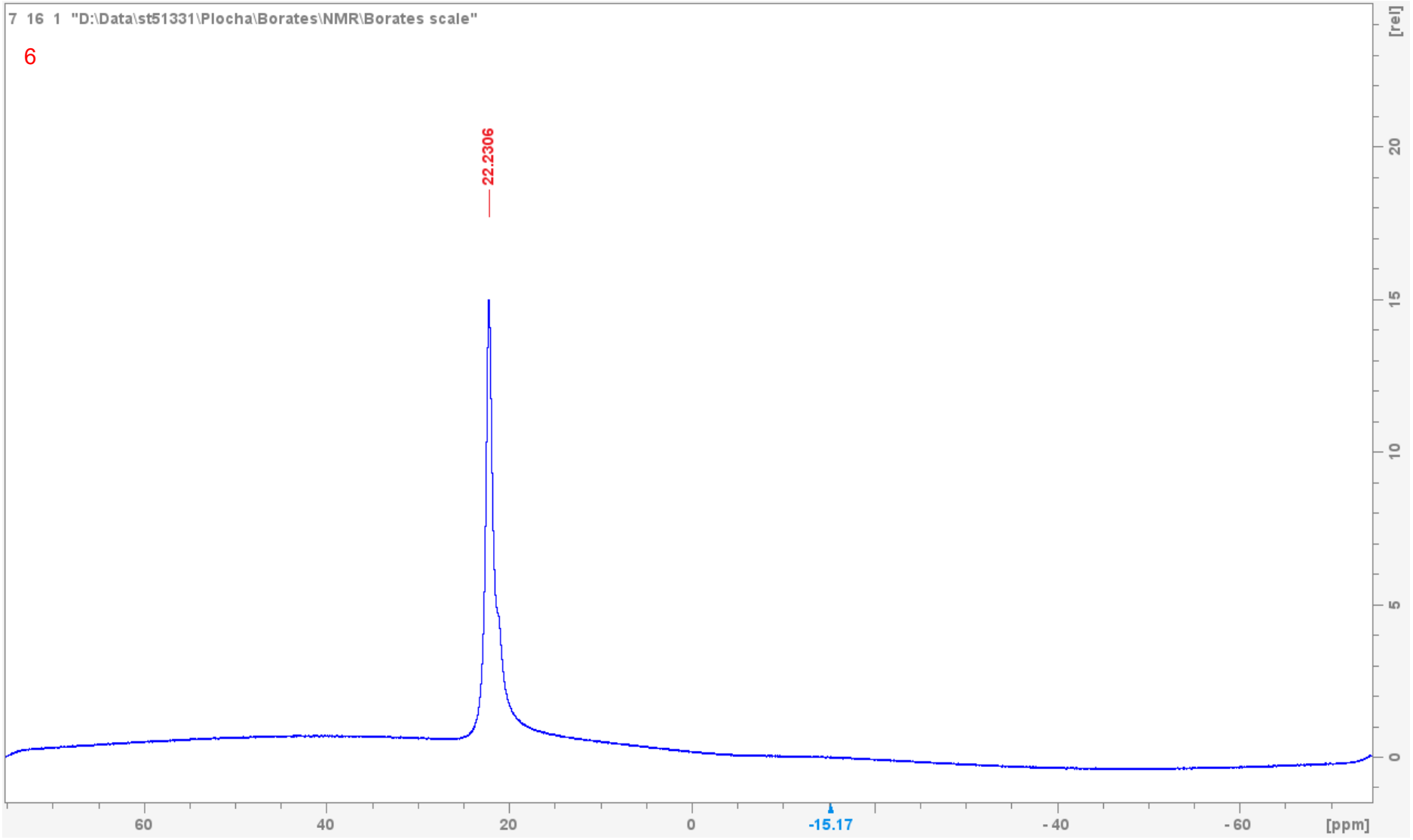

Figure S48. $^{11}B\{^{1}H\}$ NMR (C_6D_6, 160.462 MHz, 300 K) of **6**.

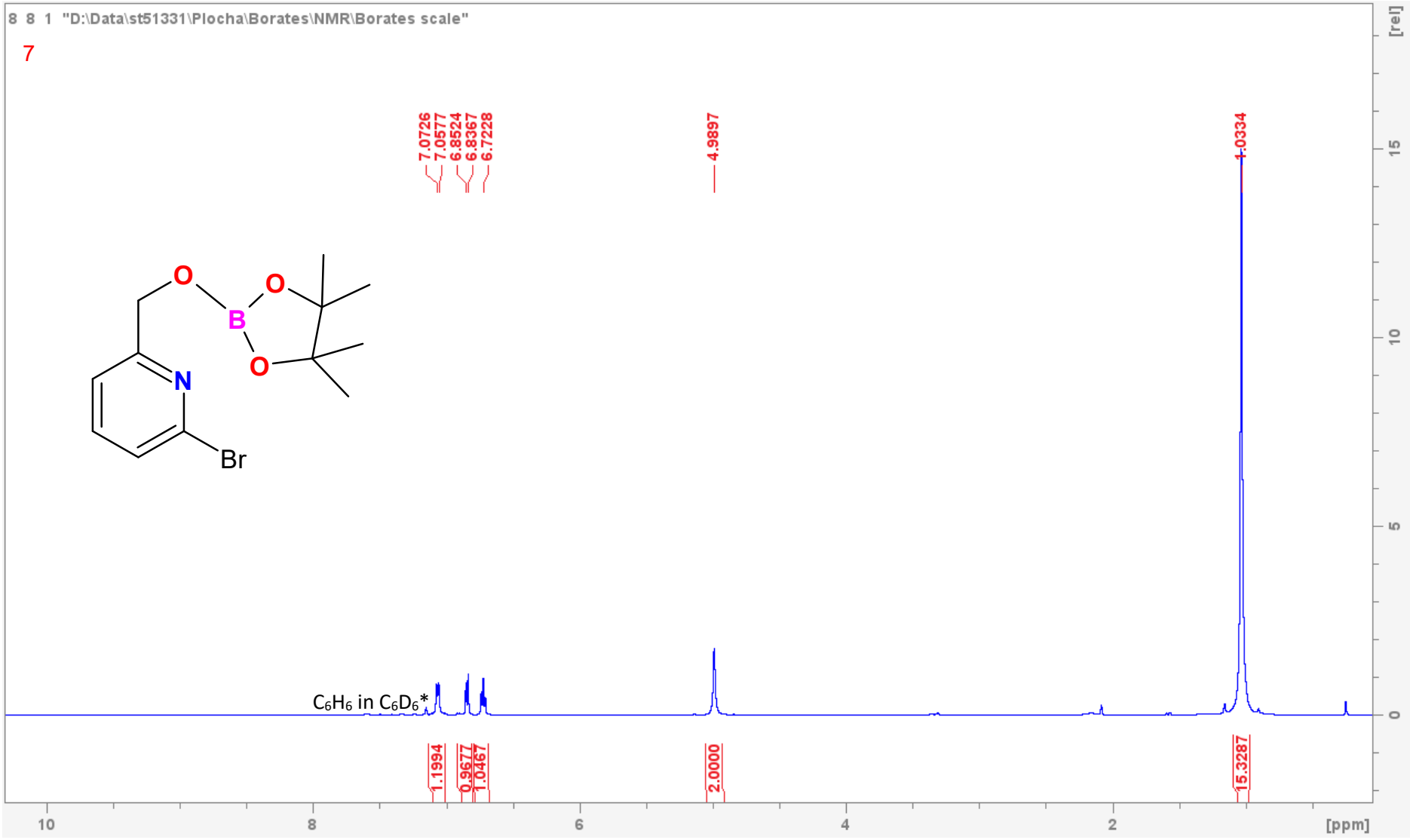

Figure S49. ^{1}H NMR (C_6D_6, 400.13 MHz, 300 K) of **7.**

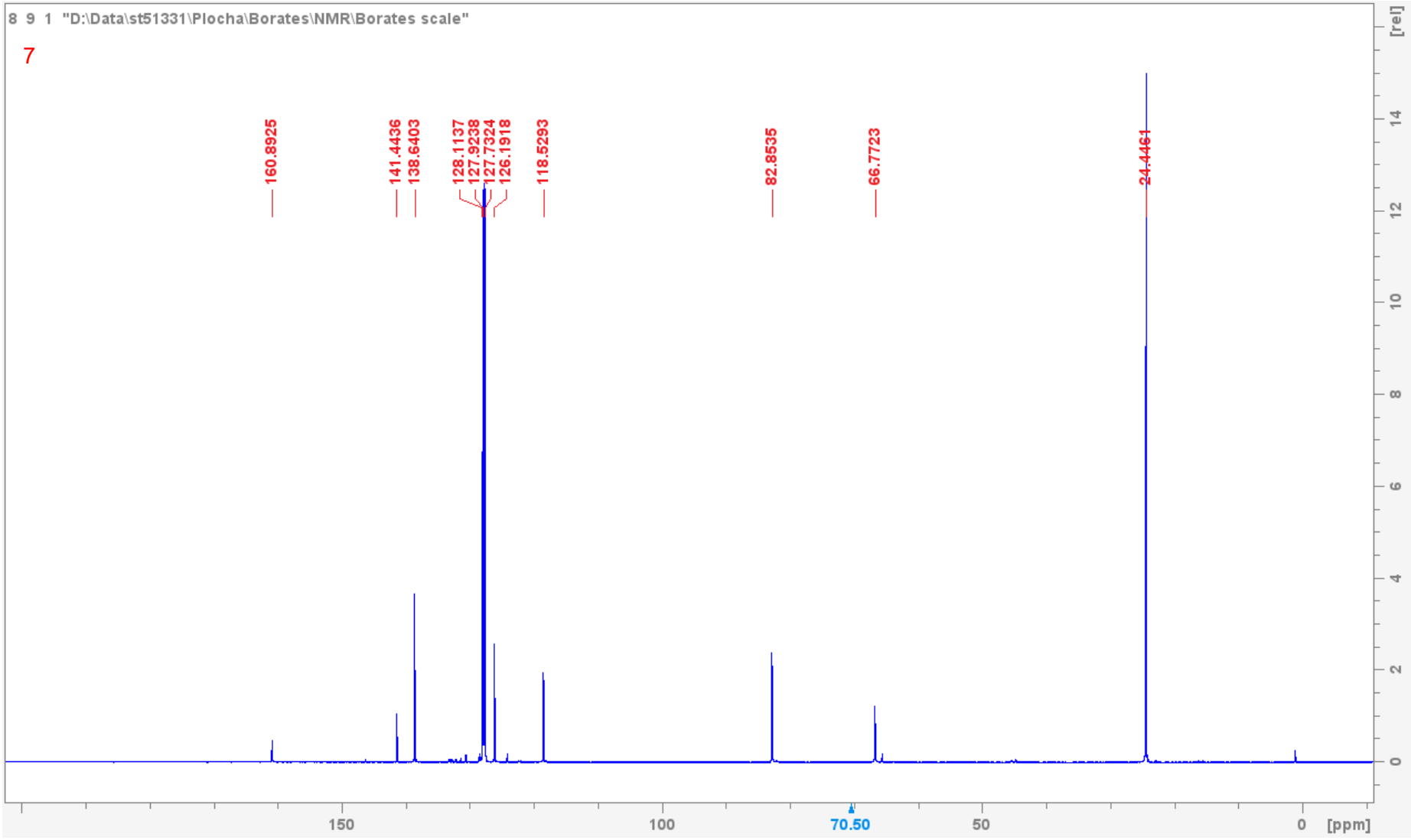

Figure S50. $^{13}C\{^{1}H\}$ NMR (C_6D_6, 125.76 MHz, 300 K) of **7**.

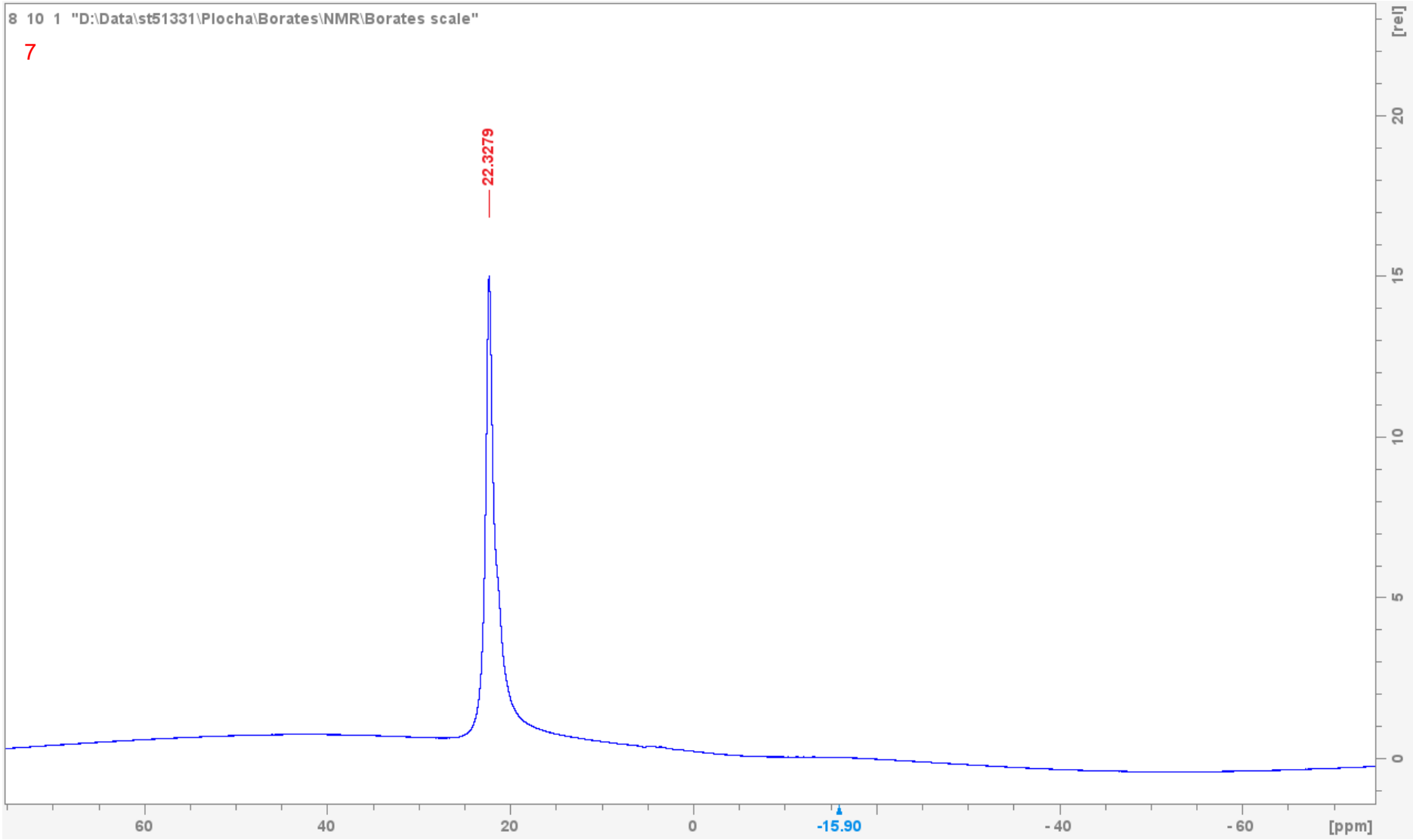

Figure S51. $^{11}B\{^{1}H\}$ NMR (C_6D_6, 128.378 MHz, 300 K) of **7**.

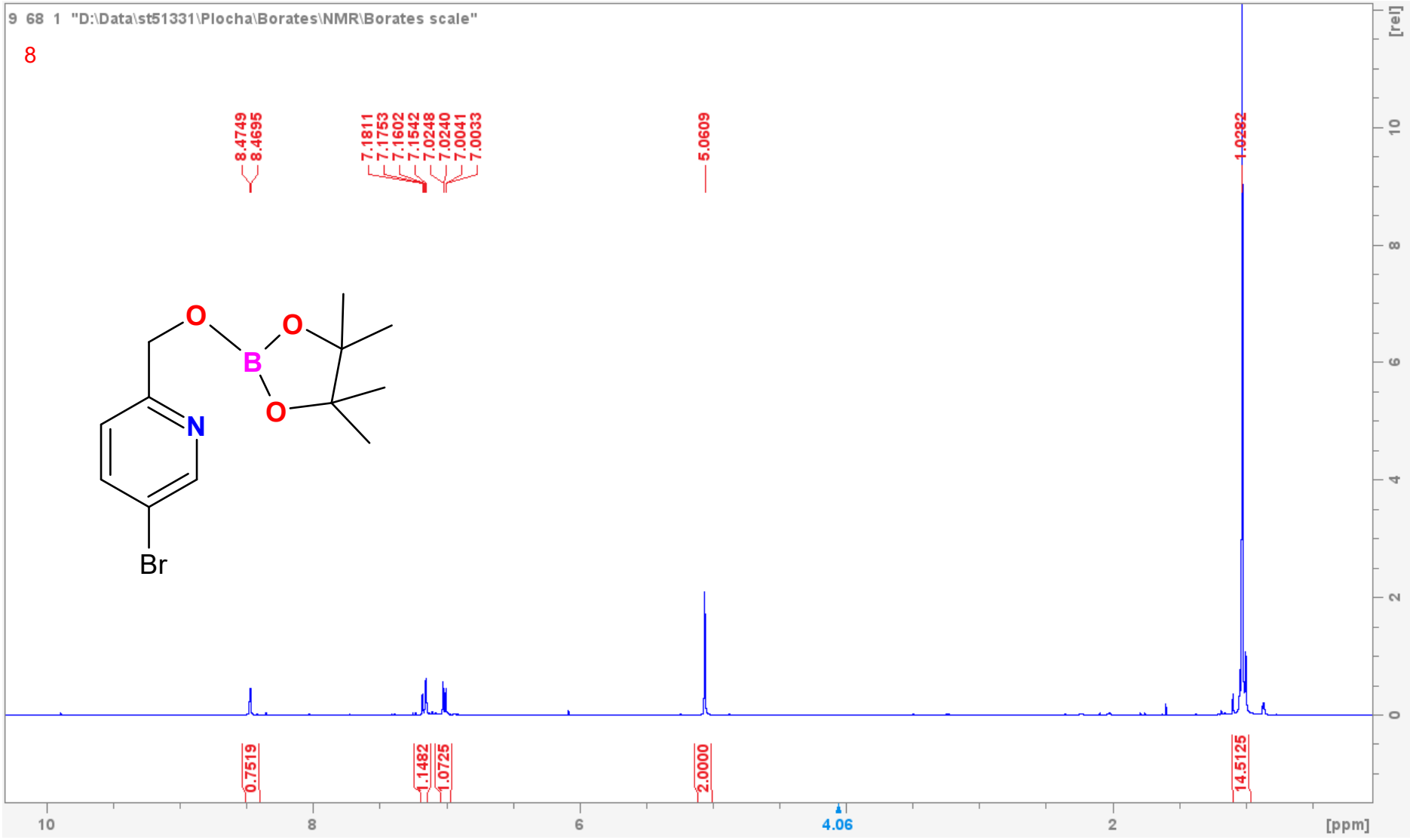

Figure S52. ^{1}H NMR (C_6D_6, 400.13 MHz, 300 K) of **8.**

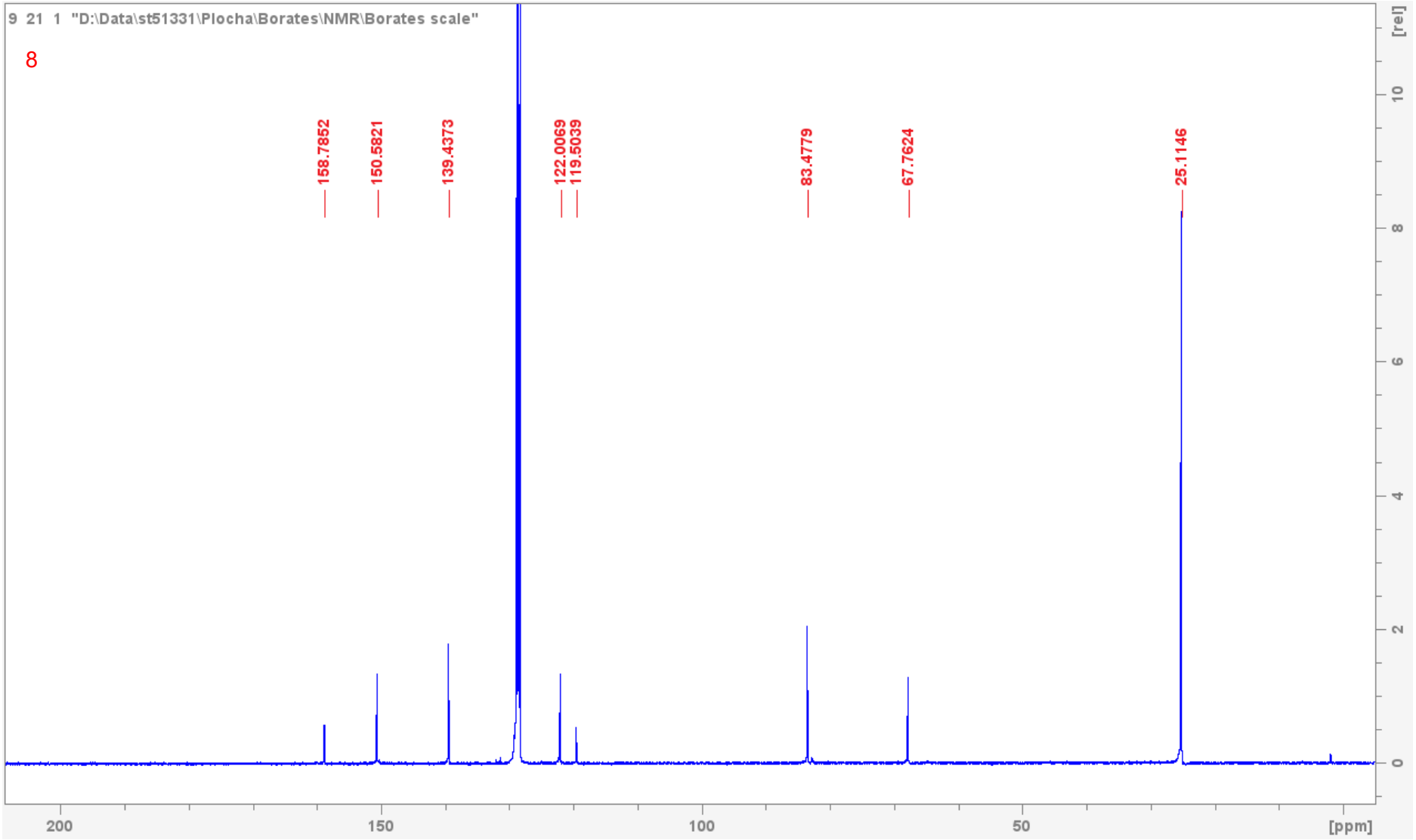

Figure S53. $^{13}C\{^{1}H\}$ NMR (C_6D_6, 100.76 MHz, 300 K) of **8**.

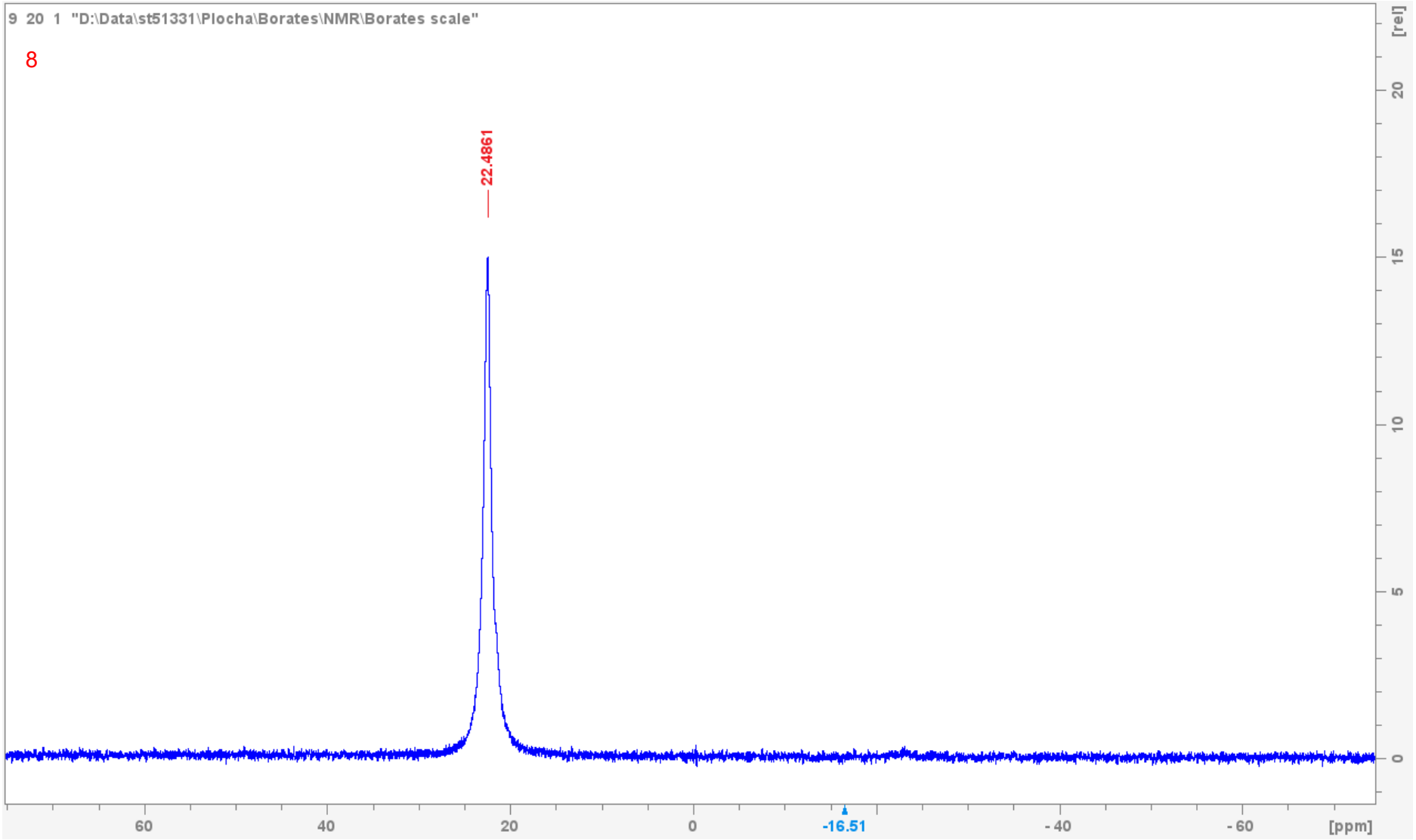

Figure S54. $^{11}B\{^{1}H\}$ NMR (C_6D_6, 128.378 MHz, 300 K) of **8**.

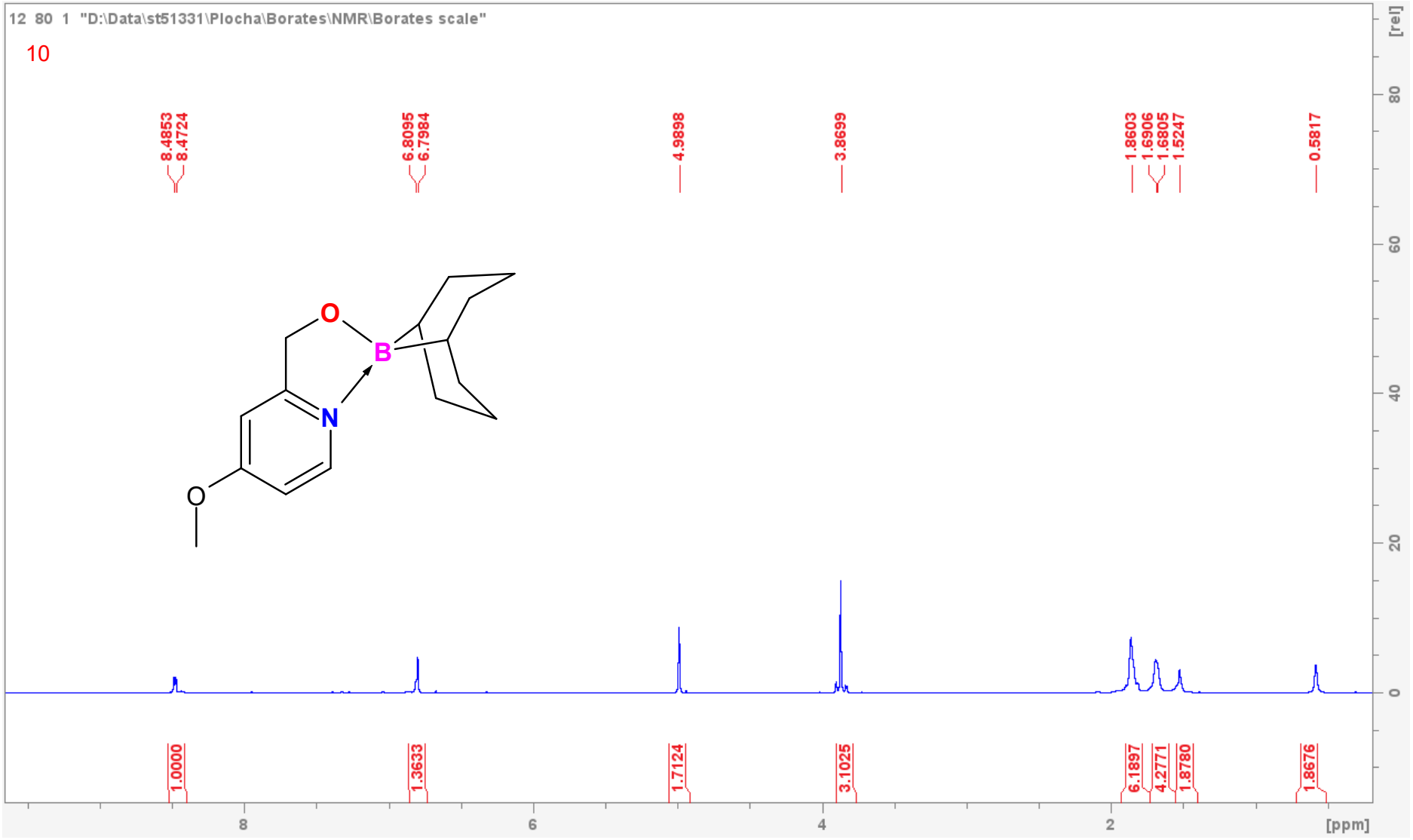

Figure S55. ^{1}H NMR ($CDCl_3$, 500.13 MHz, 300 K) of **10.**

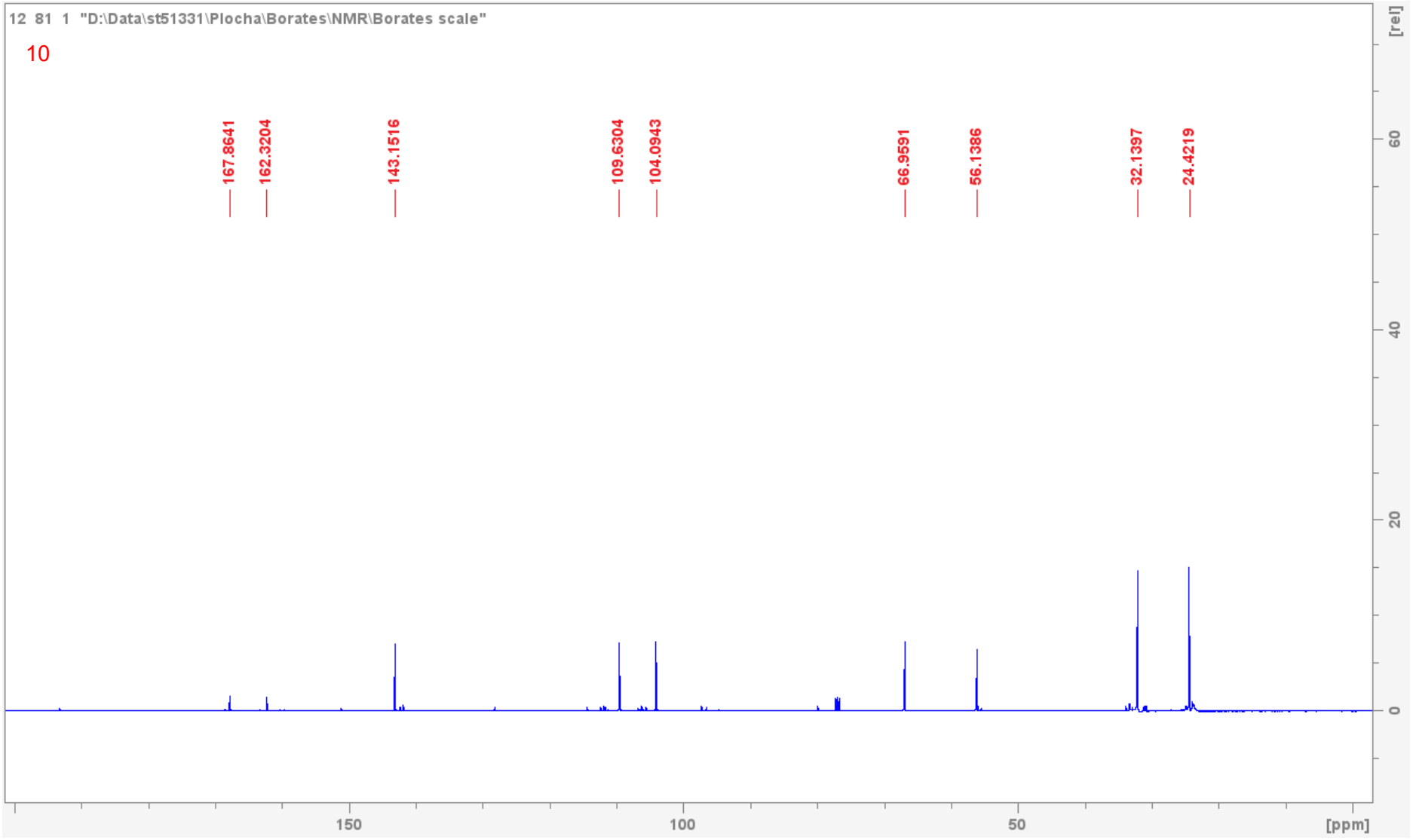

Figure S56. $^{13}C\{^{1}H\}$ NMR ($CDCl_3$, 125.76 MHz, 300 K) of **10**.

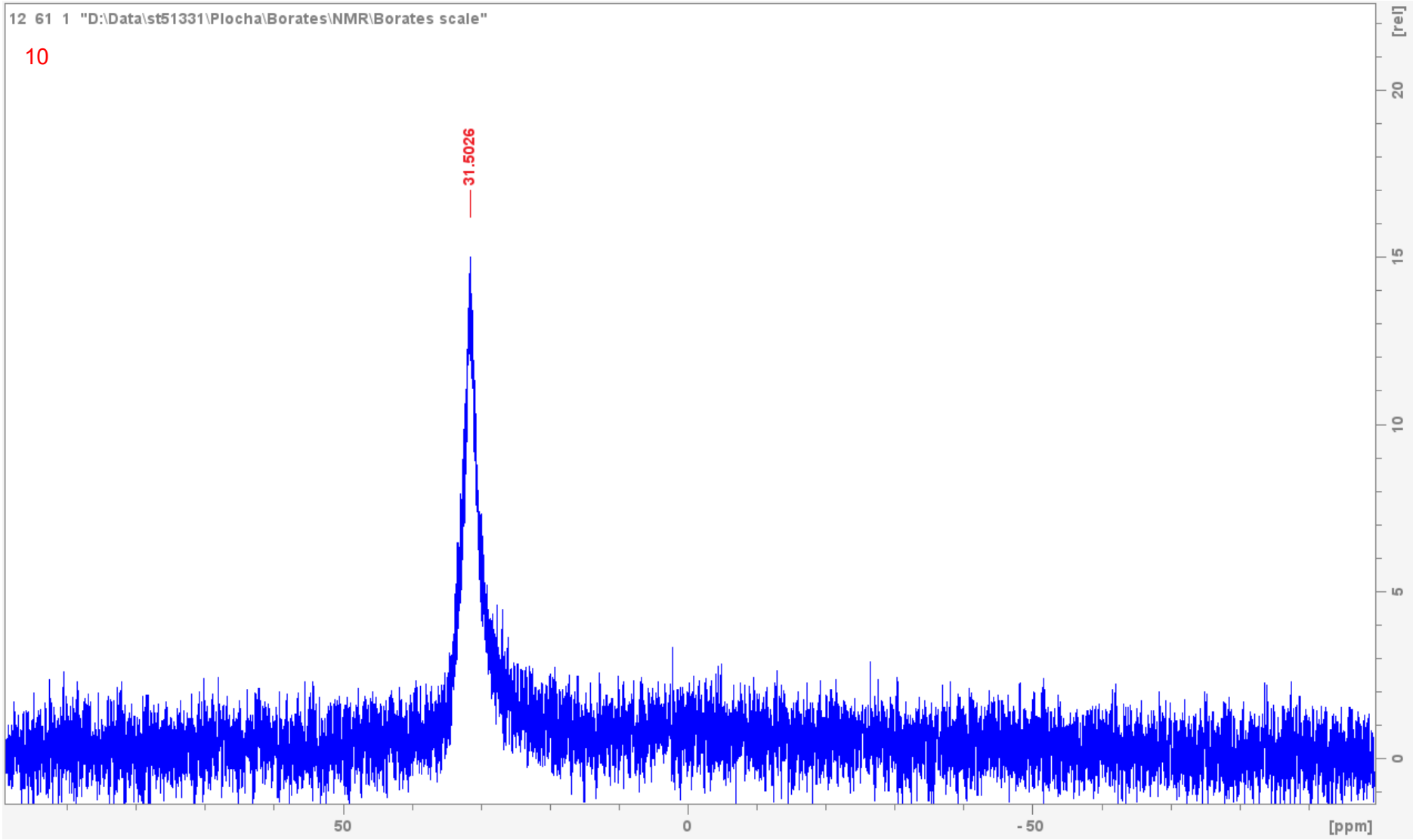

Figure S57. $^{11}B\{^{1}H\}$ NMR ($CDCl_3$, 128.378 MHz, 300 K) of **10**.

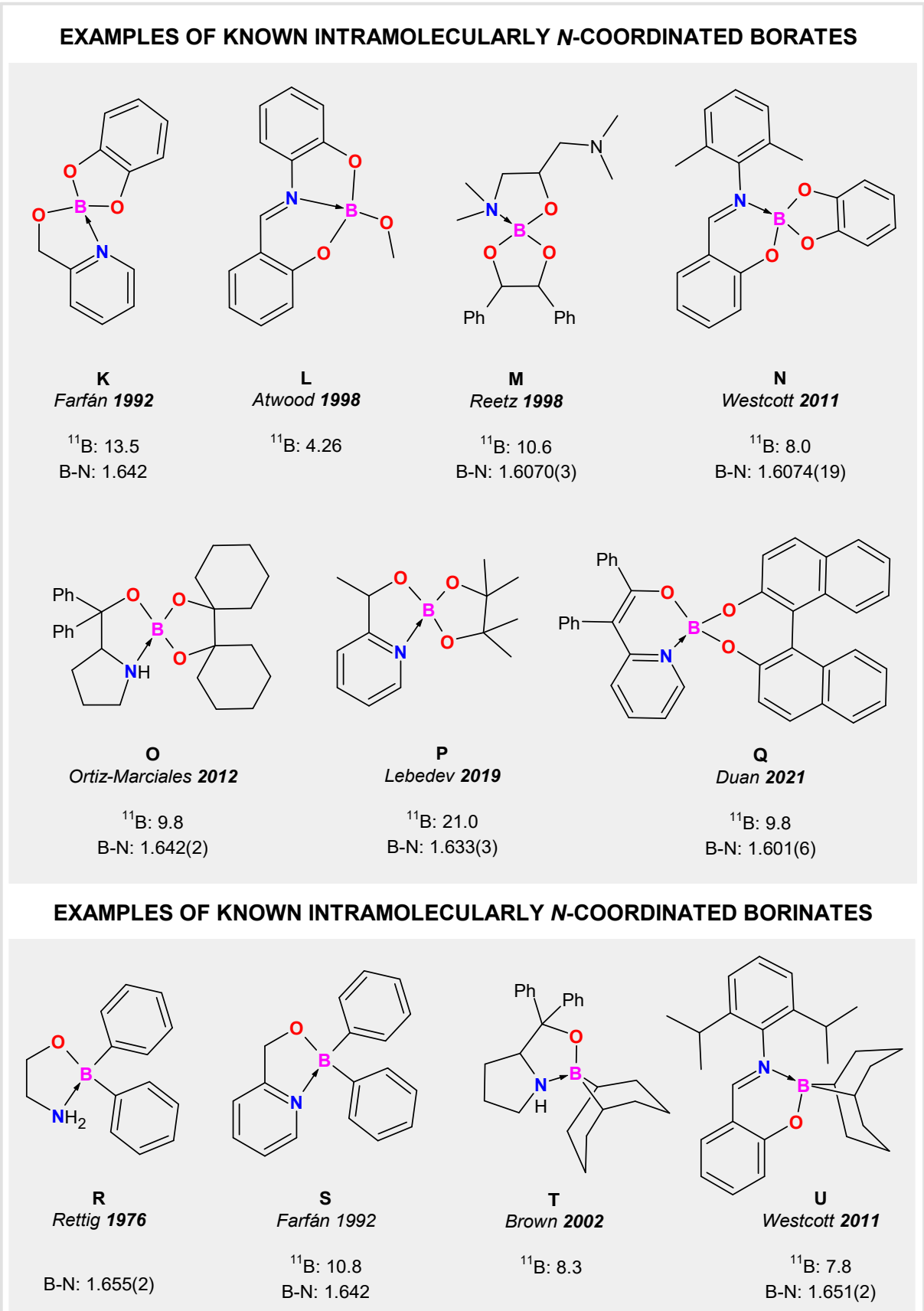

Figure S58.Examples of known intramolecularly coordinated boron esters and borinates including ^{11}B NMR (in ppm) and B-N bond length (in Å)[1]

Table S1. Crystallographic data of compounds **4**, **5** and **10**.

	4	**5**	**10**
Empirical formula	$C_{12}H_{18}BNO_3$	$C_{13}H_{20}BNO_4$	$C_{15}H_{22}BNO_2$
Formula mass [g.mol^{-1}]	235.08	265.11	259.14
λ [Å]	0.71073	0.71073	0.71073
T [K]	150(2)	150(2)	150(2)
Crystal system	Orthorombic	Monoclinic	Monoclinic
Space group	*Pbcn*	*C2/c*	*$P2_1/m$*
Crystal size [mm]	*0.193;0.253;0.552*	*0.102;0.251;0.332*	*0.093;0.098;0.344*
Crystal habit	*Colourless block*	*Colourless block*	*Colourless block*
a [Å]	26.086(3)	28.8105(8)	7.8412(3)
b [Å]	7.2573(8)	7.7335(2)	7.0999(4)
c [Å]	13.8616(16)	14.1767(4)	12.1963(6)
α [°]	90	90	90
β [°]	90	116.884(2)	103.264(2)
γ [°]	90	90	90
V [Å^3]	2624.2(5)	2817.28(14)	660.88(6)
Z	8	8	2
$\rho_{calcd.}$[gcm^{-3}]	1.190	1.250	1.302
μ [mm^{-1}]	0.083	0.090	0.084
F(000)	1008	1136	280
θ range [°]	2.913-26.498	3.001-28.353	2.669-28.301
No. of reflections collected	47157	68438	10942
No. of independent reflections / $R_{int.}$	2702 / 0.0311	3356 / 0.1062	1774 / 0.0368
No. of reflections observed with [I > 2σ(I)]	2409	2723	1521
Absorption correction	multi-scan	multi-scan	multi-scan
T_{max} / T_{min}	0.6205 / 0.4752	0.7457 / 0.7123	0.7457 / 0.6801
No. of refined parameters (restraints)	0	168	120
R(F) [I > 2σ(I)]	0.0870	0.0433	0.0645
$wR_2(F^2)$ (all data)	0.1942	0.1028	0.1636
$(\Delta/\sigma)_{max.}$	0.000	0.001	0.000
Diff. peak/hole [eÅ^{-3}]	0.344 / -0.495	0.282 / -0.163	0.693 / -0.471

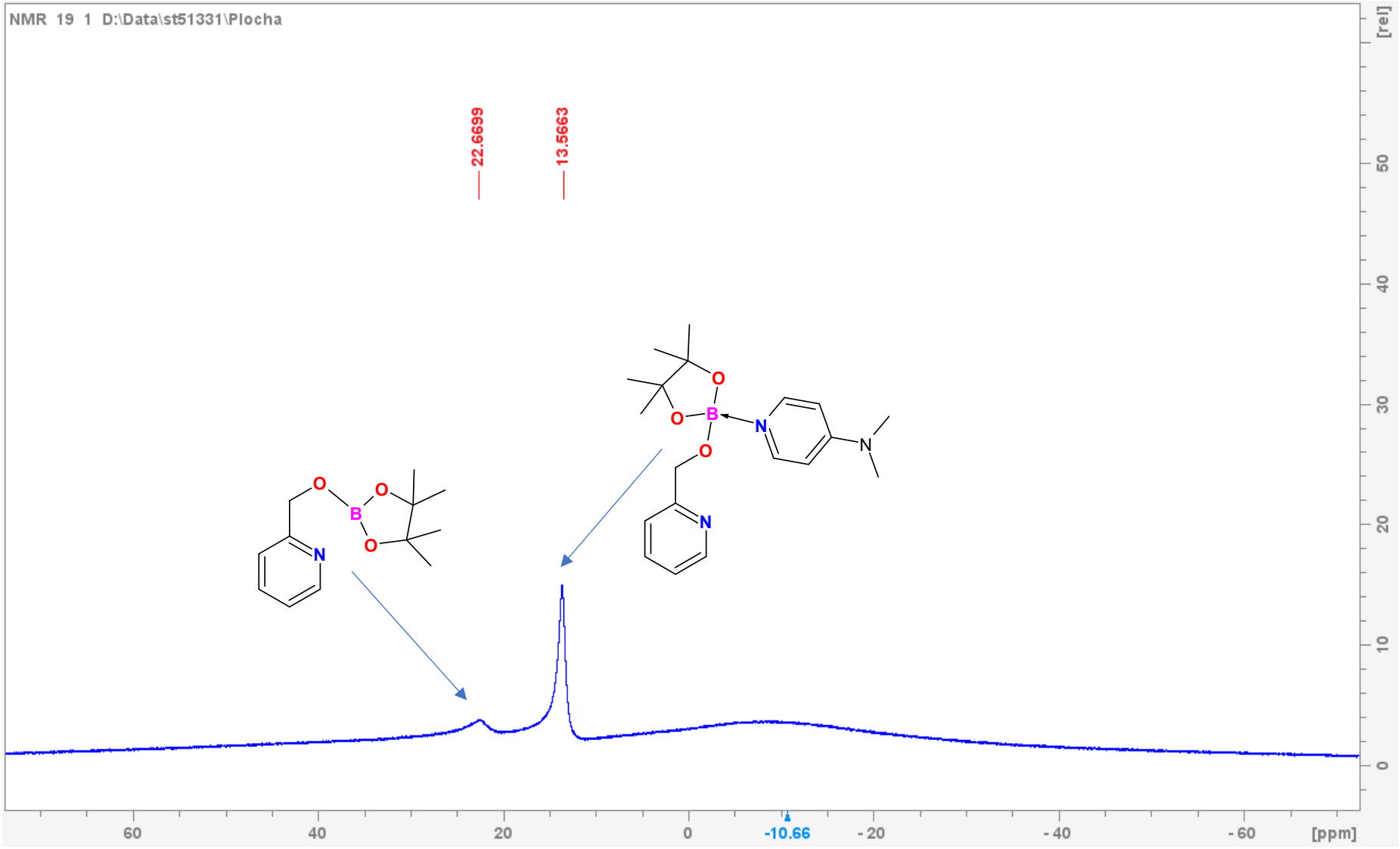

Figure S59. $^{11}B\{^{1}H\}$ NMR (C_6D_6, 128.378 MHz, 300 K). **4** + excess of DMAP, NMR scale reaction.

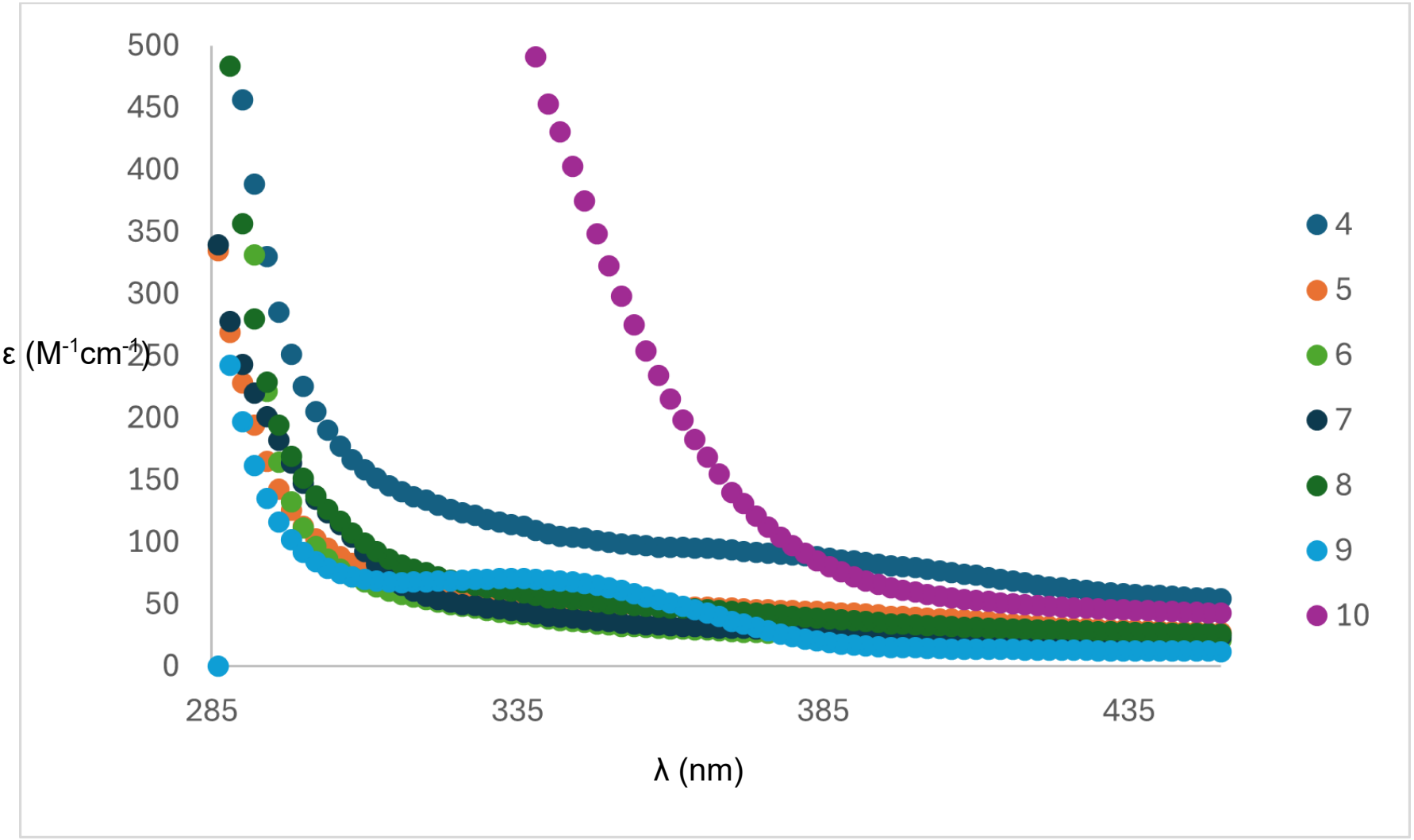

Figure S60. Absorption spectra of **4 - 10** in toluene.

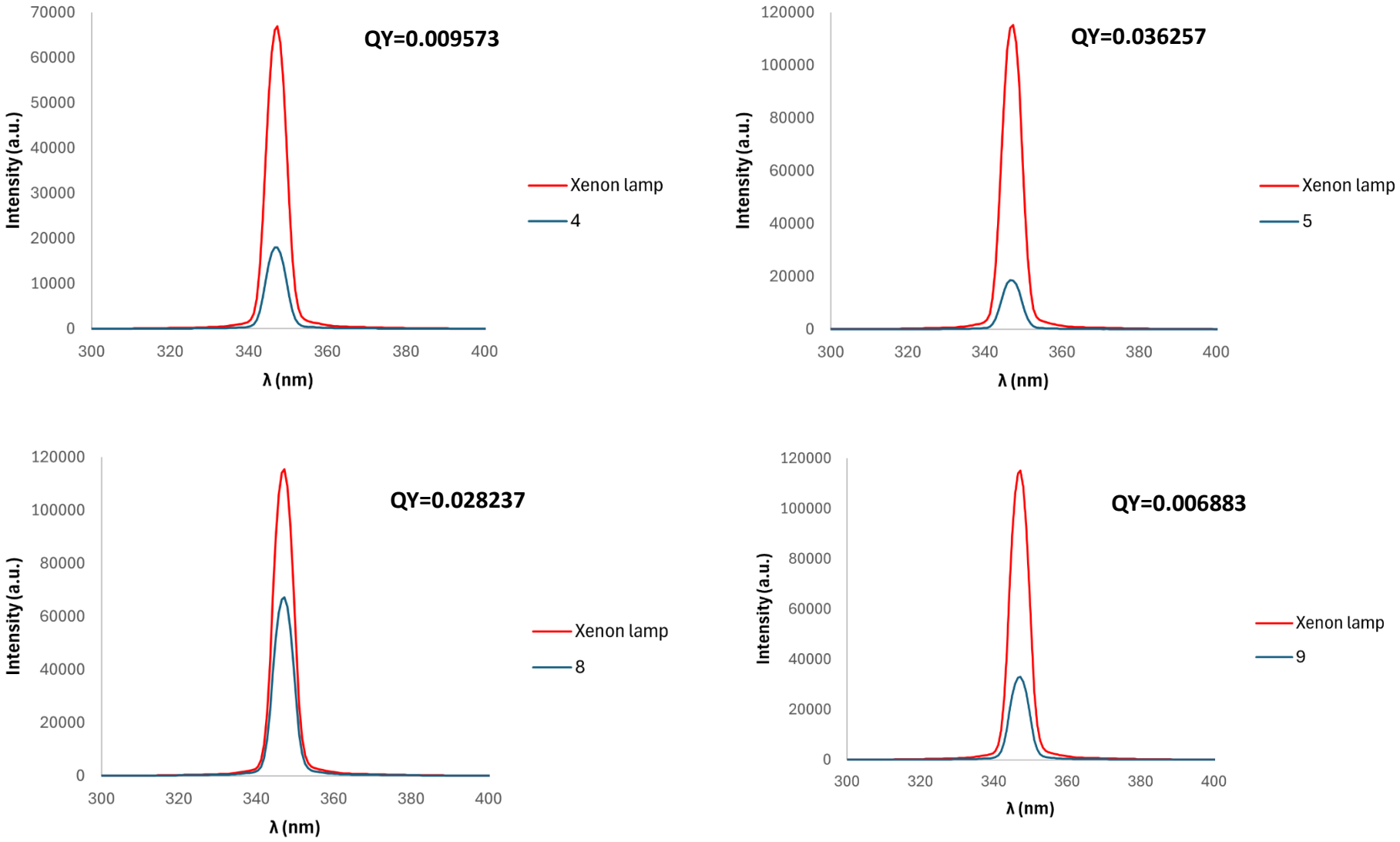

Figure S61. Quantum yield determination for **4**, **5**, **8** and **9** in toluene.

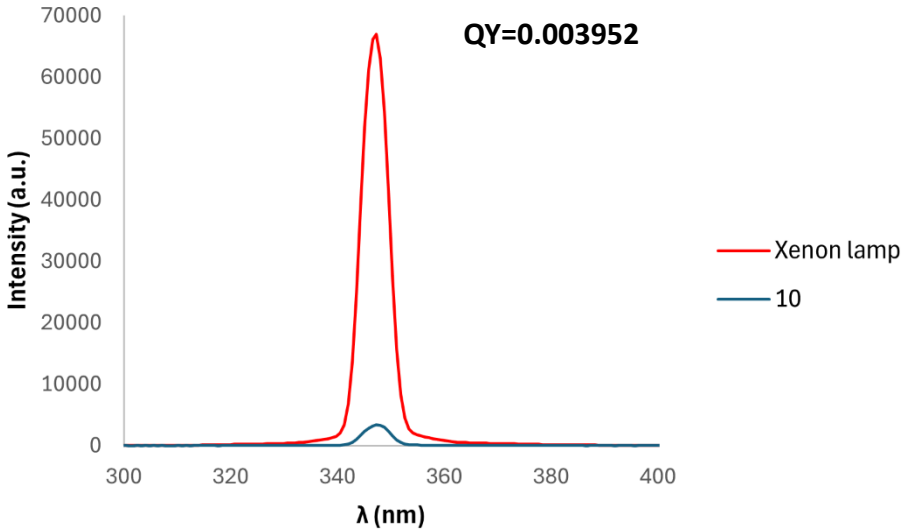

Figure S62. Quantum yield determination for **10** in toluene.

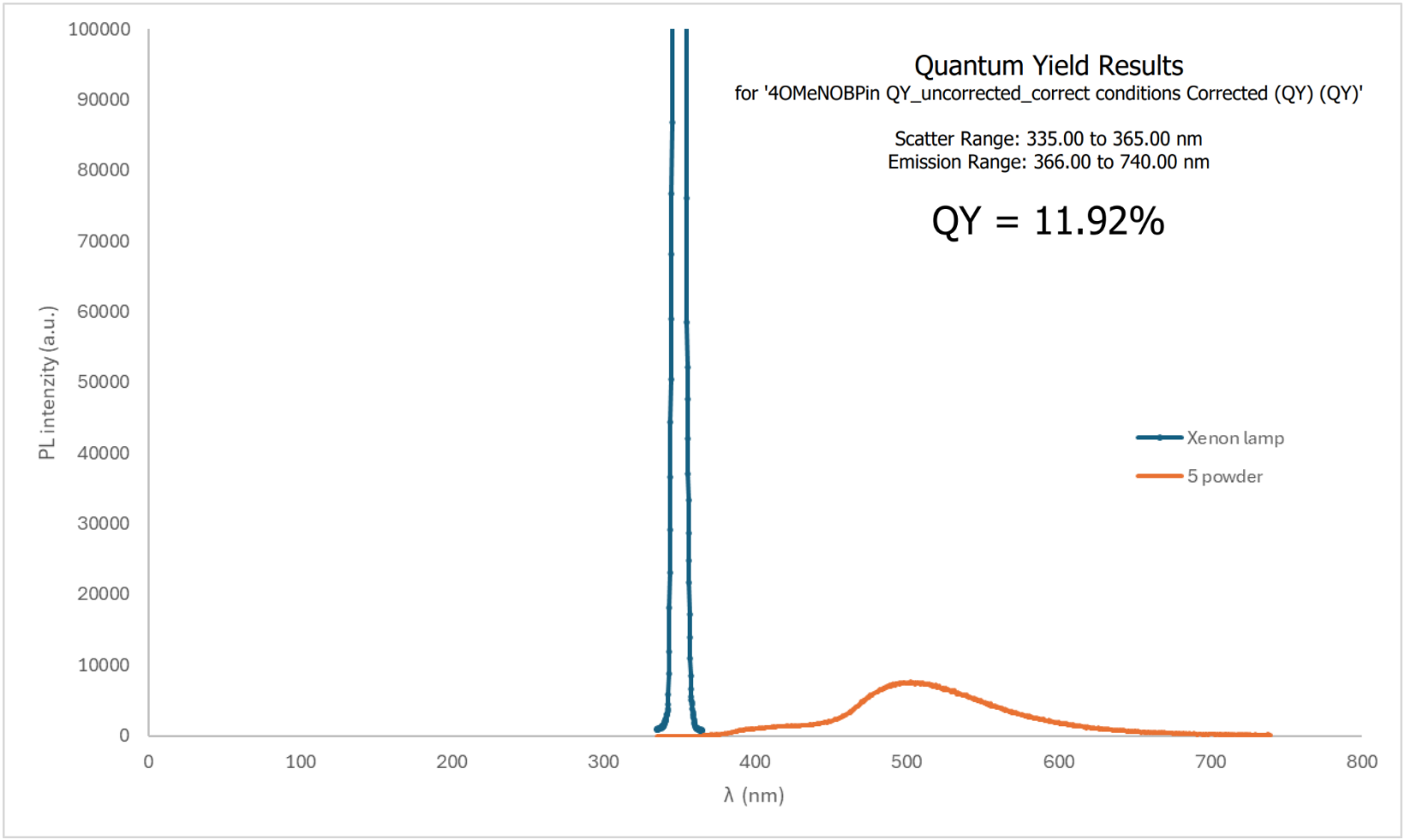

Figure S63. Quantum yield determination for powder of **5**.

DFT Computations

General methodology. Geometry Optimizations were carried out using density functional theory (DFT) at the B3PW91/6-311+G(2df,p)[2,3] level of theory using the Gaussian16[4] software package. For the Sn atom, effective core potentials and corresponding cc-pVTZ basis sets[5] were used. Dispersion effects were modelled using Grimme's GD3BJ parameters.[6] Solvent effects have been modelled by including the polarizable continuum model (IEF-PCM[7] and universal force field (UFF) atomic radii) with tetrahydrofuran as solvent.

Table S2. Computed thermochemistry data for the species involved in the proposed reaction mechanism.

	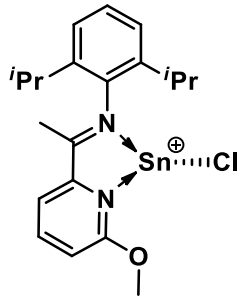	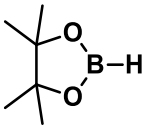	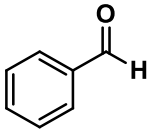	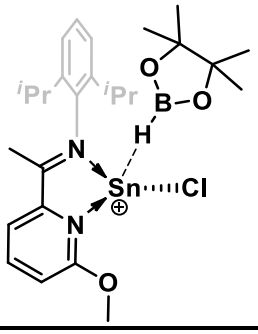
E	–1637.1230	–411.8851	–345.5749	–2048.6847
ZPE	0.4239	0.1897	0.1097	0.6147
E+ZPE	–1636.6991	–411.6954	–345.4651	–2048.0700
H	–1636.6710	–411.6849	–345.4578	–2048.0303
G	–1636.7573	–411.7284	–345.4958	–2048.1417

	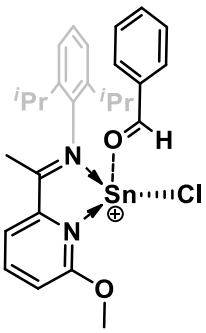	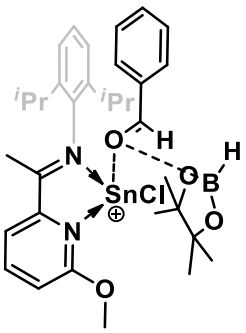	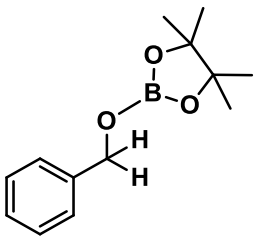
E	–1982.7200	–2394.6182	–757.5280
ZPE	0.5349	0.7262	0.3053
E+ZPE	–1982.1851	–2393.8921	–757.2227
H	–1982.1487	–2393.8445	–757.2053
G	–1982.2558	–2393.9749	–757.2671

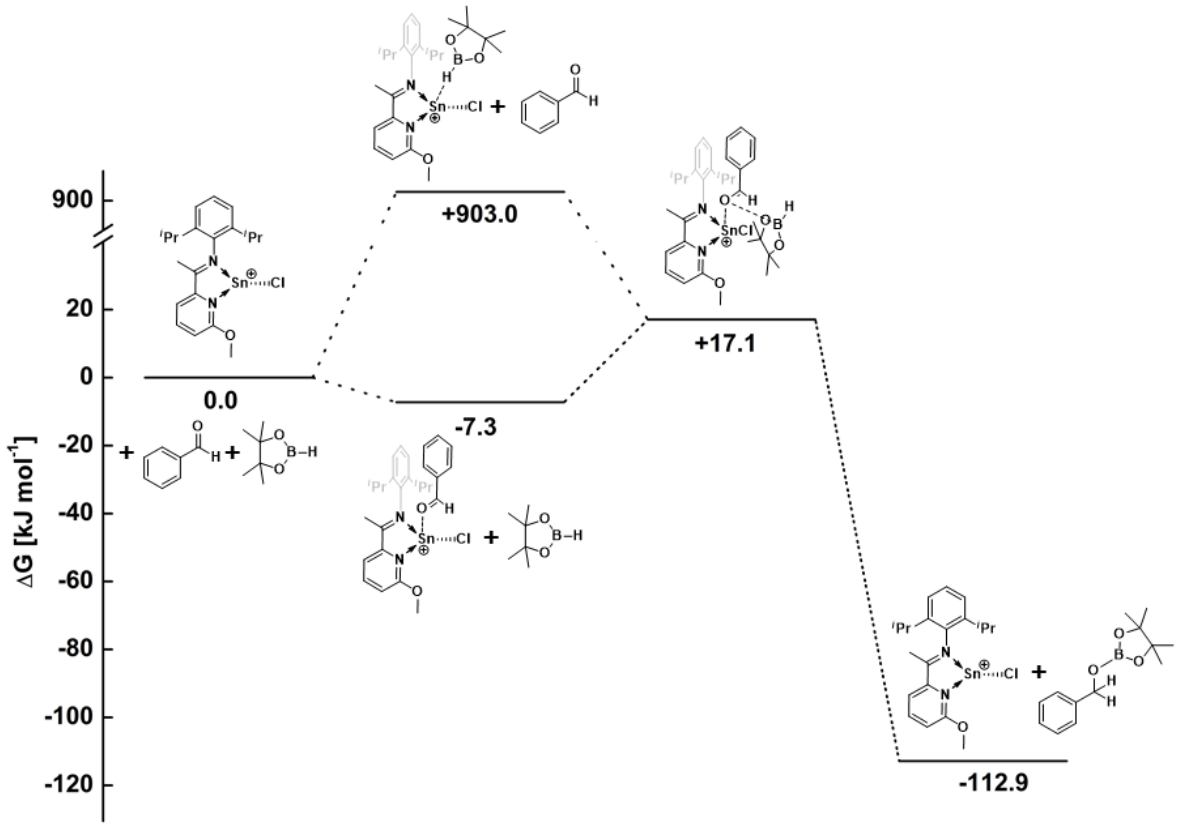

Figure S64. Possible reaction mechanism based on the computed thermochemistry data.

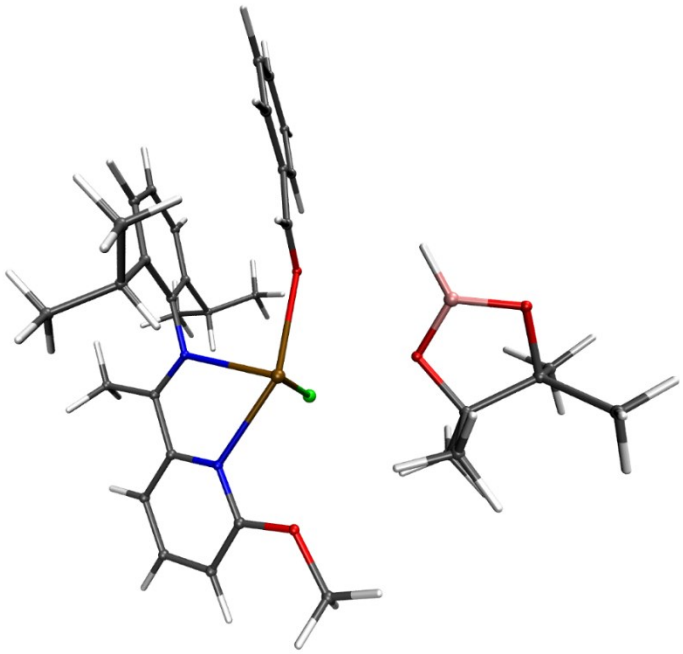

Figure S65. Optimized Geometry of a possible intermediate of **Int-1** with HBPin.

References

[1] For N-coordinated boron esters: (a) N. Farfán, D. Castillo, P. Joseph-Nathan, R. Contreras, L. Szentpály *J. Chem. Soc., Perkin Trans. 2* **1992**, 527–532. (b) Pingrong Wei and David A. Atwood *Inorg. Chem.* **1998**, *37*, 4934–4938. (c) J. Huskens, R. Goddard, M. T. Reetz, *J. Am. Chem. Soc.* **1998**, *120*, 6617-6618. (d) S. S. Barnes, C. M. Vogels, A. Decken, S. A. Westcott, Dalton Trans. **2011**, *40*, 4707–4714. (e) V. Stepanenko, M. de Jesús, C. Garcia, C. L. Barnes, M. Ortiz-Marciales, Tetrahedron Letters **2012**, *53*, 910–913. (f) W. Duan, K. Li, H. Ji, Y. Huo, Q. Yao, H. Liu, S. Gong *Dyes and Pigments* **2021**, *193*, 109538. (g) S. J. Rettig, J. Trotter, Can. J. Chem., **1976**, *54*, 3130-3141. (h) J. V. B. Kanth, H. C. Brown *Tetrahedron* **2002**, *58*, 1069–1074.

[2] (a) A. D. Becke, *J. Chem. Phys.* **1993**, *98*, 5648−5652; (b) J. P. Perdew, J. A. Chevary, S. H. Vosko, K. A. Jackson, M. R. Pederson, D. J. Singh, C. Fiolhais, *Phys. Rev. B: Condens. Matter Mater. Phys.* **1992**, *46*, 6671-6687.

[3] (a) R. Krishnan, J. S. Binkley, R. Seeger, J. A. Pople, *J. Chem. Phys.* **1980**, *72*, 650-654; (b) A. D. McLean, G. S. Chandler, *J. Chem. Phys.* **1980**, *72*, 5639-5648.

[4] Gaussian16 (RevisionC.01), M. J. Frisch, G. W. Trucks, H. B. Schlegel, G. E. Scuseria, M. A. Robb, J. R. Cheeseman, G. Scalmani, V. Barone, G. A. Petersson, H. Nakatsuji, X. Li, M. Caricato, A. V. Marenich, J. Bloino, B. G. Janesko, R. Gomperts, B. Mennucci, H. P. Hratchian, J. V. Ortiz, A. F. Izmaylov, J. L. Sonnenberg, D. Williams-Young, F. Ding, F. Lipparini, F. Egidi, J. Goings, B. Peng, A. Petrone, T. Henderson, D. Ranasinghe, V. G. Zakrzewski, J. Gao, N. Rega, G. Zheng, W. Liang, M. Hada, M.Ehara, K. Toyota, R. Fukuda, J. Hasegawa, M. Ishida, T. Nakajima, Y. Honda, O. Kitao, H. Nakai, T. Vreven, K. Throssell, J. A. Montgomery, Jr., J. E.Peralta, F. Ogliaro, M. J. Bearpark, J. J. Heyd, E. N. Brothers, K. N. Kudin, V. N. Staroverov, T. A. Keith, R. Kobayashi, J. Normand, K. Raghavachari, A. P. Rendell, J. C. Burant, S. S. Iyengar, J. Tomasi, M. Cossi, J. M. Millam, M. Klene, C. Adamo, R. Cammi, J. W. Ochterski, R. L. Martin, K. Morokuma, O. Farkas, J. B. Foresman and D. J. Fox, Gaussian, Inc., Wallingford CT, 2019.

[5] (a) B. Metz, H. Stoll, M. Dolg, *J. Chem. Phys.* **2000**, *113*, 2563-2569; (b) K. A. Peterson, *J. Chem. Phys.* **2003**, *119*, 11099-11112. (c) K. A. Peterson, D. Figgen, E. Goll, H. Stoll, M. Dolg, *J. Chem. Phys.* **2003**, *119*, 11113-11123.

[6] S. Grimme, S. Ehrlich, L. Goerigk, *J. Comp. Chem.* **2011**, *32*, 1456-1465.

[7] (a) E. Cances, B. Mennucci, J. Tomasi, *J. Chem. Phys.* **1997**, *107*, 3032–3041; (b) M. Cossi, G. Scalmani, N. Rega, V. Barone, *J. Chem. Phys.* **2002**, *117*, 43-54.